

Dissertation of the Faculty of Biology  
at the Ludwig-Maximilians-University Munich

Molecular delineation of cellular pathways  
associated with the antidepressant treatment response

Dongik Park

2016





# Eidesstattliche Versicherung

Ich versichere hiermit an Eides statt, dass die vorgelegte Dissertation von mir selbständig und ohne unerlaubte Hilfe angefertigt ist.

München,  
den .....

(Dongik Park)

# Erklärung

Hiermit erkläre ich, dass ich mich anderweitig einer Doktorprüfung ohne Erfolg nicht unterzogen habe und dass die Dissertation nicht ganz oder in wesentlichen Teilen einer anderen Prüfungskommission vorgelegt worden ist.

München,  
den .....

(Dongik Park)

First reviewer/supervisor: PD Dr. Mathias V. Schmidt

Second reviewer: Prof. Dr. Laura Busse

Date of submission: 20.06.2016

Date of oral examination: 30.11.2016



## Summary

A substantial number of psychiatric patients do not benefit from chronic antidepressant treatment. To identify biochemical pathways that can stratify antidepressant response sub-groups, DBA/2J mice were subjected to paroxetine administration for 28 days and classified into drug responder and non-responder groups based on floating time during the forced swim test (FST). Hippocampal metabolome and proteome profiles were analyzed and integrated to identify significant molecular pathway differences between paroxetine-responding and non-responding animals. I identified metabolites and proteins involved in purine and pyrimidine metabolism pathways whose levels were significantly different between paroxetine responding and non-responding mice. In addition, the glutamate/ubiquitin proteasome system (UPS)-associated pathways were associated with the chronic paroxetine treatment response. Specifically, N-Methyl-D-aspartate (NMDA) receptor, postsynaptic density protein 95 (PSD-95), and neuronal nitric oxide synthase (nNOS) levels significantly correlated with FST floating time suggesting their potential role in the antidepressant treatment response. The results from mice were further corroborated in human peripheral blood mononuclear cells (PBMCs) of major depressive disorder (MDD) patients. Protein signatures including ATIC, CPS2, PM2A, sGC- $\beta$ 1 and protein ubiquitination significantly correlated with clinical antidepressant treatment response. In my thesis project I have identified affected pathways and biomarker candidates related to the heterogeneous antidepressant treatment response using integrated -omics analyses combined with sub-group stratification based on behavioral phenotyping.

# Table of contents

Summary.....	VI
1. Introduction.....	1
1.1. Neuroanatomy of major depressive disorder.....	1
1.2. Neurobiology of major depressive disorder.....	3
1.2.1. Neurotrophic hypothesis of depression.....	3
1.2.2. HPA axis hypothesis of depression.....	3
1.2.3. Monoamine hypothesis of depression.....	4
1.2.4. Neuroplasticity theory of depression.....	5
1.3. Biomarkers for major depressive disorder.....	6
1.4. Antidepressant drugs.....	7
1.4.1. First generation of antidepressants.....	7
1.4.2. Second generation of antidepressants.....	7
1.4.3. Antidepressant treatment response.....	7
1.5. Personalized medicine strategy.....	9
1.6. Omics analyses.....	10
1.6.1. Quantitative proteomics.....	10
1.6.1.1. Metabolic labeling.....	10
1.6.1.2. Post-synthesis labeling.....	11
1.6.1.3. Label-free method.....	11
1.6.2. Targeted metabolomics.....	11
1.7. Aim of the thesis.....	12
2. Materials and Methods.....	13
2.1. Animal housing and husbandry.....	13
2.2. Drug administration.....	13
2.3. Mouse brain and blood collection.....	13
2.4. Behavioral analyses.....	14
2.4.1. Forced Swim Test.....	14
2.4.2. Female urine sniffing test.....	14
2.5. Paroxetine measurements.....	14
2.6. Omics analyses.....	15
2.6.1. Proteomics analysis.....	15

2.6.2. Metabolomics analysis.....	16
2.7. Molecular techniques.....	17
2.7.1. qRT-PCR.....	17
2.7.2. Immunoprecipitation.....	18
2.7.3. Western blot analysis.....	19
2.8. Patient samples.....	20
2.8.1. Paroxetine treatment of PBMCs.....	21
2.8.2. Protein level quantitation in cultured PBMCs.....	22
2.9. Statistical Analysis.....	22
3. Results.....	24
3.1. Sub-grouping of paroxetine responder and non-responder mice .....	25
3.2. Covariate analysis.....	27
3.3. Identification of purine and pyrimidine metabolism.....	28
3.4. Metabolomics analysis of mouse plasma.....	35
3.5. Analysis of peripheral patient sepcimens.....	43
3.6. Identification of glutamatergic and ubiquitin proteasomesystem pathways..	44
3.7. Validation of glutamatergic and ubiquitin proteasome system pathways.....	48
3.8. Candidate biomarker validation in human PBMCs from MDD patients.....	54
4. Discussion.....	56
4.1. Purine and pyrimidine metabolism pathway.....	56
4.2. Glutamatergic pathway.....	62
4.3. UPS pathway.....	66
4.4. Outlook.....	69
Appendix.....	70
References.....	70
List of abbreviations.....	93
List of figures.....	96
List of tables.....	98
Publications.....	99
Acknowledgements.....	100
Curriculum Vitae.....	102



# 1. Introduction

Major depressive disorder (MDD) is one of the most common psychiatric disorders which is characterized by persistent decrease/loss of interest and low mood (Hori et al., 2016). The World Health Organization estimates 350 million people suffer from MDD. MDD is often associated with suicide attempts and ranked second for global disease burden (Beautrais et al., 1996; Murray and Lopez, 1997).

## 1.1. Neuroanatomy of major depressive disorder

Several brain regions involved in cognitive and emotional processing have been shown to be affected in MDD (Figure 1).

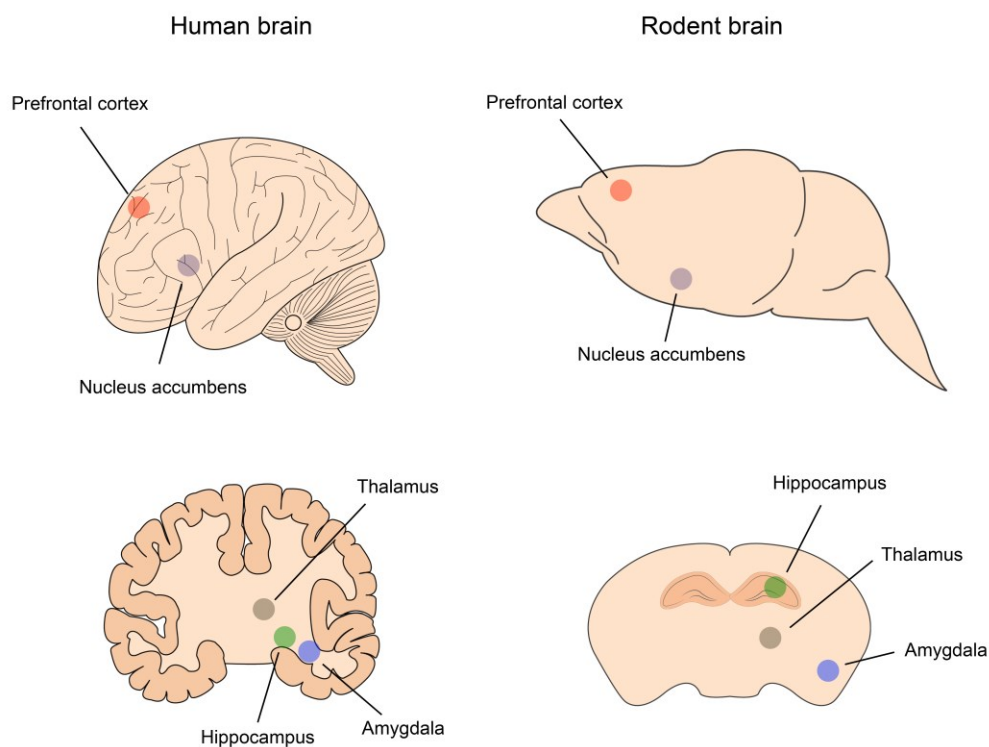


**Figure 1.** Brain regions affected in MDD.

The prefrontal cortex is part of the limbic system that controls emotional and cognitive functions. The association of prefrontal cortex with mood disorders has been extensively studied in animals and humans. Chronic stress has been shown to cause dendritic spine atrophy in rodents (Qiao et al., 2016). Prefrontal cortex dysfunction has been implicated in depressed patients (Merriam et al., 1999; Murray et

al., 2011). Structural atrophy has been shown in the prefrontal cortex of depressed patients (Drevets et al., 1997; Bremner et al., 2002).

Hippocampal volume loss and structural atrophy have been frequently reported in MDD patients (Sheline et al., 1996; 1999; Campbell et al., 2004; Opel et al., 2014). In the hippocampus adult neurogenesis takes place and this process plays important roles in various brain functions including synaptic plasticity, learning and memory, and emotional regulation (Jun et al., 2012). Hippocampal adult neurogenesis has been associated with MDD pathology and antidepressant treatment response (Malberg et al., 2000; Anacker et al., 2011; Lee et al., 2013; Mahar et al., 2014; Rotheneichner et al., 2014).

Nucleus accumbens (NAc) has also been strongly associated with stress-related neuropsychiatric conditions. Chronic mild stress was shown to induce decreased dopamine D2 receptor expression in the NAc (Papp et al., 1994). Altered serotonin and dopamine turnover was shown in the Flinders sensitive line, a rat model of depression (Zangen et al., 1999; 2001). Reduced NAc activity and volume have been reported in patients with mood disorders (Baumann et al., 1999; Heller et al., 2009). Its extensive functional connectivity with other brain regions including prefrontal cortex, hippocampus and amygdala that are also significantly associated with depressive disorders implicate a critical role of NAc in MDD pathophysiology (Shirayama and Chaki, 2006).

Volumetric abnormality has been observed in the amygdala of MDD subjects. Unmedicated depression patients showed a decrease of amygdala volume compared to controls (Hamilton et al., 2008). Depressed female individuals were shown to have a smaller amygdala (Hastings et al., 2004) and a hyperactive amygdala has been shown in depressed individuals (Drevets et al., 1992; Yang et al., 2010).

Like other brain regions involved in MDD, a significant volume decrease of the thalamus has also been observed in MDD individuals (Nugent et al., 2013). Thalamic area hyperactivity was shown to correlate with treatment-resistant depression and antidepressant treatment response (Yamamura et al., 2016).

## 1.2. Neurobiology of major depressive disorder

### 1.2.1. Neurotrophic hypothesis of depression

Neurotrophic factors are growth factors that are essential for neuronal cell proliferation and survival. Based on observations in rodents and depression patients low levels of neurotrophic factors have been implicated in the pathobiology of depression. They include brain-derived neurotrophic factor (BDNF), nerve growth factor (NGF), neurotrophin-3 (NT-3) and neurotrophin-4 (NT-4). Particularly BDNF has been extensively studied and associated with depressive disorders. BDNF level alterations have also been found in animal models of chronic stress (Murakami et al., 2005; Dwivedi, 2009). Antidepressants increase BDNF expression in brain regions including the hippocampus and prefrontal cortex (Lee and Kim, 2010). BDNF was shown to produce antidepressant-like effects (Shirayama et al., 2002) implying its critical role in the pathology and treatment of depressive disorders.

### 1.2.2. HPA axis hypothesis of depression

The hypothalamic-pituitary-adrenal (HPA) axis is a network that spans three endocrine systems, hypothalamus, pituitary gland and adrenal gland. In response to a stressor, neuropeptides including corticotrophin releasing hormone (CRH) and arginine vasopressin (AVP) are secreted from the paraventricular nucleus of hypothalamus. This causes adrenocorticotrophic hormone (ACTH) release from the anterior pituitary, which stimulates adrenal cortex to synthesize and release glucocorticoids into the blood stream. Negative feedback control of the HPA axis is mediated by glucocorticoid receptor (Figure 2). HPA axis abnormalities have been found in depressive disorders. Depression patients have increased cortisol levels in body fluids including saliva, plasma and urine (Nemeroff and Vale, 2005). An increased volume of the pituitary (MacMaster and Kusumakar, 2004; MacMaster et al., 2006) and adrenal gland (Rubin et al., 1995) have been found in patients with depressive disorder reflecting stress-induced HPA axis dysregulation.

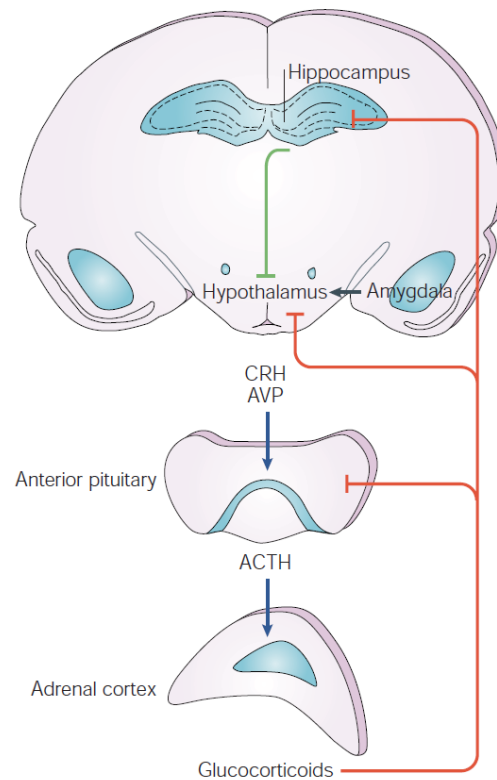


**Figure 2.** Diagram of the HPA axis (adapted from Sandi, 2004).

### 1.2.3. Monoamine hypothesis of depression

Drugs and agents that increase monoamine neurotransmitter levels and availability in the synaptic cleft have been found to be effective for alleviating depressive symptoms (Sangkuhl et al., 2009; Dell'Osso et al., 2011). These observations led to the hypothesis that monoamine deficiency may cause depressive symptoms. In this regard, depressive disorders have been associated with impaired neurotransmission of monoaminergic pathways (D'Aquila et al., 2000; Schmidt and Reith, 2005; Popik et al., 2006). Conventional antidepressants including TCAs, SSRIs and MAOIs affect monoamine levels including serotonin, norepinephrine and dopamine. Drugs of the tricyclic antidepressant (TCA) and selective serotonin reuptake inhibitor (SSRI) type inhibit monoamine transporters that regulate extracellular monoamine levels by reuptake from the synaptic cleft. The resulting increased neurotransmitter levels activate post-synaptic monoaminergic pathways. Monoamine oxidase inhibitor (MAOI) increases neurotransmitter levels by inhibiting monoamine oxidase (MAO) activity that catalyzes the degradation of monoamine neurotransmitters (Figure 3).

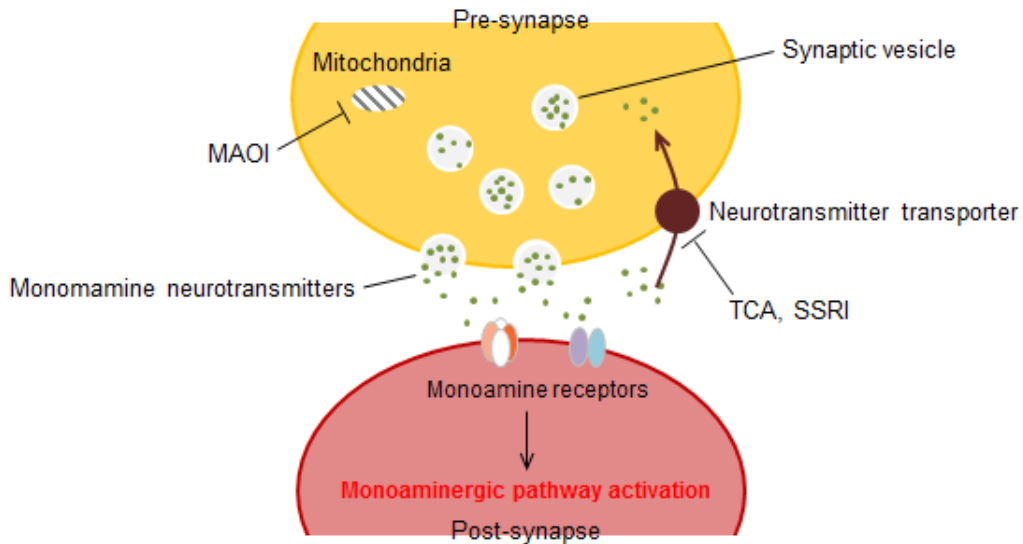


**Figure 3.** Monoamine neurotransmission in the synapse.

#### 1.2.4. Neuroplasticity theory of depression

Neuroplasticity defines neuronal adaptation which includes structural and functional activity changes. Hippocampal synaptic plasticity in the form of long-term potentiation (LTP) persistently strengthens electrical signals in the synapse. Calcium,  $\alpha$ -amino-3-hydroxy-5-methyl-4-isoxazolepropionic acid (AMPA) and N-Methyl-D-aspartate (NMDA) receptors, cyclic adenosine monophosphate (cAMP), calcium-calmodulin-dependent kinase II (CaMKII) and cAMP response element binding protein (CREB) are important for the regulation of neuronal plasticity (Pittenger and Duman, 2008). Stress was shown to impair LTP in the rodent hippocampus (Kim and Diamond, 2002). High levels of glucocorticoid, a stress hormone, suppress hippocampal LTP (De Kloet, 2004). In the prefrontal cortex, chronic stress not only induces pyramidal cell dendrite atrophy (Cook and Wellman, 2004; Radley et al., 2004), but also leads to glia and endothelial cell number reduction in animal models of stress (Banasr et al., 2007). Depressed individuals show decreased neuroplasticity, which was measured by motor cortical excitability in response to transient brain stimulation (Ford and Erlinger, 2004; Liukkonen et al., 2006; Elovainio et al., 2009; Vogelzangs et al., 2012; Player et al., 2013; Valkanova et al., 2013; Hickman et al., 2014b).

### 1.3. Biomarkers for major depressive disorder

Research using animal models and patient specimens has resulted in several biomarker candidates for major depressive disorder (MDD).

C-reactive protein (CRP) is an acute phase protein circulating in blood whose concentration rises rapidly in response to physiological changes including infection and inflammation (Thompson et al., 1999). Several studies have found that elevated CRP level are associated with MDD (Ford and Erlinger, 2004; Liukkonen et al., 2006; Elovainio et al., 2009; Howren et al., 2009; Vogelzangs et al., 2012; Valkanova et al., 2013; Hickman et al., 2014a).

The HPA axis activity has been suggested as a potential biomarker of MDD. The dexamethasone suppression test (DST) has been used to test adrenal gland activity. Dexamethasone, a synthetic analogue of cortisol, induces negative feedback control to the pituitary gland and suppresses cortisol release from the adrenal gland. Plasma cortisol levels in response to dexamethasone injection can be used as a measure for HPA axis dysfunction (Targum et al., 1983; Dam et al., 1985; Fountoulakis et al., 2008).

BDNF serum levels have been proposed as an MDD biomarker in the clinic (Karege et al., 2002; Shimizu et al., 2003; Karege et al., 2005). FK506-binding protein 51 (FKBP51) is a co-chaperone protein that interacts with glucocorticoid receptor and regulates its activity. FKBP51 has been found to be a risk factor for stress-related neuropsychiatric disorders including MDD (Lekman et al., 2008; Binder, 2009). Several *FKBP5* gene polymorphisms have been found to be associated with depressive disorders (Appel et al., 2011; Szczepankiewicz et al., 2014). Reduced p11 mRNA and protein expression in NAc and hippocampus have been reported in depressed patients and suicide victims (Svenningsson et al., 2006; Anisman et al., 2008; Alexander et al., 2010). Despite all the promising research findings none of these biomarkers have made it to the clinic to guide diagnosis of depressive disorders.

## 1.4. Antidepressant drugs

### 1.4.1. First generation of antidepressants

The first generation of antidepressants was developed in 1950s. Isoniazid and iproniazid were used as anti-tuberculosis agents and found to be potent inhibitors of MAO and to have psycho-stimulant effects (Healy, 2000). The TCA imipramine was subsequently developed by the Swiss psychiatrist Ronald Kuhn. Tricyclics were first found to inhibit norepinephrine reuptake and later also shown to block the serotonin transporter (López-Muñoz and Alamo, 2009). Hence TCAs act as serotonin-norepinephrine reuptake inhibitors (SNRIs) resulting in elevated neurotransmitter levels in the synaptic cleft.

### 1.4.2. Second generation of antidepressants

MAOIs and TCAs mode of action led to the hypothesis that the drugs' antidepressant activities are related to elevated neurotransmitter levels (Pletscher, 1991). Novel SSRIs and selective norepinephrine reuptake inhibitors (SNRIs) were subsequently developed and introduced on the market. SSRIs and SNRIs have fewer adverse side effects compared to other types of antidepressants. Currently they are used as first line medications for the treatment of a wide range of psychiatric disorders.

### 1.4.3. Antidepressant treatment response

Approximately 50% of MDD patients do not respond adequately to conventional antidepressant treatment (Trivedi et al., 2006; Papakostas, 2009). The patients who fail to achieve remission after two or more of antidepressant trials are diagnosed to have treatment resistant depression (TRD) (Malhi et al., 2005). The development of novel more targeted antidepressant drugs has not been very successful. According to several meta-analyses with SSRIs, patients' response rate remains at around 47% (Nelson, 1998).

To overcome this high rate of drug non-response, several clinical strategies have been conducted. Augmentation therapy uses a second non-antidepressant agent with antidepressant medication. Augmentation treatment with lithium has shown a significant increase of response rate (de Montigny et al., 1983; Heninger et al., 1983;

Schöpf et al., 1989; Joffe and Schuller, 1993; Stein and Bernadt, 1993). Augmentation therapies with thyroid hormone and 5-HT<sub>2A</sub> receptor antagonists such as trazodone have been reported to be more effective than antidepressant monotherapy (Maes et al., 1996; Joffe, 1997). Various other substances including pindolol, omega-3 fatty acids, modafinil, bupropion/bupropion and methylphenidate, testosterone, mecamylamine and inositol have been used for augmentation therapy (Papakostas, 2009).

Combination therapy uses multiple antidepressants. The combination of desipramine (noradrenergic TCA) with fluoxetine has been shown to be more effective for achieving a response in MDD patients (Fava et al., 1994; Nemeroff et al., 1996). Using mirtazapine in combination with SSRIs was also found to be effective for TRD treatment (Carpenter et al., 1998). The adjunctive effect of mianserin was also found superior compared to SSRI monotherapy (Maes et al., 1999; Ferreri et al., 2001).

Electric and magnetic brain stimulations induce an antidepressant-like effect in TRD patients. Deep brain stimulation (DBS) is a surgical method that implants electrodes and stimulates certain brain regions (Mayberg et al., 2005; Kennedy et al., 2011). Transcranial magnetic stimulation (TMS) applies electro-magnetic fields to stimulate a population of nerve cells. Because of its non-invasive and safe nature, TMS is a promising therapeutic strategy to treat TRD (George et al., 1995; Pascual-Leone et al., 1996; Lee et al., 2012). Electroconvulsive therapy is a procedure that applies electric current through the brain to induce biochemical and functional activity changes. This method has been shown to be effective for the treatment of TRD (Khalid et al., 2008; Dierckx et al., 2012; Kellner et al., 2012).

Novel fast-acting antidepressant-like agents have also been investigated for the treatment of TRD. They include scopolamine and ketamine. Scopolamine, an antagonist for muscarinic cholinergic receptors has rapid antidepressant-like effects in TRD patients (Furey and Drevets, 2006; Drevets et al., 2013; Jaffe et al., 2013). Ketamine, an NMDA receptor blocker, also produces a rapid antidepressant effect (Murrough et al., 2013; Lally et al., 2014) in TRD patients (Murrough et al., 2013; Lally et al., 2014).

Recent research has delineated potential candidates associated with antidepressant treatment resistance. Serotonin transporter (Huezo-Diaz et al., 2009) and serotonin autoreceptors (Malagié et al., 2001; Samuels et al., 2015) have been found to be critical for the antidepressant response. In addition, alterations and abnormalities of the HPA axis have been associated with antidepressant treatment outcome (Binder et

al., 2008; Ventura-Juncá et al., 2014). BDNF gene Val66Met polymorphism has been also studied with regard to the antidepressant treatment response and was shown to result in antidepressant treatment resistance in rodents and humans (Chen et al., 2006; Zou et al., 2010a; 2010b; Kocabas et al., 2011). A link between inflammatory cytokines and antidepressant response has been documented. Cerebrospinal fluid IL-1, IL-6 and TNF- $\alpha$  blood levels in MDD patients were significantly correlated with depression severity (Martinez et al., 2012). High cytokine concentrations have been found in antidepressant treatment resistant depression patients (Sluzewska et al., 1997; Lanquillon et al., 2000; Fitzgerald et al., 2006).

### 1.5. Personalized medicine strategy

The high heterogeneity of the antidepressant treatment response requires a tailored treatment to improve therapeutic efficacy. Several studies have been conducted to identify biological markers that predict and/or evaluate the antidepressant treatment response. Genetic polymorphism studies have found polymorphisms in tryptophan hydroxylase, serotonin transporter and serotonin 5-HT<sub>2</sub> receptor to be statistically associated with SSRI treatment outcome (Serretti et al., 2001; Zanardi et al., 2001; Arias et al., 2003; Serretti et al., 2006; Ham et al., 2007; Serretti et al., 2007).

Neuroimaging measurements have identified neurophysiological markers for the antidepressant response. Mayberg et al. found that brain region-specific blood glucose metabolism changes were observed only in 6-week fluoxetine treatment responder MDD patients (Mayberg et al., 2000; 2002). Several studies have reported that a decrease of theta cordance from prefrontal electroencephalography during the first weeks with either SSRI or SNRI treatment is able to predict symptom improvement for the following weeks of continued treatment (Cook et al., 2002; 2005; Bares et al., 2007).

Omics data promise to have great potential for the personalized medicine approach in psychiatry. Psychiatric patient sub-group stratification based on omics profiling data allows a more precise and tailored treatment (Guest et al., 2013; Sethi and Brietzke, 2015).

## 1.6. Omics analyses

### 1.6.1. Quantitative proteomics

The shotgun proteomics approach has been very successful for the high-throughput analysis of complex protein mixtures (Domon and Aebersold, 2010; Meissner and Mann, 2014). The method involves enzymatic digestion of proteins into peptides that are subjected to tandem mass spectrometry. With the help of stable isotopes proteomes can be profiled and compared by quantitative mass spectrometry.

#### 1.6.1.1. Metabolic labeling

Stable isotopes can be incorporated into proteins during cellular synthesis *in vitro* and *in vivo* (Figure 4). For the stable isotope labeling of amino acids in cell culture (SILAC) method labeled essential amino acids (arginine, lysine and methionine) are added to the cell culture medium (Ong et al., 2002). Due to the mass difference between light and heavy isotopes, mass spectrum signals of unlabeled and labeled peptides have different mass-to-charge ratio ( $m/z$ ) values and their intensities can be used for quantification.

Stable isotope labeling in mammals (SILAM) refers to *in vivo* labeling of the entire mammalian proteome with stable isotopes.  $^{13}\text{C}$ - or  $^{15}\text{N}$ -containing diets are used for partial or full proteome labeling in rodents (Kruger et al., 2008; Zhang et al., 2011b). Labeled rodent tissues and organs can serve as reference material to investigate *in vivo* proteome turnover and expression changes (Filiou et al., 2011; Zhang et al., 2011b; Webhofer et al., 2013).

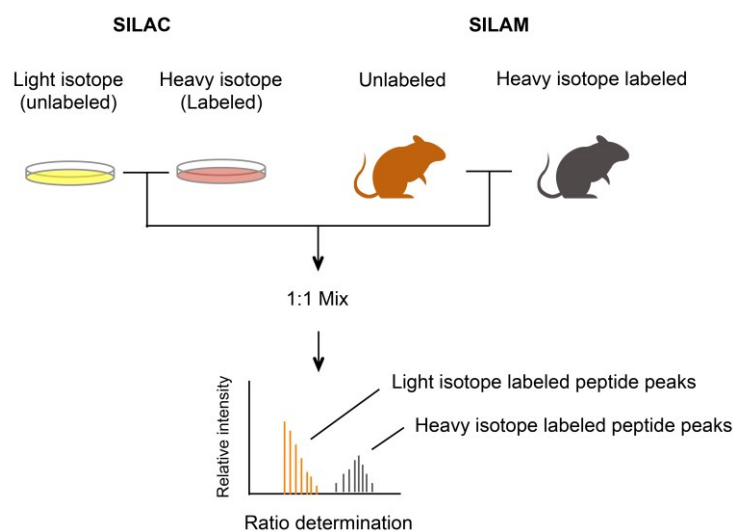


**Figure 4.** SILAC and SILAM metabolic labeling methods.

### 1.6.1.2. Post-synthesis labeling

Chemical probes have been used for post-synthesis labeling of peptides and proteins. Whereas metabolic labeling methods require cellular protein synthesis, non-metabolic labeling with chemical probes is applied to investigate body fluids.

Isotope-coded affinity tag (ICAT) consists of three domains, a reactive group for labeling amino acids, an isotopically coded linker region and a tag for affinity isolation. The ratio of signal intensities between light and heavy ICATs is used for the relative quantification of two samples. Four sets of isotope-coded protein label (ICPL) probes, ICPL0, ICPL4, ICPL6 and ICPL10, are available for the comparison of four different samples. Each probe has a different mass by replacing  $^1\text{H}$  or  $^{12}\text{C}$  with deuterium or  $^{13}\text{C}$ , respectively.

Isobaric tags for relative and absolute quantification (iTRAQ) and tandem mass tag (TMT) are used for the comparison of multiple biological conditions (Tonack et al., 2013; Núñez Galindo et al., 2015; Yao et al., 2015). Isobaric tags consist of three components, an amine reactive group that allows covalent binding to amino acids, a reporter group that includes a differential mass, and balance group between the other two components. The different reporter masses from multiple samples can be analyzed in one mass spectrometry run. TMT isobaric tags with various combinations of  $^{13}\text{C}$  and  $^{15}\text{N}$  allow comparison of 10 different samples.

### 1.6.1.3. Label-free quantitation

Label-free quantitation is a method based on measuring peptide peak areas, intensities or spectral counts. In contrast to protein labeling methods that combine labeled and unlabeled samples, during label-free quantitation samples are subjected separately to mass spectrometry analysis (Zhu et al., 2010).

## 1.6.2. Targeted metabolomics

Metabolomics has been an important method to investigate biological pathway and metabolism changes (Sato et al., 2012; Shah et al., 2012; Inoue et al., 2013). It has been extensively applied for biomarker research and the identification of affected biological pathway (Griffiths et al., 2010; Armitage and Barbas, 2014).

Metabolomics analysis has been conducted with several platforms including nuclear magnetic resonance, liquid chromatography coupled to mass spectrometry and gas chromatography coupled to mass spectrometry.

Two different strategies can be utilized for metabolomics analysis – untargeted and targeted. Untargeted metabolomics assesses all measurable analytes including the ones with unknown identity, which requires follow-ups for their identification and characterization. Targeted metabolomics captures biochemically characterized small molecules. By using internal standards or metabolite signal intensity, targeted metabolomics data can be quantitative. Relevant biochemical pathways can be enriched by a list of identified metabolites. Quantified metabolite levels also reflect pathway activity.

## 1.7. Aim of the thesis

Using quantitative -omics analyses and *in silico* data integration this thesis aims at identifying biosignatures and molecular pathways relevant for the stratification of antidepressant treatment sub-groups and antidepressant efficacy. The study represents an attempt to address the high rate of antidepressant non-response, one of the major problems in psychiatry, and to bridge the translational gap between preclinical and clinical studies.

The separation of antidepressant responder and non-responder sub-groups is a prerequisite for biomarker identification. My -omics analyses were carried out with specimens from an animal model that reflects clinical bimodal distribution of patient sub-groups, which was established in Prof. Marianne Müllers laboratory during her tenure at the *Max Planck Institute of Psychiatry*.

Resulting from -omics profiles of the mouse model, protein signatures that are part of the identified pathways were further corroborated in mice and MDD patients' peripheral blood mononuclear cells (PBMCs) with the aim of identifying biomarker candidates relevant for assessing antidepressant treatment response.

## 2. Materials and Methods

### 2.1. Animal housing and husbandry

The experiments were performed with male DBA/2J mice (Charles River Laboratories, Chatillon-sur-Chalaronne, France). All animals were between 8-10 weeks old and single-housed for at least one week prior to the beginning of the experiments. Mice were held under normal light and temperature conditions (12 light: 12 dark light cycle, lights on at 7 pm, temperature at  $23 \pm 2^\circ\text{C}$ , and humidity at  $55 \pm 5\%$ ) with standard bedding and nesting material, in polycarbonate cages (21 x 15 x 14 cm). Water and Altromin 1324 standard mouse chow (Altromin GmbH, Lage, Germany) were provided *ad libitum*. All procedures were carried out in accordance with the European Communities Council Directive 2010/63/EU and approved by the committee for the Care and Use of Laboratory animals of the Government of Upper Bavaria, Germany.

### 2.2. Drug administration

Mice were treated with either vehicle or 5 mg/kg paroxetine pills (Paroxetine hydrochloride Carbone Scientific, London, UK) for 28 days twice a day. Animals were randomly assigned to the vehicle- or paroxetine-treated groups. Either vehicle or paroxetine was voluntarily self-administered via customized palatable pellets (40mg PQPellets, Phenoquest AG, Martinsried, Germany). Animals that did not take the pills properly were excluded from further analyses.

### 2.3. Mouse brain and blood collection

Blood was collected at least one month before commencing paroxetine treatment from retro-orbital puncture and after 28 days of paroxetine treatment through cardiac puncture or trunk blood. On day 29, the animals were subjected to a forced swim test (FST) and sacrificed. Trunk blood and brains of the animals were collected and stored at  $-80^\circ\text{C}$  until further use. Blood was centrifuged to separate plasma and erythrocytes (1300g, 10 min,  $4^\circ\text{C}$ ) before storage.

## 2.4. Behavioral analysis

### 2.4.1. Forced Swim Test

The forced swim test was performed to evaluate antidepressant-like activity of chronic paroxetine treatment in DBA2/J mice, and to further stratify paroxetine-treated mouse sub-groups based on behavior profiles. After 28 days of paroxetine pill administration, mice were subjected to the forced swim test on day 29. Mice were placed into a glass beaker (height 24 cm, diameter 13 cm) filled with water ( $21 \pm 1^\circ\text{C}$ ) up to a height of 15 cm, so that the animals were unable to reach the ground or escape for 6 min testing. After the test, animals were immediately dried and returned to home cage. Main parameter of interest is floating time scored by an experienced observer blind to treatment.

### 2.4.2. Female urine sniffing test

The female urine sniffing test was conducted to assess anhedonia-like behavior of animals before and after chronic paroxetine treatment. The test was performed prior to commencing paroxetine treatment and 28 days after treatment. Mice were habituated to a cotton swab inserted into their home cage for 1 h prior to testing. Mice were exposed to a sterile cotton swab dipped into water for 3 min and after a 45 min inter trial interval. Then they were exposed to a sterile cotton swab dipped in estrous female urine from the same strain. Total sniffing time was recorded.

## 2.5. Paroxetine measurements

Mouse whole brains were homogenized in a fivefold volume of phosphate buffered saline containing protease inhibitor cocktail tablets (Roche, Penzberg, Germany) using a Dispomix Drive (Medic Tools AG, Zug, Switzerland). All samples were prepared using Ostro protein precipitation and phospholipid removal plates (Waters, Eschborn, Germany). Plasma and brain homogenates were analyzed by liquid chromatography-electrospray tandem mass spectrometry (LC-MS/MS) using an Agilent 1100 Series (Agilent, Waldbronn, Germany) liquid chromatograph interfaced with an Applied Biosystems API 4000 (ABSciex, Darmstadt, Germany) triple quadrupole mass spectrometer. Deuterated paroxetine (Paro-D6) was used as internal

standard. Five  $\mu\text{l}$  samples were loaded and gradient eluted from an Accucore RP-MS 2.6  $\mu\text{m}$  column (2.1 x 50 mm, Thermo Scientific, Dreieich, Germany) at a flow rate of 0.3 ml/min and 30°C (eluent A: methanol, 10 mM ammonium formate, 0.1% formic acid eluent B: 10 mM ammonium formate, 0.1% formic acid). Gradient: 0-0.5 min 20% A, 0.5-2 min 20- 90% A, 1 min held at 90% A, 3-3.5 min 90-20% A and 3.5-8 min 20% A. The ion source was operated in positive mode at 500°C and multiple reaction monitoring collision-induced dissociation was performed using nitrogen collision gas. The collision energy was set to 29 V for paroxetine and 33 V for Paro-D6. The transitions monitored during analysis were  $m/z$  330  $\rightarrow$  192 for paroxetine and  $m/z$  336  $\rightarrow$  198 for Paro-D6.

## 2.6. Omics analyses

### 2.6.1. Proteomics analysis

Mouse hippocampus was homogenized in a buffer containing 2M NaCl, 10mM HEPES/NaOH, 1mM EDTA and protease inhibitor cocktail tablets (Roche Diagnostics, Mannheim, Germany) and phosphatase inhibitors (Sigma, St. Louis, MO, USA). Homogenates were sonicated with an ultra-sonicator (Branson, Danbury, CT, USA) and centrifuged (16100g, 20 min, 4°C). The protein concentration was quantified by Bradford assay.

Protein extracts were mixed with equal amounts of  $^{15}\text{N}$ -labeled DBA/2 mouse hippocampal protein extract (Sato et al., 2012; Shah et al., 2012; Inoue et al., 2013). Forty  $\mu\text{g}$  of  $^{14}\text{N}$ -  $^{15}\text{N}$  hippocampal protein mixture was separated in a 10% SDS-PAGE gel and stained with Coomassie Brilliant Blue R-250 (BioRad, Hercules, CA, USA) overnight. After destaining and cutting the gel lane into slices, gel bands were further destained 3 times with 25 mM  $\text{NH}_4\text{HCO}_3$ /50% acetonitrile (Merck, Darmstadt, Germany). The gel slices were then reduced with 10 mM dithiothreitol (BioRad, Hercules, CA, USA) for 30 min at 56°C and carboxyaminomethylated with 50 mM iodoacetamide (Biorad, Hercules, CA, USA) for 30 min at room temperature, followed by additional twice of washing with with 25 mM  $\text{NH}_4\text{HCO}_3$ /50% acetonitrile. The gel slices were subjected to tryptic digestion to produce peptides (overnight, 37°C). Tryptic peptides were extracted with 2% formic acid/50%

acetonitrile (Merck, Darmstadt, Germany) with shaking. The peptides were lyophilized and dissolved in 1% formic acid (Merck, Darmstadt, Germany). The extracted peptides were analyzed by LC-MS/MS using a nanoflow HPLC-2D system (Eksigent, Dublin, California) coupled online to an LTQ-Orbitrap mass spectrometer (Thermo Fisher Scientific, Bremen, Germany). Proteins were identified by Sequest (Thermo Fischer, Scientific, Bremen, Germany) search using a decoy Uniprot mouse protein  $^{14}\text{N}$  and  $^{15}\text{N}$  database. Peptide search results were filtered and combined with the help of Trans-Proteomic Pipeline (TPP). Based on protein group detection data from TPP, protein quantitation was carried out using ProRata software (version 1.0).

### 2.6.2. Metabolomics analysis

A 30-fold excess (w/v) of 80% cold methanol was added to the hippocampus and prefrontal cortex. Brain tissues were homogenized ( $1200\text{ min}^{-1}$ , 2 min, Potter-S homogenizer, Sartorius, Göttingen, Germany) on ice and centrifuged (14000g, 10 min,  $4^{\circ}\text{C}$ ). Supernatants were transferred and a 6-fold excess (w/v) of 80% cold methanol was added to the pellets. Pellets were sonicated to further extract metabolites and combined with the previous supernatants. Combined samples were vortexed, centrifuged (14000g, 10 min,  $4^{\circ}\text{C}$ ) and lyophilized.

Mouse plasma metabolites were extracted with a 4-fold excess (v/v) of 100% cold methanol. After vortexing for 2 min, samples were incubated on dry ice for 2 h and centrifuged (2053 g, 10 min,  $4^{\circ}\text{C}$ ). Supernatants were filtered using a  $0.22\text{ }\mu\text{m}$  ultrafiltration tube (1105g, 2 min,  $4^{\circ}\text{C}$ ) and the filtrates were lyophilized. The lyophilized metabolites were stored at  $-80^{\circ}\text{C}$  until further use. Samples were dissolved in  $20\text{ }\mu\text{l}$  liquid chromatography-mass spectrometry grade water. Ten microliters were injected and analyzed using a 5500 QTRAP triple quadrupole mass spectrometer (AB/SCIEX, Framingham, MA, USA) coupled to a Prominence UFLC high-performance liquid chromatography system (Shimadzu, Columbia, MD, USA) via selected reaction monitoring of a total of 280 endogenous water-soluble metabolites for steady-state analyses of samples. Samples were delivered to the mass spectrometer via normal phase chromatography using a  $4.6\text{-mm i.d} \times 10\text{ cm}$  Amide Xbridge HILIC column (Waters, Milford, MA, USA) at  $350\text{ }\mu\text{l min}^{-1}$ . Gradients were run starting from 85% buffer B (high-performance liquid chromatography grade acetonitrile) to 42% B from 0 to 5 min 42% B to 0% B from 5 to 16 min 0% B was

held from 16 to 24 min 0% B to 85% B from 24 to 25 min 85% B was held for 7 min to re-equilibrate the column. Buffer A comprised 20mM ammonium hydroxide/20mM ammonium acetate (pH = 9.0) in 95:5 water:acetonitrile. Some metabolites were targeted in both positive and negative ion modes for a total of 291 selected reaction monitoring transitions using positive/negative polarity switching. Electrospray ionization voltage was +4900 V in positive ion mode and – 4500 V in negative ion mode. The dwell time was 4ms per selected reaction monitoring transition and the total cycle time was 1.89 s. Approximately 9–12 data points were acquired per detected metabolite. Peak areas from the total ion current for each metabolite-selected reaction monitoring transition were integrated using the MultiQuant v2.0 software (AB/SCIEX). Animals from the same cohort were used for all metabolomics analyses. Animals from the same cohort were used for all metabolomics analyses.

## 2.7. Molecular techniques

### 2.7.1. qRT-PCR

Hippocampal total RNA was isolated with TRIzol reagent (Invitrogen, Karlsruhe, Germany) as previously described (Schmidt et al., 2010). RNA levels were quantified using NanoPhotometer (IMPLEN, Munich, Germany). One ug of RNA was subjected to reverse transcription using Omniscript RT kit according to manufacturer's protocol (Quiagen, Santa Clarita, CA, USA). QuantFast SYBR Green PCR kit (Quiagen, Santa Clarita, CA, USA) was used for Quantitative Reverse Transcription Polymerase Chain Reaction (qRT-PCR). The reaction was performed using LightCycler 480 (Roche Diagnostics, Penzberg, Germany). The cycling condition used was as follows: denaturation step at 95°C for 10min, followed by 45 cycles of amplification step (95°C for 10sec, 60°C for 30sec, for each cycle). Each set of primer was used for detection of glyceraldehyde-3-phosphate dehydrogenase (GAPDH), nNOS, NR1, NR2A, NR2B and PSD95 (Eurofins MWG Operon, Ebersberg, Germany) (Table 1). Each sample was analyzed in duplicate and normalized with GAPDH level. Relative quantitation was performed based on crossing points value (Pfaffl, 2001).

Gene	Primer sequence (5' to 3')
NR1	Forward: CTGCGACCCCAAGATTGTCAA
	Reverse: TATTGGCCTGGTTTACTGCCT
NR2A	Forward: ACGTGACAGAACGCGAACTT
	Reverse: TCAGTGCGGTTTCATCAATAACG
NR2B	Forward: CAGCAAAGCTCGTTCCCAAAA
	Reverse: GTCAGTCTCGTTCATGGCTAC
PSD-95	Forward: TCCGGGAGGTGACCCATTC
	Reverse: TTTCCGGCGCATGACGTAG
nNOS	Forward: AGCTCCTGGAACGACTACCTG
	Reverse: CCGGCACACAGCTCTAGTG
GAPDH	Forward: AACTTTGGCATTGTGGAAGG
	Reverse: GGATGCAGGGATGATGTT

**Table 1.** List of primers used for qRT-PCR analysis.

### 2.7.2. Immunoprecipitation

Hippocampal proteins were extracted and immunoprecipitated using Pierce Direct IP kit (Thermo Fisher Scientific, Rockford, IL, USA). Mouse hippocampus was homogenized with IP lysis/wash buffer containing 2% SDS (Sigma, St. Louis, MO, USA), protease inhibitor cocktail tablets (Roche Diagnostics, Mannheim, Germany) and phosphatase inhibitors (Sigma, St. Louis, MO, USA). Lowry assay was performed to measure protein concentration with DC Protein Assay kit (Bio-Rad Laboratories, Munich, Germany). 10ug of Ub antibody (Santa Cruz, Dallas, TX, USA) was covalently bound to the resin according to manufacturer's protocol. 500ug of hippocampal lysates were boiled (95°C, 10 min) and diluted with 5 volumes of IP lysis/wash buffer containing 2% Triton X-100, protease inhibitor cocktail tablets (Roche Diagnostics, Mannheim, Germany) and phosphatase inhibitors (Sigma, St. Louis, MO, USA). The lysates were incubated with Ub antibody-coupled resin (4°C, overnight). The resin was washed three times with IP lysis/wash buffer and was boiled with 1×SDS loading buffer for elution (95°C, 10 min). Immunoprecipitates were separated in a 10% SDS-PAGE gel, and Western blot analysis was performed with NR1, NR2A and PSD-95 antibodies. Ubiquitinated protein levels were normalized by total ubiquitination intensity.

### 2.7.3. Western blot analysis

Mouse hippocampus, prefrontal cortex and erythrocytes were homogenized with the same buffer used for proteomics sample preparation, or RIPA buffer containing protease inhibitor cocktail tablets (Roche Diagnostics, Mannheim, Germany) and phosphatase inhibitors (Sigma, St. Louis, MO, USA). Patient PBMCs were homogenized with RIPA buffer containing protease and phosphatase inhibitors. Homogenates were sonicated and centrifuged (16100g, 20 min, 4°C). Bradford assay was used to quantify extracted protein concentration. Proteins were separated in 10-15% gradient SDS-PAGE gels. Subsequently, they were transferred to a PVDF membrane (Millipore, Billerica, MA, USA). After blotting, the membrane was blocked with 5% skim milk solution for 1 h at room temperature and incubated with  $\beta$ -actin (1:4000, Sigma, St. Louis, MO, USA), aminoimidazole-4-carboxamide ribonucleotide transformylase/IMP cyclohydrolase (ATIC) (1:500, Santa Cruz, Dallas, TX, USA),  $\text{Ca}^{2+}$ /calmodulin-dependent protein kinase (CaMK) II (1:2000, Abcam, Cambridge, UK), carboxy-terminal PDZ ligand of *nNOS* (CAPON) (1:500, Santa Cruz, Dallas, TX, USA), carbamoyl phosphate synthase 2 (CPS2) (1:500, Santa Cruz, Dallas, TX, USA), extracellular signal-regulated kinase (ERK) (1:1000, Cell Signaling, Danvers, MA, USA), glutamate dehydrogenase 1 (GDH1) (1:1000, Aviva System Biology, San Diego, CA, USA), glutamine synthetase (GS) (1:1000, Sigma, St. Louis, MO, USA), glycogen synthase kinase-3 $\beta$  (GSK-3 $\beta$ ) (1:1000, Cell Signaling, Danvers, MA, USA), soluble guanylate cyclase- $\beta$ 1 (sGC- $\beta$ 1) (1:500, Santa Cruz, Dallas, TX, USA), hypoxanthine-guanine phosphoribosyltransferase (HPRT) (1:500, Sigma, St. Louis, MO, USA), mitochondrial aspartate transaminase (mAST) (1:500, Sigma, St. Louis, MO, USA), mitogen-activated protein kinase kinase (MEK) (1:1000, Cell Signaling, Danvers, MA, USA), neuronal nitric oxide synthase (nNOS) (1:1000, Cell Signaling, Danvers, MA, USA), N-Methyl-D-aspartate (NMDA) receptor subunit (NR) 1 (1:500, Santa Cruz, Dallas, TX, USA), NR2A (1:500, Santa Cruz, Dallas, TX, USA), NR2B (1:500, Santa Cruz, Dallas, TX, USA), phospho-CaMKII (P-CaMKII) (1:1000, Cell Signaling, Danvers, MA, USA), phospho-ERK (P-ERK) (1:1000, Cell Signaling, Danvers, MA, USA), phospho-GSK-3 $\beta$  (Ser9) (P-GSK-3 $\beta$ ) (1:1000, Cell Signaling, Danvers, MA, USA), phospho-MEK (P-MEK) (1:1000, Cell Signaling, Danvers, MA, USA), phospho-NR1 (P-NR1) (1:500, Santa Cruz, Dallas, TX, USA), phospho-NR2A (P-NR2A) (1:500, Santa Cruz, Dallas, TX, USA), phospho-NR2B (P-NR2B)

(1:500, Santa Cruz, Dallas, TX, USA), postsynaptic density protein 95 (PSD-95) (1:1000, GeneTex, Irvine, CA, USA), proteasome subunit  $\alpha$  type-2 (PMSA2), synapsin (1:1000, Cell Signaling, Danvers, MA, USA), synaptic vesicle glycoprotein 2A (SV2A), synaptojanin 1 (SYNJ1), syntaxin binding protein1 (STXBP1) or ubiquitin (Ub) (1:500, Santa Cruz, Dallas, TX, USA) antibody at 4°C overnight. PMSA2, SYNJ1, STXBP1 and SV2A antibodies were provided by the Human Protein Atlas (HPA) program (Albanova University Center, Royal Institute of Technology, Sweden).

The membranes were washed and then incubated with horseradish peroxidase (HRP) conjugated-secondary antibodies. The blots were developed with Luminata<sup>TM</sup> Forte Western HRP Substrate (Millipore, Billerica, MA, USA). Images were acquired by ChemiDoc<sup>TM</sup> MP imaging system (Bio-Rad Laboratories, Munich, Germany). Densitometric data analyses were carried out with ImageJ software (National Institute of Health, USA).

## 2.8. Patient samples

For *in vivo* and *ex vivo* studies, two distinct PBMC batches from different individuals were chosen. PBMCs obtained from 17 participants of the Munich Antidepressant Response Signature (MARS) study were included for assessing protein expression levels (Table 2). PBMCs from 32 individuals were subjected to *ex vivo* cultivation and paroxetine treatment (Table 3). Diagnosis was conducted according to DSM-IV criteria, and all participants were diagnosed as having MDD. Depression severity was evaluated using the 21-item Hamilton Depression Rating Scale (HDRS). Responder and non-responder patients were classified based on clinical antidepressant treatment response corresponding to minimal 50% reduction in HDRS score between baseline (T0) and after 6 weeks of admission (T6). The Munich Antidepressant Response Signature (MARS) project was approved by the ethics committee of the Medical Faculty at *Ludwig Maximilians University* of Munich, Germany (submission number 318/00). Participants included in the study gave oral and written consents after receiving a complete description of the study.

Characteristic	Responders	Non-responders	Statistics
	Mean ( $\pm$ SD)	Mean ( $\pm$ SD)	
Age	49 (14)	49 (11.6)	$p = 0.58$
Males/Females	6/4	3/4	$\chi^2 = 0.4857, p = 0.49$
HDRS at admittance	23.8 (5.7)	22.5 (4.2)	$p = 0.35$
HDRS at T6	7 (3.6)	17.1 (4.2)	$p = 2.0 \times E^4$

HDRS, Hamilton Depression Rating Score  
T6, after six weeks of admission

**Table 2.** Demographic features of antidepressant treatment responder and non-responder patients.

Characteristic	Responders	Non-responders	Statistics
	Mean ( $\pm$ SD)	Mean ( $\pm$ SD)	
Age	47.1 (16.1)	51.5 (16.1)	$p = 1.0$
Males/Females	5/10	6/11	$\chi^2 = 0.136, p = 0.91$
HDRS at admittance	23.4 (5.3)	22.5 (4.2)	$p = 0.52$
HDRS at T6	4.6 (3.7)	18.9 (5.2)	$p < 0.0001$

HDRS, Hamilton Depression Rating Score  
T6, after six weeks of admission

**Table 3.** Demographic and clinical characteristics of antidepressant responders and non-responders included in *ex vivo* PBMCs cultivation and paroxetine treatment.

### 2.8.1. Paroxetine treatment of PBMCs

Blood of patients with MDD was collected between 08:00 and 09:00 h within 5 days after admittance. PBMCs were prepared as described previously (Gassen et al., 2014). Blood was collected from depression patients via venepuncture, and centrifuged (800g, 20 min) to separate PBMCs. Using Biocoll separating solution, PBMCs were enriched and washed with ice-cold PBS. PBMCs were plated at  $4 \times 10^5$  cells/cm<sup>2</sup>. After 6 hours, cells were treated with 120ng/ml paroxetine for 2 days according to the consensus guidelines for therapeutic drug monitoring in psychiatry (Lotrich and Pollock, 2005; Hiemke et al., 2011).

### 2.8.2. Protein level quantitation in cultivated PBMCs

In *ex vivo* cultivated PBMCs, ATIC, CPS2, HPRT and  $\beta$ -actin protein levels were detected and quantitated with an automated capillary immunoassay system, Simple Western<sup>TM</sup> (ProteinSimple, Santa Clara, CA, USA). PBMCs lysates were prepared according to manufacturer's instruction. Fluorescent master mix was prepared with 400mM DTT, 5 $\times$  fluorescent master mix solution and biotinylated protein ladder. Protein lysates were incubated with master mix solution and denatured at 95°C for 5 min. Protein samples, primary and secondary antibodies were loaded on 96 well plate. All following steps were fully automated. Protein levels were quantified using antibodies for  $\beta$ -actin (1:150, Sigma, St.Louis, MO, USA), ATIC (1:25, Santa Cruz, Dallas, TX, USA) and CPS2 (1:50, Santa Cruz, Dallas, TX, USA). Protein quantitation data were normalized with  $\beta$ -actin. Quantitative analysis was performed using Compass software (ProteinSimple, Santa Clara, CA, USA).

## 2.9. Statistical Analysis

Hierarchical clustering analysis (HCA) was performed to separate paroxetine-treated sub-groups of mice, using SPSS (SPSS version 21, IBM SPSS Inc., Chicago, IL, USA). Statistical analysis of behavioral data (FST and FUST) and covariates were performed with GraphPad Prism 5 (GraphPad Software, Inc., La Jolla, CA, USA). Student *t*-test, one-way or two-way ANOVA was used to evaluate statistical significance between groups. Pearson correlation coefficients (*r*) with *p* values were used to evaluate correlation between floating time and body weight gain. For the identification of significantly altered metabolites, metabolite peak intensities were median and auto-scaled normalized. Metabolites with missing values, 30 for the hippocampus and 27 for the prefrontal cortex in all replicates, were excluded from data analysis. Significant analysis of microarrays (and metabolites) (SAM) method was used to identify significantly altered metabolites ( $q < 0.05$ , FDR  $< 0.1$ ). Significantly altered metabolites were subjected to pathway enrichment analysis of MetaboAnalyst (<http://www.metaboanalyst.ca>) to identify differentially affected pathways between the PLF and PSF groups. Pathways with Holm adjusted  $p < 0.05$  and FDR  $< 0.05$  were considered significantly affected. To identify sub-pathways interacting with a differentially affected pathway between the PLF and PSF groups, correlates of each SAM signature were combined and used to enrich relevant

metabolic pathways using MetaboAnalyst (Pearson correlation coefficients ( $r$ )  $> 0.7$ , FDR  $< 0.1$ ). Pathways with Holm adjusted  $p < 0.05$  and FDR  $< 0.05$  were considered significant. Proteomics pathway enrichment was performed using DAVID bioinformatics resources 6.7 according to a Kyoto Encyclopedia of Genes and Genomes (KEGG) database (Huang et al., 2007). Enriched pathways were considered significant at Bonferroni adjusted  $p < 0.05$  and FDR  $< 0.01$ . Proteins common to several pathways were further extracted from the enriched pathways using a Venn diagram comparison. Protein interaction network was created using STRING database. Western blot data were analyzed with GraphPad Prism 5. Two-tailed  $t$ -test was used to evaluate the difference between the groups. Data were expressed as the mean  $\pm$  the standard error of the mean (SEM). Correlations between pathway protein levels and FST floating time/HDRS change were assessed using Pearson correlation coefficients ( $r$ ) with  $p$  values. Statistical data were considered significant at  $p < 0.05$ . D'Agostino & Pearson omnibus normality test was used to check normal distribution.

### 3. Results

Figure 5 shows a schematic overview of the workflow.

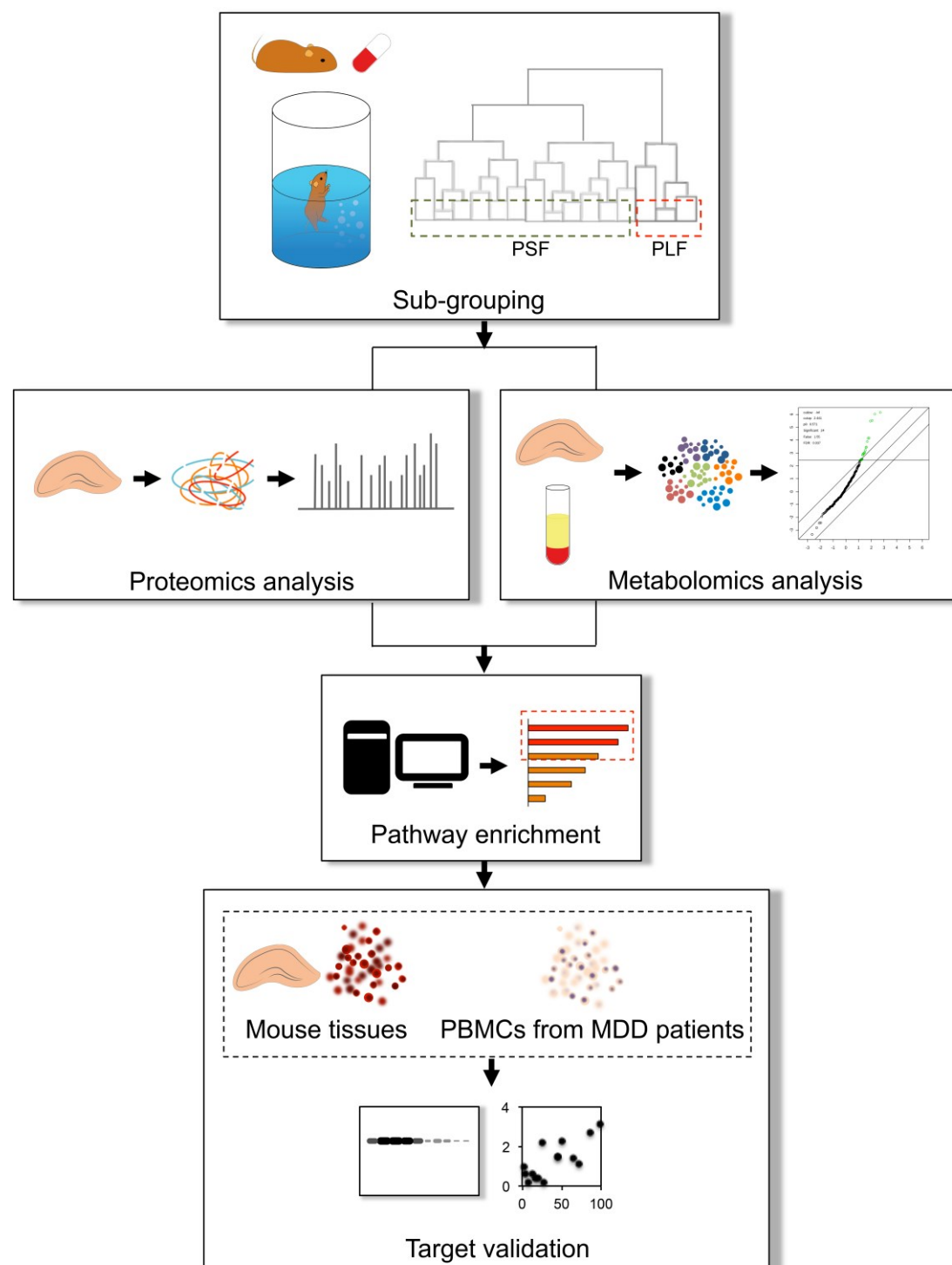


**Figure 5.** A schematic overview of the workflow.

### 3.1. Sub-grouping of paroxetine responder and non-responder mice

DBA/2J mice were administered with vehicle or paroxetine pills (2 x 5 mg/kg/day) for 28 days. The paroxetine-treated group (PAR) showed significantly reduced FST floating time compared to vehicle-treated (VEH) mice ( $t = 13.90$ ,  $df = 143$ ,  $p < 0.0001$ ) (Figure 6).

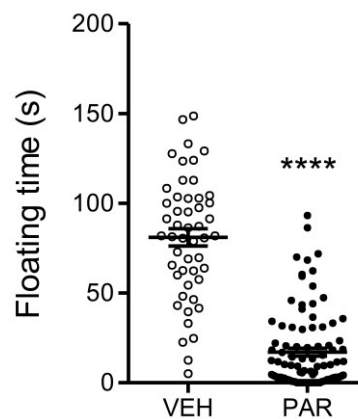


**Figure 6.** The effect of chronic paroxetine treatment on FST floating time. Male DBA/2J mice received paroxetine (5 mg/kg, twice a day, 28 days) and floating time was recorded for 6 min. PAR mice displayed significantly shorter floating time compared to vehicle-treated group (VEH).  $n(\text{VEH}/\text{PAR})=50/95$ . Data are expressed as mean  $\pm$  SEM. \*\*\*\*  $p < 0.0001$  (two-tailed  $t$ -test).

I was able to separate paroxetine-treated mice into long-time floating (PLF) and short-time floating (PSF) groups according to their FST floating time using hierarchical cluster analysis (HCA) ( $F = 159.5$ ,  $df = 144$ ,  $p < 0.001$ ) (Figure 7). PSF mice floating time was significantly lower than for VEH mice ( $p < 0.001$ ) while no floating time difference was observed between PLF and VEH mice. During the female urine sniffing test (FUST) PLF and PSF mice did not show differential sniffing time prior to paroxetine treatment ( $F_{(5,192)} = 104.5$ ,  $p > 0.05$ ) (Figure 8a). A slightly different sniffing time became apparent after 28 days of paroxetine treatment ( $p = 0.052$ ). The time for sniffing female urine was longer for PSF mice compared to VEH and PLF mice ( $F_{(5,192)} = 84.24$ ,  $df = 197$ ,  $p < 0.0001$ ) (Figure 8b). Two-way ANOVA identified no interaction between time points and treatment.

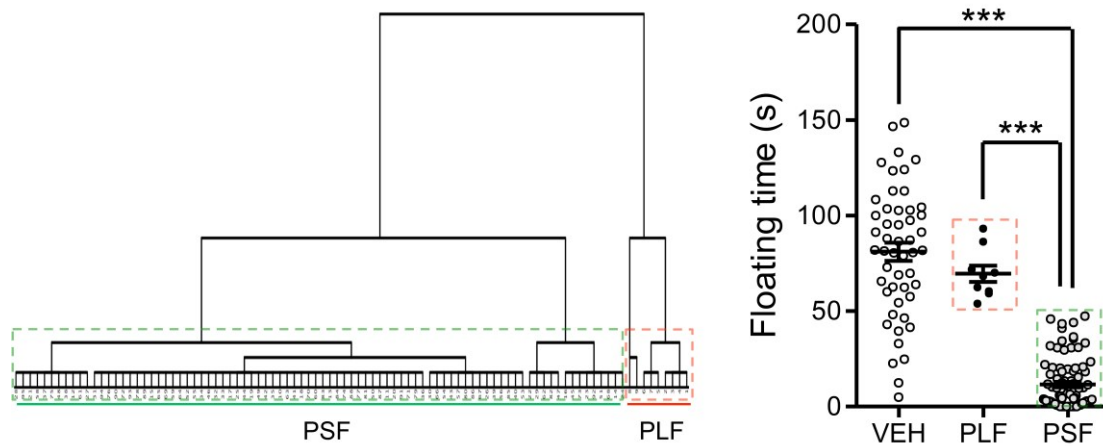


**Figure 7.** Sub-grouping of paroxetine-treated mice. Dendrogram of paroxetine-treated mice. Mice treated with paroxetine were separated into PLF and PSF groups using hierarchical clustering analysis (HCA).  $n(\text{VEH/PLF/PSF})=50/9/86$ . Data are expressed as mean  $\pm$  SEM. \*\*\* $p < 0.001$  (one-way ANOVA with Tukey's test for multiple comparisons).

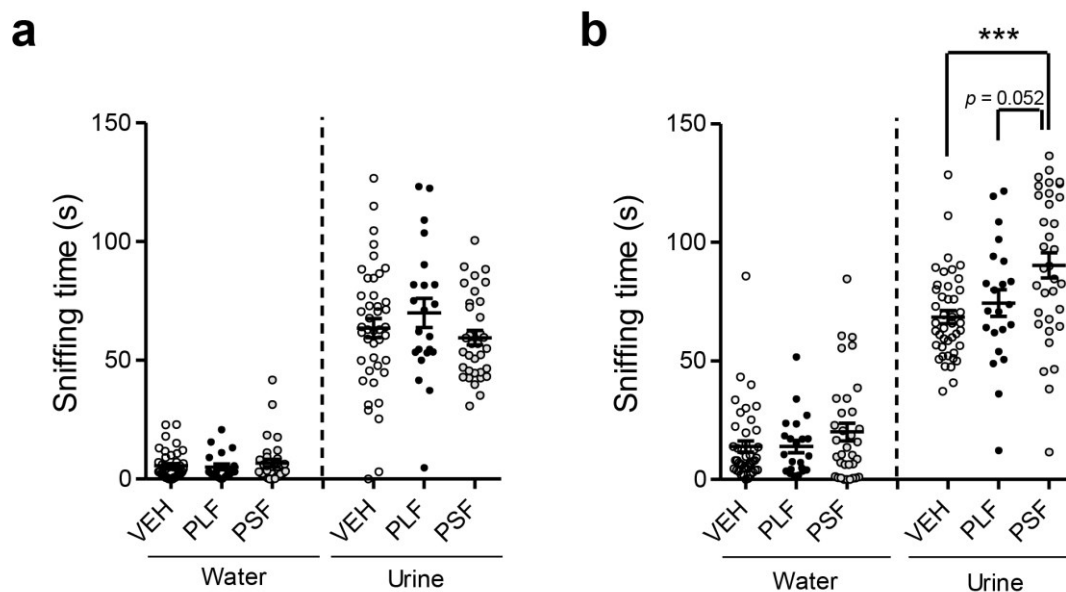


**Figure 8.** The effect of chronic paroxetine treatment on female urine sniffing test (FUST). The effect of chronic paroxetine treatment on female urine sniffing test (FUST). Sniffing time at (a) baseline and (b) after 28 days of paroxetine treatment. Chronic paroxetine treatment induced a slightly significant difference of sniffing time between paroxetine-treated long- time floating (PLF) and paroxetine-treated short-time floating (PSF) groups.  $n(\text{VEH/PLF/PSF}) = 43/22/34$ . \* $p < 0.05$  (two-tailed  $t$ -test), \*\*\* $p < 0.001$  (one-way ANOVA with Tukey's test for multiple comparisons).

### 3.2. Covariate analysis

Covariates that may be relevant for paroxetine treatment response were examined. Paroxetine concentrations in whole brain and plasma did not differ between groups ( $p > 0.05$ ) and did not correlate with FST floating time ( $r = 0.26$ ,  $p = 0.387$ ) (Figure 9a and b). I also analyzed mouse age and body weight gain. A significant age effect on FST floating time was not observed ( $F_{(4,81)} = 2.184$ ,  $p > 0.05$ ) (Figure 10).

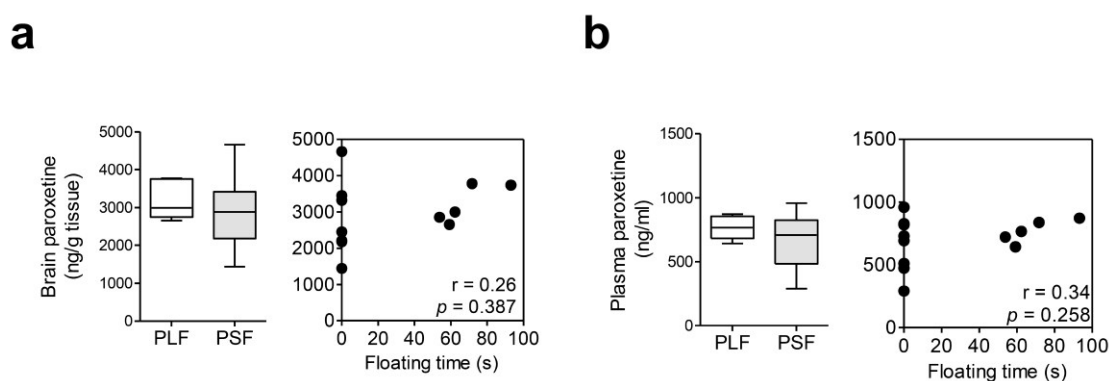


**Figure 9.** Paroxetine levels in (a) whole brain and (b) plasma. PLF and PSF groups did not show significant paroxetine level differences,  $n(\text{PLF/PSF})=5/8$ . Pearson correlation coefficients ( $r$ ) with  $P$  values are indicated in the correlation graphs.

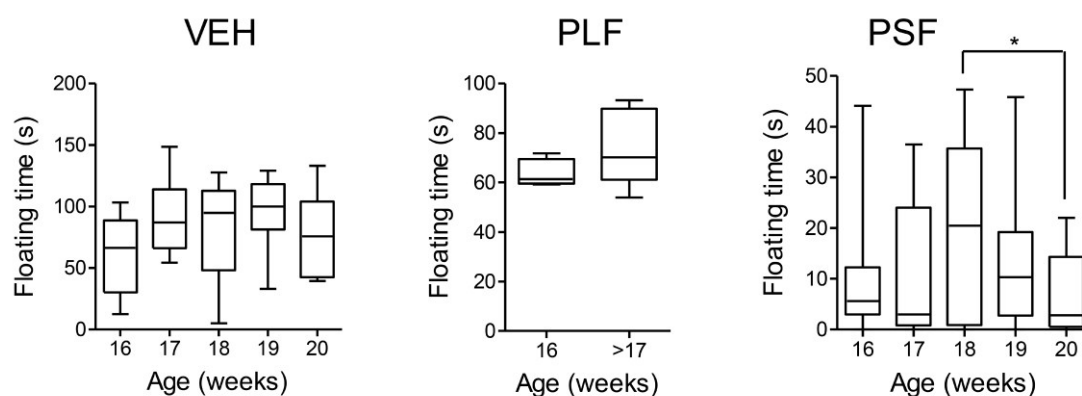


**Figure 10.** The effect of age on FST floating time,  $n(\text{VEH/PLF/PSF})=50/9/86$ .  $*p < 0.05$  (one-way ANOVA with Tukey's test for multiple comparisons).

Body weight gain did not vary between PLF and PSF mice. Both groups had a significantly higher body weight gain after chronic paroxetine treatment compared to VEH mice ( $F_{(2,42)} = 29.51$ ,  $p < 0.0001$ ). Correlation between body weight gain and FST floating time was not significant (VEH:  $r = -0.02$ ,  $p = 0.876$  PLF:  $r = -0.32$ ,  $p = 0.405$  PSF:  $r = -0.15$ ,  $p = 0.169$ ) (Figure 11).

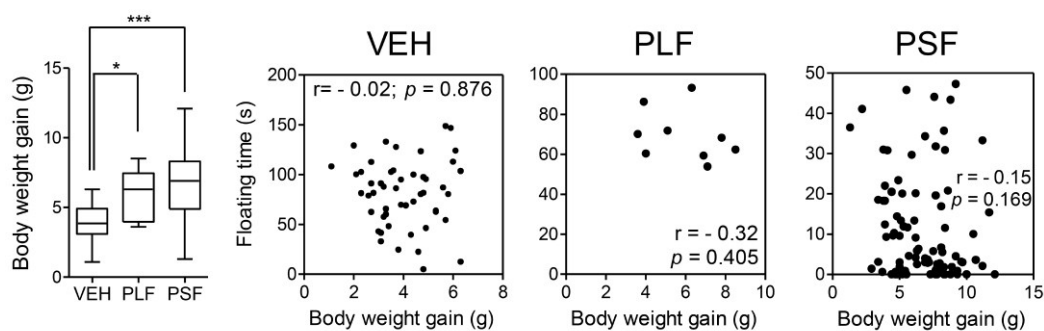


**Figure 11.** The effect of body weight gain on FST floating time,  $n(\text{VEH/PLF/PSF})=50/9/86$ . Data are expressed as the mean  $\pm$  SEM. \* $p < 0.05$ , \*\*\* $p < 0.001$  (one-way ANOVA with Tukey's test for multiple comparisons). Pearson correlation coefficients ( $r$ ) with  $P$  values are indicated in the correlation graphs.

### 3.3. Identification of purine and pyrimidine metabolism

After clustering paroxetine-treated mice into long-floating and short-floating groups, I performed metabolomics and proteomics analyses of the hippocampus. Both -omics analyses showed purine/pyrimidine metabolites and proteins with significant differences between the two groups ( $\log_2|\text{FC}| > 0.3$ ,  $-\log_{10}(p \text{ value}) > 1.3$ ) (Figure 12).

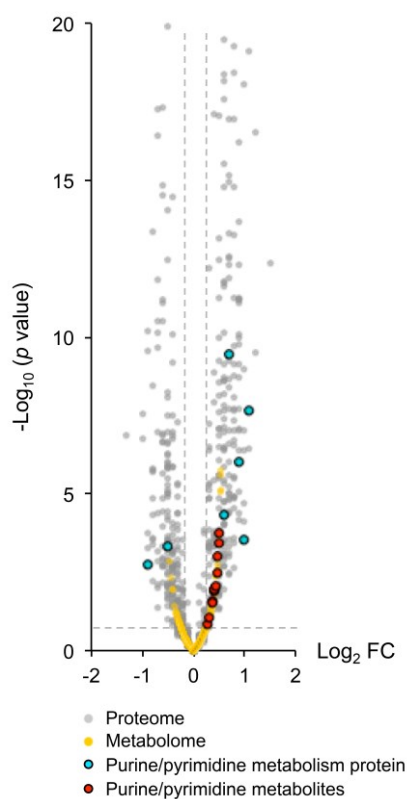


**Figure 12.** A volcano plot of hippocampal metabolome and proteome. Metabolites and proteins with  $\log_2|\text{FC}| > 0.3$  and  $-\log_{10}(p \text{ value}) > 1.3$  were considered significant. Purine/pyrimidine

metabolites and metabolism-related proteins were found to be significantly different between the sub-groups,  $n=3-5$ /group.

In metabolomics analysis, significant analysis of microarrays (and metabolites) (SAM) and SAM-driven correlation analysis revealed that chronic paroxetine treatment differentially affected the hippocampal metabolome of the PLF and PSF mice (Figure 13).

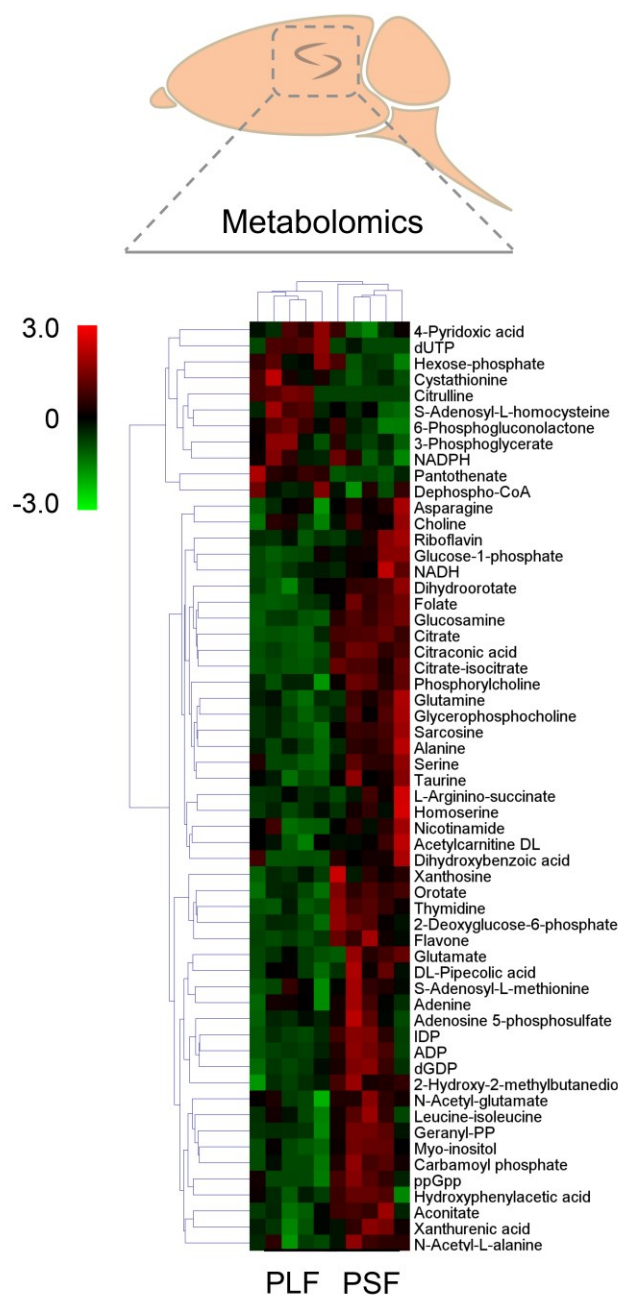


**Figure 13.** A heat map with combined profiles of SAM signatures ( $q < 0.05$ ,  $FDR < 0.1$ ) and their significant correlates ( $r > 0.7$ ,  $p < 0.05$ ). Heat map colors denote normalized metabolite intensity,  $n=5$ /group.

Sixteen metabolites were differentially regulated showing significantly higher levels in PSF compared to PLF mice ( $q < 0.05$ ,  $FDR < 0.1$ ). In addition, I found significant correlations with 42 other hippocampal metabolites ( $r > 0.7$ ,  $FDR < 0.1$ ) (Figure 14).

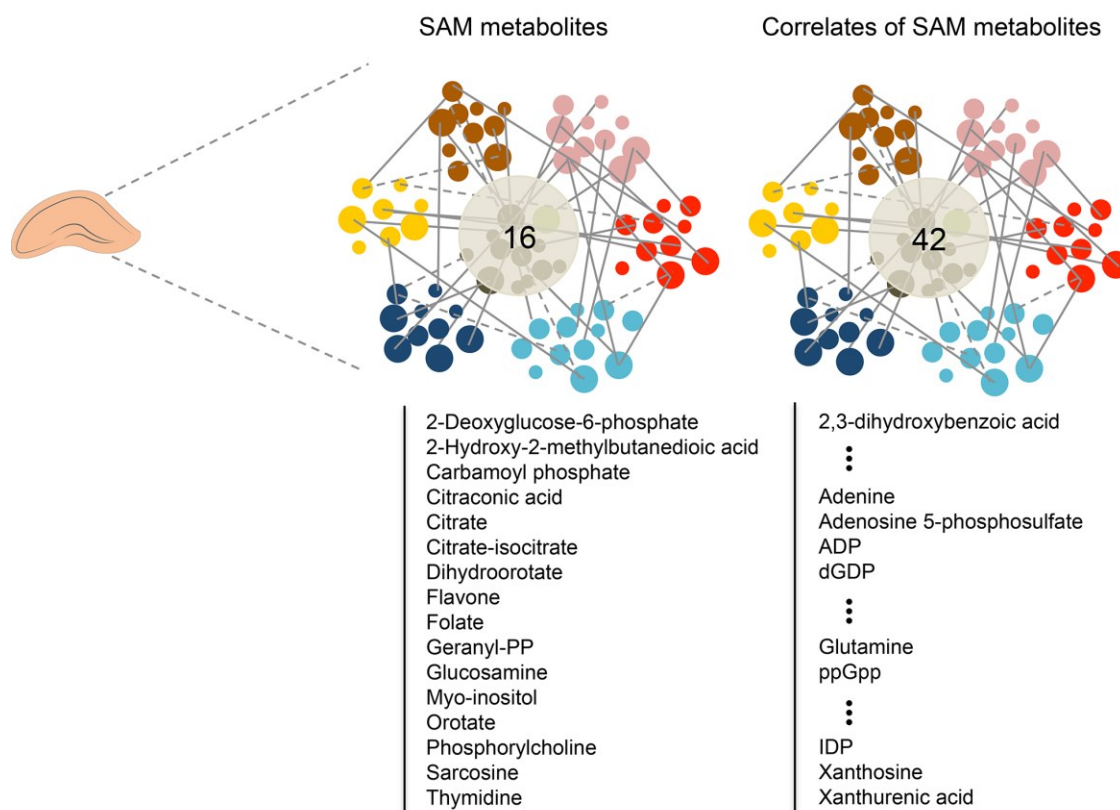


**Figure 14.** Hippocampal SAM metabolites ( $q < 0.05$ ,  $FDR < 0.1$ ) and their significant correlates ( $r > 0.7$ ,  $p < 0.05$ )

In proteomics analysis, I found that purine/pyrimidine metabolism proteins including S-adenosyl-L-homocysteine hydrolase (AdoHcyase), S-adenosyl-L-homocysteine hydrolase 2 (AdoHcyase 2), guanine deaminase (GDA), inosine triphosphate pyrophosphatase (ITPase), purine nucleoside phosphorylase (PNP) and UMP-CMP kinase (UMP/CMPK) were differentially expressed between the PLF and PSF groups (Figure 15).

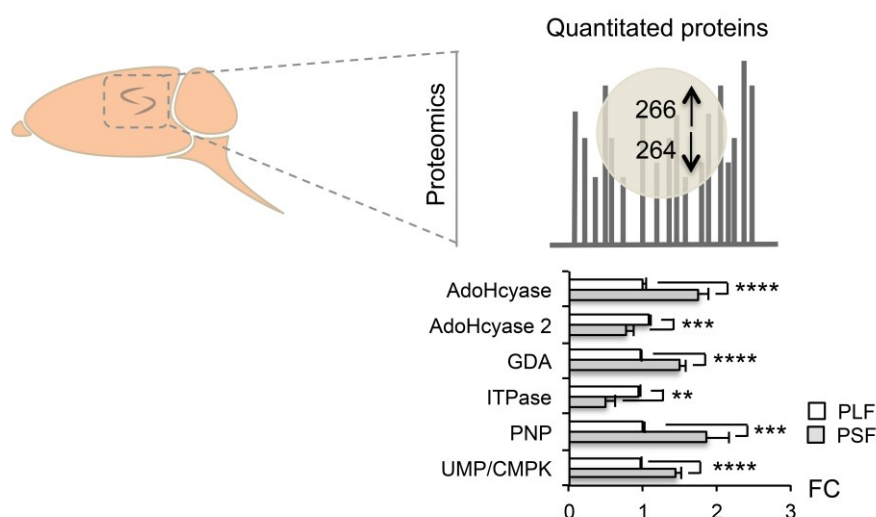


**Figure 15.** Identification of purine and pyrimidine metabolism pathway proteins in proteomics analysis. 266 and 264 proteins were found to be up- and down-regulated between PLF and PSF mice. Purine and pyrimidine metabolisms protein levels were significantly different between the PLF and PSF mice ( $p < 0.05$ ),  $n=3/\text{group}$ . Data are expressed as the mean  $\pm$  SEM. \*\* $p < 0.01$ , \*\*\* $p < 0.001$ , \*\*\*\* $p < 0.0001$  (two-tailed  $t$ -test).

The pyrimidine metabolism pathway was enriched with four metabolites from hippocampal SAM analysis (carbamoyl phosphate, dihydroorotate, orotate and thymidine). Eight correlates of SAM signatures (adenine, adenosine 5-phosphosulfate, ADP, dGDP, glutamine, IDP, ppGpp, xanthosine) enriched the purine metabolism pathway (Holm adjusted  $p < 0.05$ , FDR  $< 0.05$ ) (Figure 16).

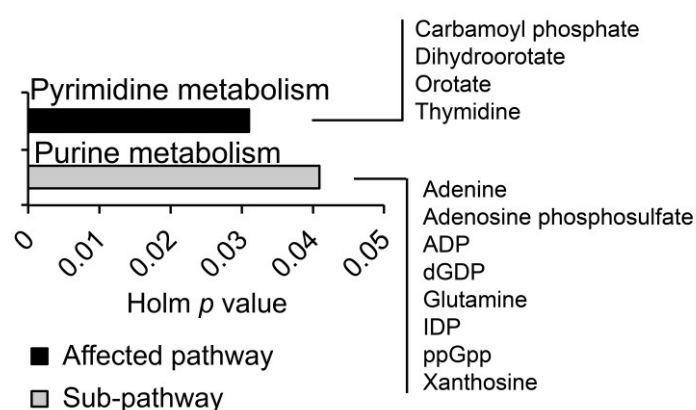


**Figure 16.** Metabolic pathway analysis in the hippocampus. Metabolomics analysis identified purine and pyrimidine metabolisms as sub-pathway and affected pathway, respectively (Holm adjusted  $p < 0.05$ , FDR  $< 0.05$ ).

Average levels of purine and pyrimidine metabolites were significantly higher in PSF than PLF mice and were strongly correlated with FST floating time (Figures 17a and b).

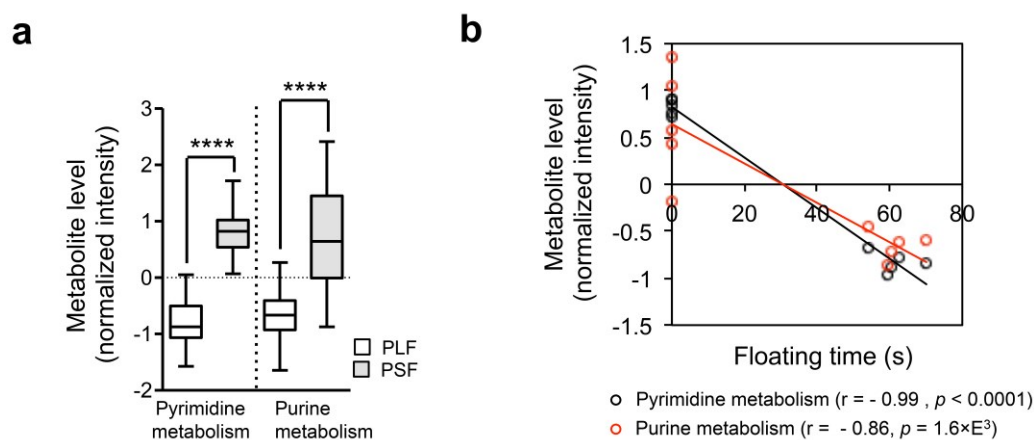


**Figure 17.** Purine and pyrimidine metabolite average levels and correlation with FST floating time. **(a)** Average level difference of purine and pyrimidine metabolites between PLF and PSF group was shown by box plots with whiskers min to max. **(b)** Average purine and pyrimidine pathways metabolite levels were strongly correlated with FST floating time. Data are expressed as the mean  $\pm$  SEM. \*\*\*\* $p < 0.0001$  (two-tailed  $t$ -test). Pearson correlation coefficients ( $r$ ) with  $p$  values are indicated under the correlation graphs.

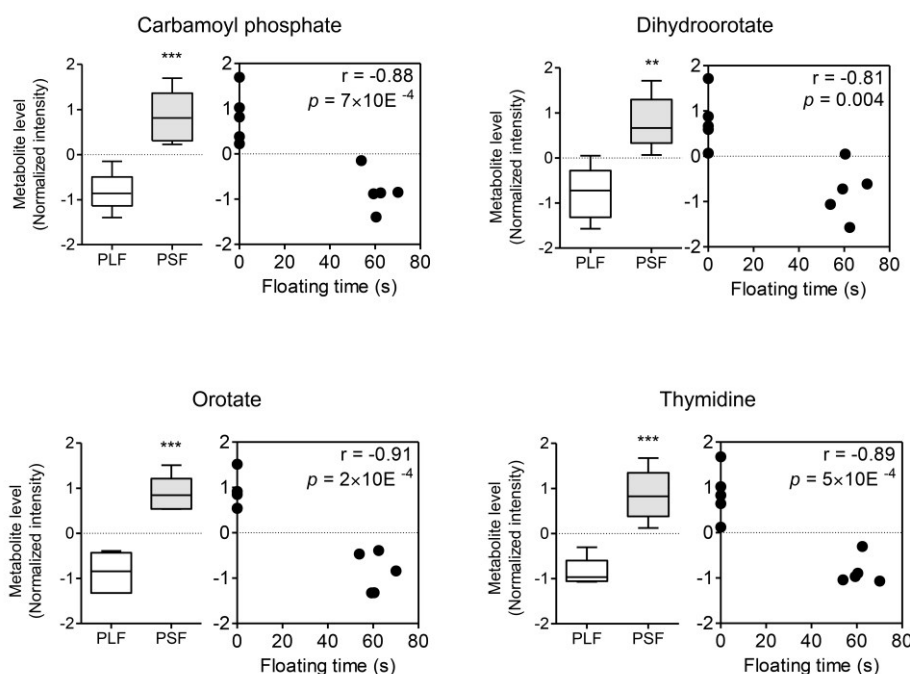


**Figure 18.** Levels of hippocampal metabolites that are part of pyrimidine metabolism pathway and correlation with FST floating time.  $n = 5$ /group. Bars represent mean  $\pm$  SEM. \*\* $p < 0.01$ , \*\*\* $p < 0.001$  vs PLF (two-tailed  $t$ -test). Pearson correlation coefficients ( $r$ ) with  $p$  values are indicated in the correlation graphs.

Purine and pyrimidine metabolite levels were higher in the PSF compared to PLF groups and with the exception of adenine and adenosine phosphosulfate showed a significant negative-correlation with FST floating time (Figures 18 and 19). Metabolomics analysis of the prefrontal cortex did not result in any metabolite and pathway differences distinguishing the PLF and PSF groups.

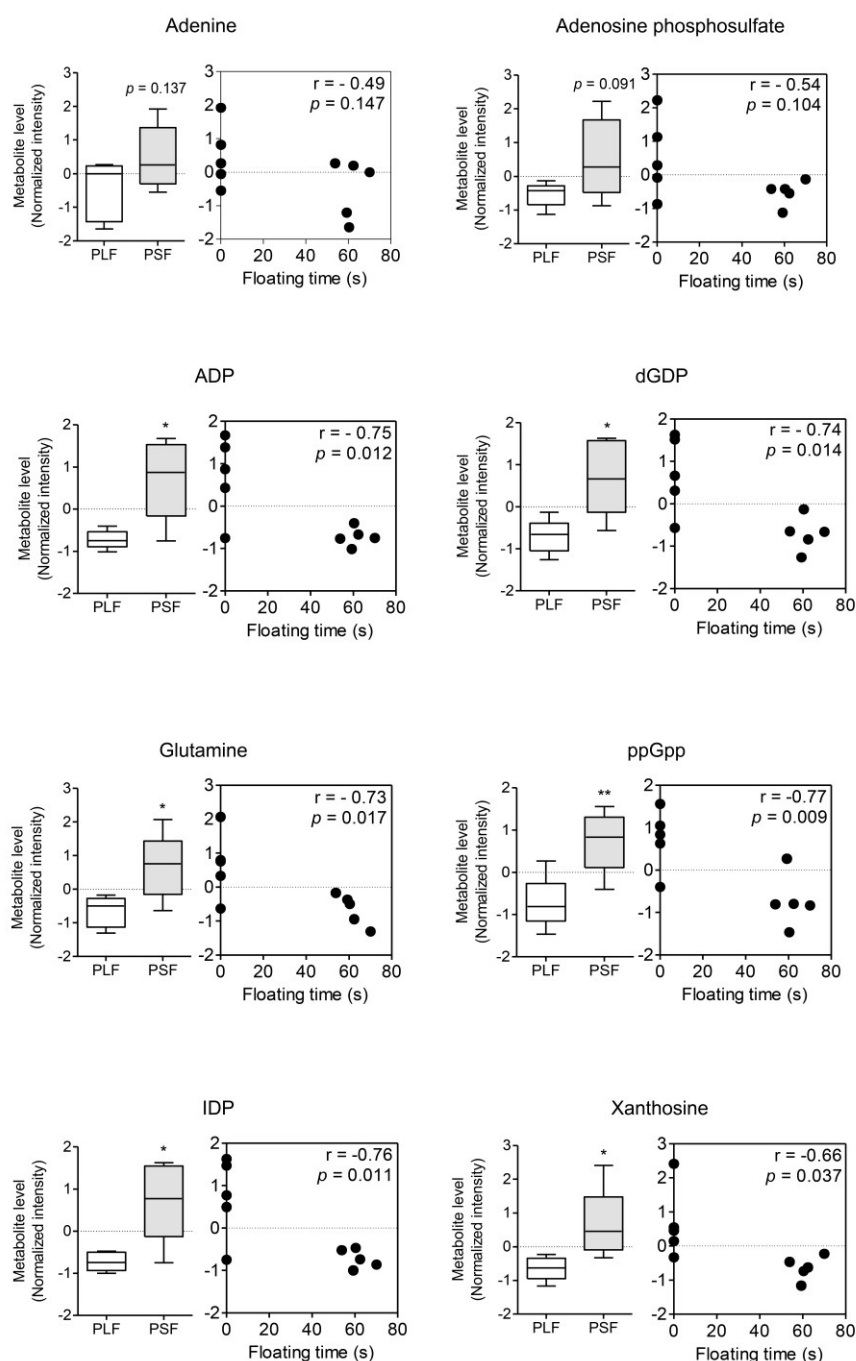


**Figure 19.** Levels of hippocampal metabolites that are part of purine metabolism pathway and correlation with FST floating time.  $n = 5/\text{group}$ . Bars represent mean  $\pm$  SEM. \* $p < 0.05$ , \*\* $p < 0.01$  vs

PLF (two-tailed *t*-test). Pearson correlation coefficients (*r*) with *p* values are indicated in the correlation graphs.

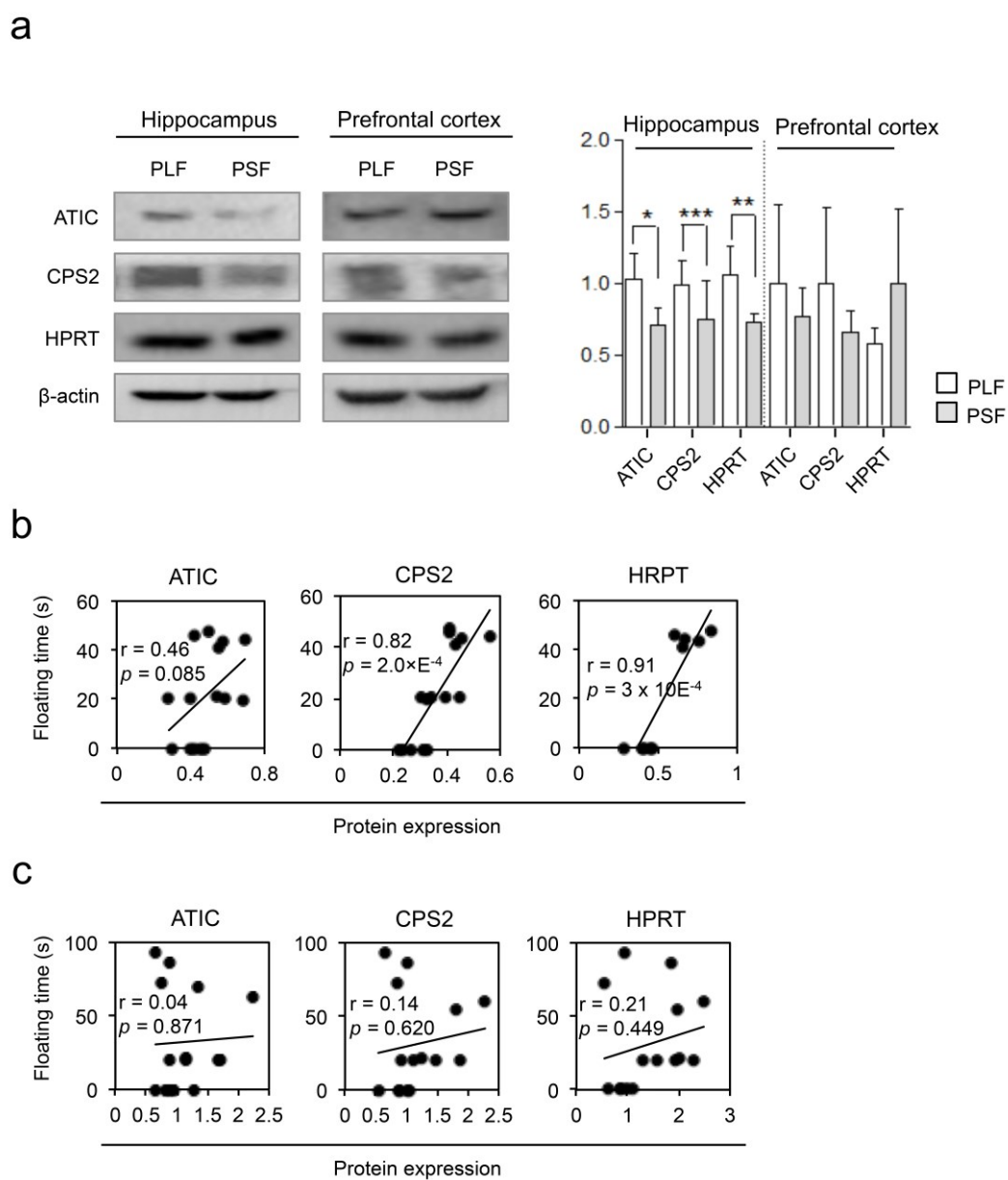


**Figure 20.** The effect of chronic paroxetine treatment on ATIC, CPS2 and HPRT protein expressions in the mouse hippocampus and prefrontal cortex. **(a)** Western blot and densitometry analyses of the pathway protein levels in the hippocampus and prefrontal cortex. Hippocampal ATIC, CPS2 and HPRT proteins showed significant expression level differences between the PLF and PSF groups,  $n=5/\text{group}$ . **(b)** Correlation of hippocampal CPS2 and HPRT protein levels with FST floating time was significant in the hippocampus. ATIC protein level showed moderate correlation with FST floating time.  $n=15$ . **(c)** Correlation of FST floating time with the pathway protein levels in the prefrontal cortex. None of the pathway protein showed significant correlation with FST floating time.  $n=15$ . Protein expression levels were normalized with  $\beta$ -actin. Data are expressed as the mean  $\pm$  SEM. \* $p < 0.05$ , \*\* $p < 0.01$ , \*\*\* $p < 0.001$  (two-

tailed *t*-test). Pearson correlation coefficients (*r*) with *p* values are indicated in the correlation graphs.

Aminoimidazole-4-carboxamide ribonucleotide transformylase/IMP cyclohydrolase (ATIC), carbamoyl phosphate synthase 2 (CPS2) and hypoxanthine-guanine phosphoribosyltransferase (HPRT) protein expression in the hippocampus and prefrontal cortex were assessed to validate differentially affected pathways between the PLF and PSF groups (Figure 20a). In the hippocampus, ATIC, CPS2 and HPRT protein levels showed significant differences between groups. Compared to the PLF group the PSF group had significantly reduced ATIC, CPS2 and HPRT protein expression levels (ATIC:  $t = 3.304$ ,  $df = 8$ ,  $p < 0.05$ , CPS2:  $t = 1.702$ ,  $df = 8$ ,  $p < 0.001$ , HPRT:  $t = 3.488$ ,  $df = 8$ ,  $p < 0.01$ ). In the prefrontal cortex protein expression showed no difference between the two groups. FST floating time significantly correlated with CPS2 and HPRT protein expression levels in the hippocampus, but not in the prefrontal cortex. Correlation between FST floating time and ATIC protein levels also showed strong tendency in the hippocampus (Figures 20b and c).

### 3.4. Metabolomics analysis of mouse plasma

To delineate peripheral metabolome changes related to chronic paroxetine treatment response, plasma metabolite levels were investigated in the PLF and PSF groups at baseline (T0) and following 28 days of drug treatment (T4). While metabolomic profiles between PLF and PSF groups showed no significant differences both at T0 and T4, the PSF group exhibited profound differences with 43 significant metabolite level changes between T0 and T4 and another 71 metabolites that were strongly correlated ( $r > 0.7$ ,  $FDR < 0.1$ ) (Figure 21a). In the PSF group pyrimidine metabolism was enriched with 6 metabolites (carbamoyl phosphate, CMP, dTMP, thymine, UDP, UMP) and another 7 metabolites (adenosine, AMP, GMP, guanine, hypoxanthine, IMP, uric acid) enriched the purine metabolism pathway (Holm adjusted  $p < 0.05$ ,  $FDR < 0.05$ ) (Figure 22). The PLF group exhibited smaller metabolome changes compared to the PSF group. Only 4 metabolites were significantly altered after chronic paroxetine treatment according to SAM with another 32 metabolites highly correlated ( $r > 0.7$ ,  $FDR < 0.1$ ) (Figure 21b). While SAM signatures revealed no significantly affected pathways for the PLF group, glycine, serine and threonine

metabolism was enriched for 5 correlates (choline, dimethylglycine, guanidoacetic acid, serine and threonine) (Holm adjusted  $p < 0.05$ , FDR  $< 0.05$ ) (Figure 23).

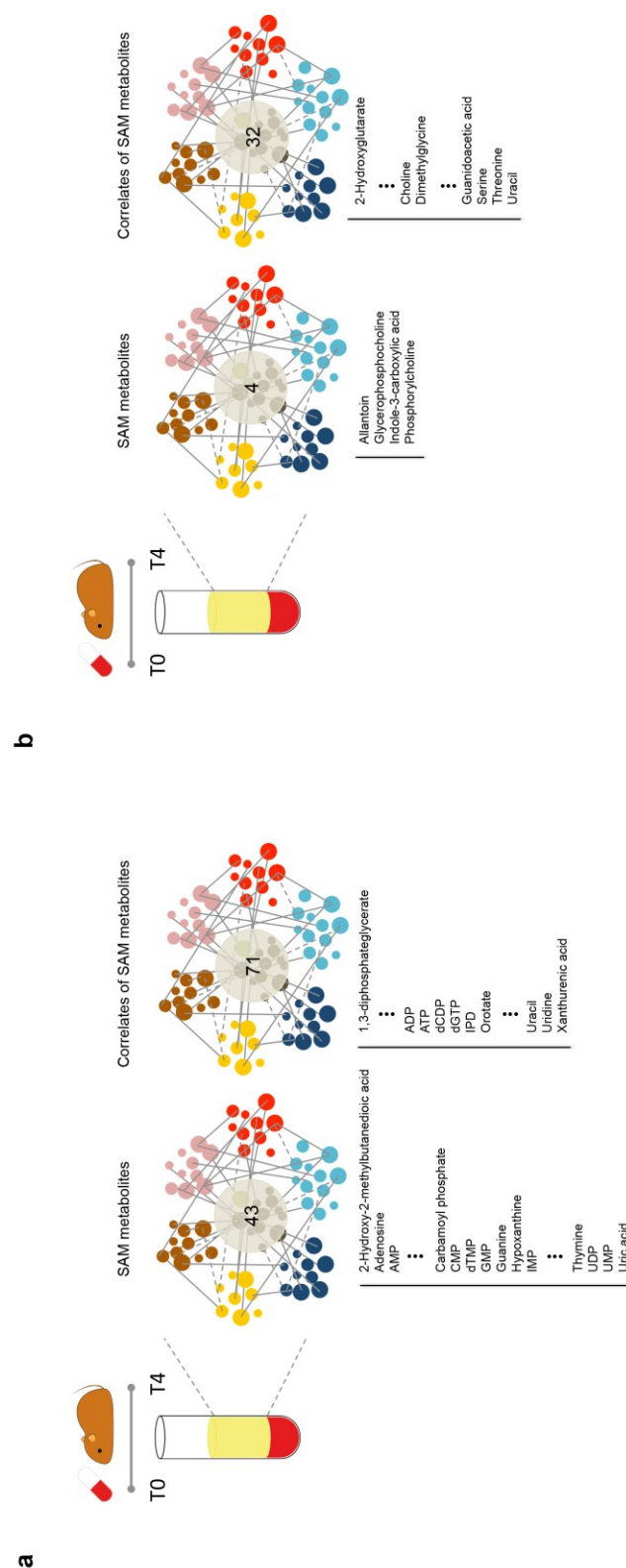


**Figure 21.** Significant plasma metabolite level changes after chronic paroxetine treatment. Plasma SAM metabolites ( $q < 0.05$ , FDR  $< 0.1$ ) and their significant correlates ( $r > 0.7$ ,  $p < 0.05$ ) in **(a)** PSF and **(b)** PLF groups.

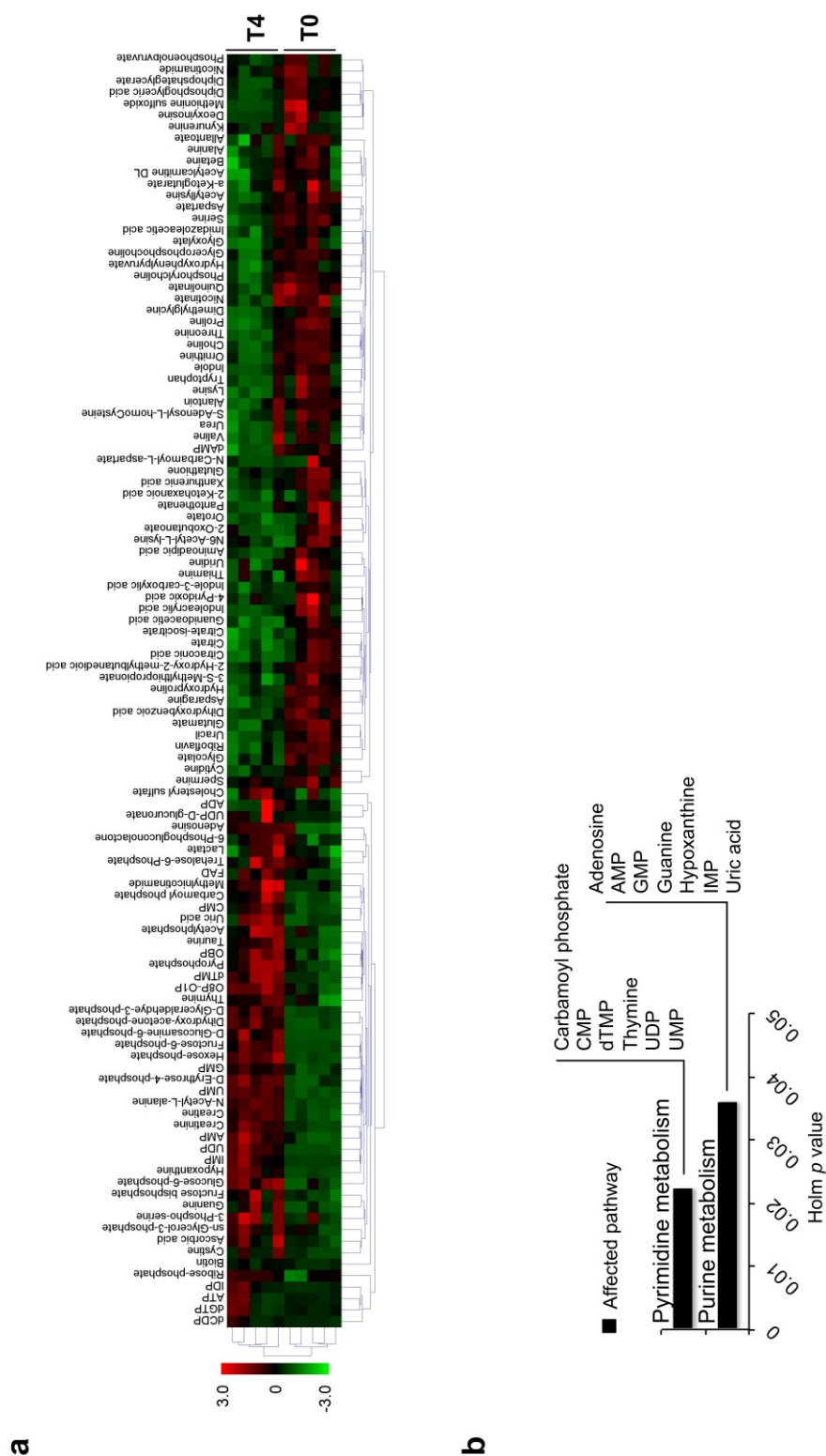


**Figure 22.** Chronic paroxetine treatment induced differential metabolome alterations in PSF mouse plasma. (a) Heat maps and (b) identified pathways of PSF groups comparing metabolome at baseline (T0) and following 28 days of treatment (T4). Purine and pyrimidine

metabolisms were the only affected pathways in the PSF group (Holm adjusted  $p < 0.05$ , FDR  $< 0.05$ ). Heat map colors denote normalized metabolite intensity,  $n=5$ /group.

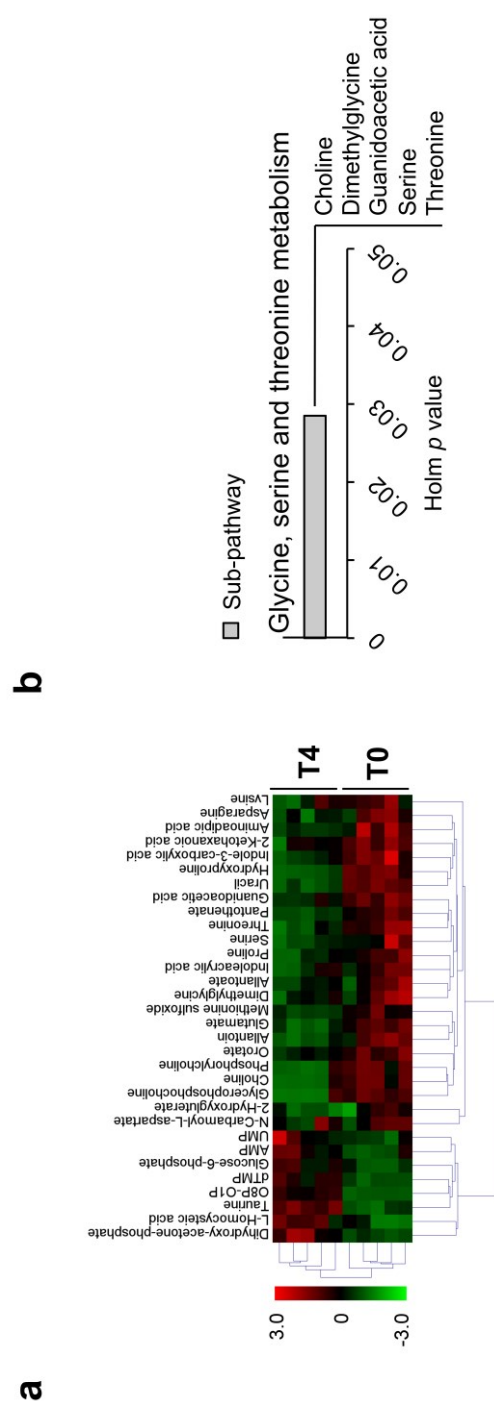


**Figure 23.** (a) Heat maps and (b) identified pathways of PLF groups comparing metabolome at baseline (T0) and following 28 days of treatment (T4). Correlates of SAM signatures identified glycine, serine and threonine metabolism as a sub-pathway (Holm adjusted  $p < 0.05$ , FDR  $< 0.05$ ). Heat map colors denote normalized metabolite intensity,  $n=5$ /group.

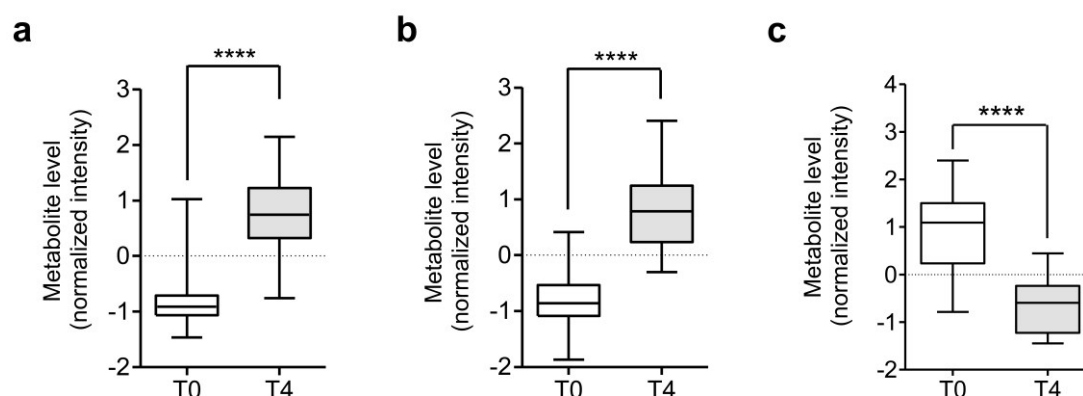


**Figure 24.** Plasma metabolite average level changes in the identified pathways. Chronic paroxetine treatment induced average level changes of (a) purine and (b) pyrimidine pathway metabolites in the PSF group, and (c) glycine/serine/threonine pathway metabolites in PLF group between T0 and T4,  $n=5/\text{group}$ . Metabolite levels are expressed with Box plots with whiskers min to max. \*\*\*\* $p < 0.0001$  (two-tailed paired  $t$ -test).

Plasma metabolite levels of identified pathways were significantly altered after mice had been treated chronically with paroxetine. Purine and pyrimidine metabolism pathway average levels were significantly upregulated by chronic paroxetine treatment in PSF mouse plasma (Figures 24a and b). In PLF mouse plasma, glycine, serine and threonine metabolism pathway was significantly downregulated by chronic paroxetine treatment (Figure 24c). Significant purine and pyrimidine metabolite level changes between T0 and T4 were observed only in the PSF mice. In PSF mice, chronic paroxetine treatment induced significant upregulation of pyrimidine pathway metabolites (carbamoyl phosphate, CMP, dTMP, thymine, UDP, UMP, Figure 25) and purine pathway metabolites (adenosine, AMP, GMP, guanine, hypoxanthine, IMP, uric acid, Figure 26). Glycine, serine and threonine pathway metabolite level changes occurred both in PLF and PSF mice (Figure 27). Plasma levels of 2,3-dihydroxybenzoic acid, aminoadipic acid, choline, pantothenate, taurine, threonine and uracil were found to be regulated to a similar extent in both PLF and PSF groups (Figure 28).

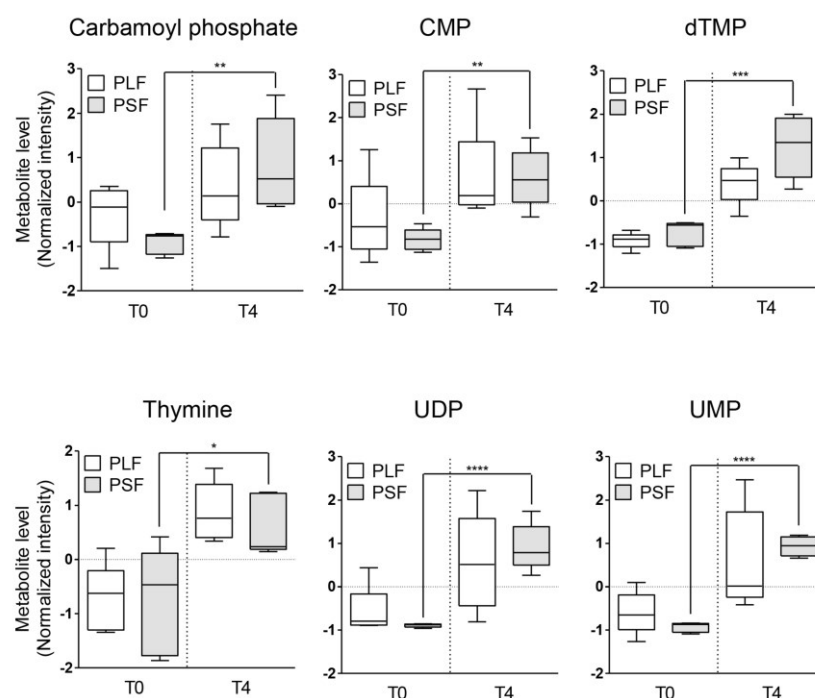


**Figure 25.** Plasma pyrimidine pathway metabolite levels. The metabolite levels in the PSF group were elevated by chronic paroxetine treatment. The PLF and PSF groups exhibited similar metabolite levels both at T0 and T4.  $n = 5/\text{group}$ . \* $p < 0.05$ , \*\* $p < 0.01$ , \*\*\* $p < 0.001$ , \*\*\*\* $p < 0.0001$  (two-tailed paired  $t$ -test).

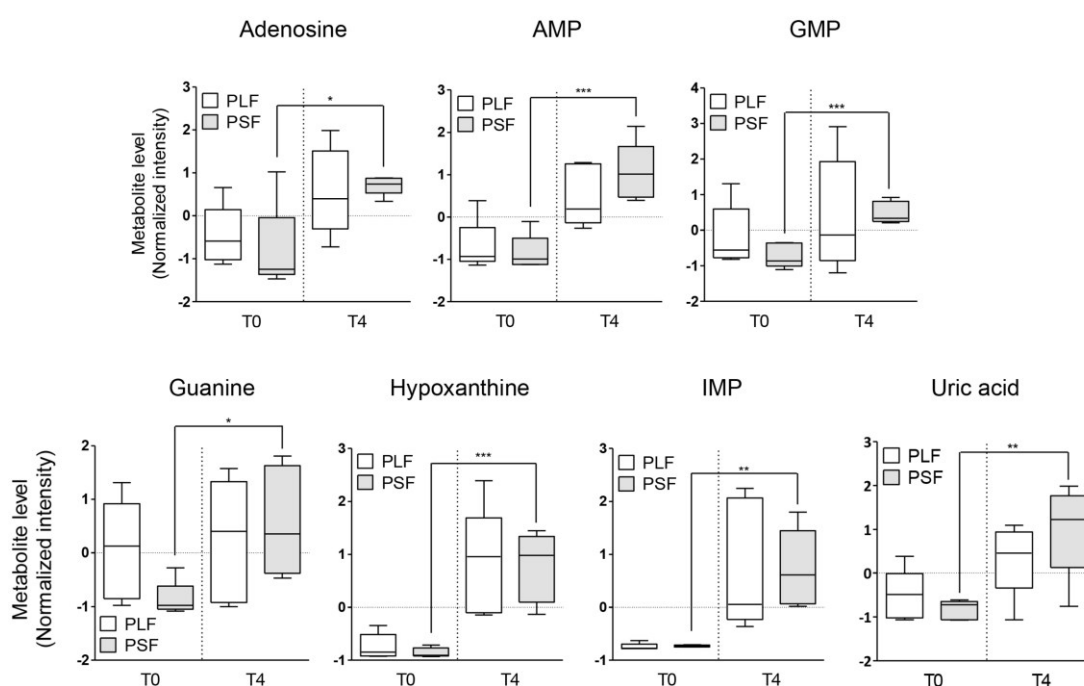


**Figure 26.** Plasma purine pathway metabolite levels. The metabolite levels in the PSF group were elevated by chronic paroxetine treatment. The PLF and PSF groups exhibited similar

metabolite levels both at T0 and T4.  $n = 5/\text{group}$ .  $*p < 0.05$ ,  $**p < 0.01$ ,  $***p < 0.001$  (two-tailed paired  $t$ -test).

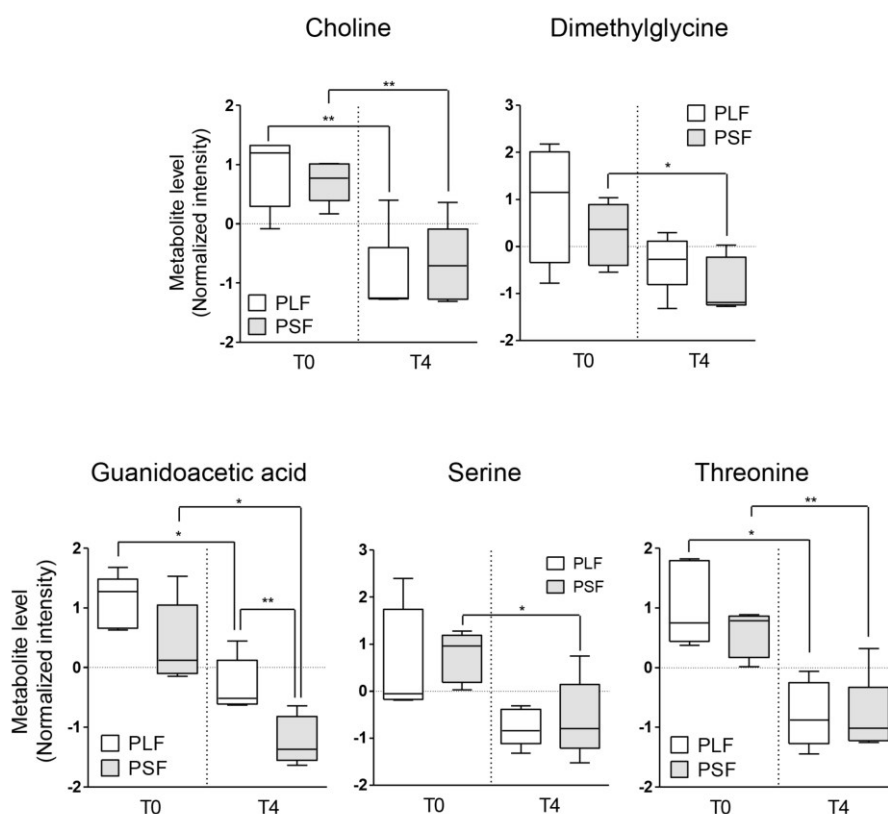


**Figure 27.** Plasma glycine, serine and threonine metabolism pathway metabolite levels. Glycine, serine and threonine metabolite levels in PLF and PSF mice. Both PLF and PSF mice showed that glycine, serine and threonine metabolite levels were significantly down-regulated by chronic paroxetine treatment.  $n = 5/\text{group}$ .  $*p < 0.05$ ,  $**p < 0.01$  (two-tailed paired  $t$ -test).

Metabolite	PLF		PSF	
	$q$ value	FC	$q$ value	FC
2,3-Dihydroxybenzoic acid	5.19E-02	0.55	2.04E-02	0.61
Amino adipic acid	5.19E-02	0.58	3.27E-02	0.63
Choline	4.48E-02	0.54	2.40E-02	0.62
Pantothenate	4.83E-02	0.60	3.14E-02	0.60
Taurine	2.29E-02	1.94	2.21E-02	1.69
Threonine	4.42E-02	0.55	2.40E-02	0.61
Uracil	1.97E-02	0.50	1.69E-02	0.58

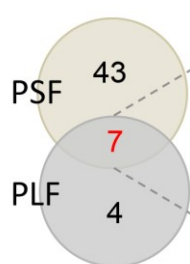


**Figure 28.** Common plasma SAM signatures between the PLF and PSF groups.  $q$  value  $< 0.05$  in either PLF or PSF groups,  $\text{FDR} < 0.1$ .

For validation of peripheral pathways identified in plasma, erythrocytes were chosen as source. Interestingly, erythrocytic ATIC, CPS2 and HPRT proteins were differentially expressed between the PLF and PSF groups. Erythrocytic ATIC and CPS2 protein expression in the PSF mice was 1.2-fold and 2.4-fold higher than in the PLF mice, respectively (ATIC:  $t = 4.991$ ,  $df = 8$ ,  $p < 0.01$ , CPS2:  $t = 4.484$ ,  $df = 8$ ,  $p < 0.01$ ). HPRT protein levels were 1.7-fold higher in the PSF compared to the PLF group ( $t = 3.145$ ,  $df = 8$ ,  $p < 0.05$ ) (Figure 29a). Furthermore, CPS2 and HPRT protein levels were significantly correlated to FST floating time. Correlation between FST floating time and ATIC protein levels showed tendency (Figure 29b).

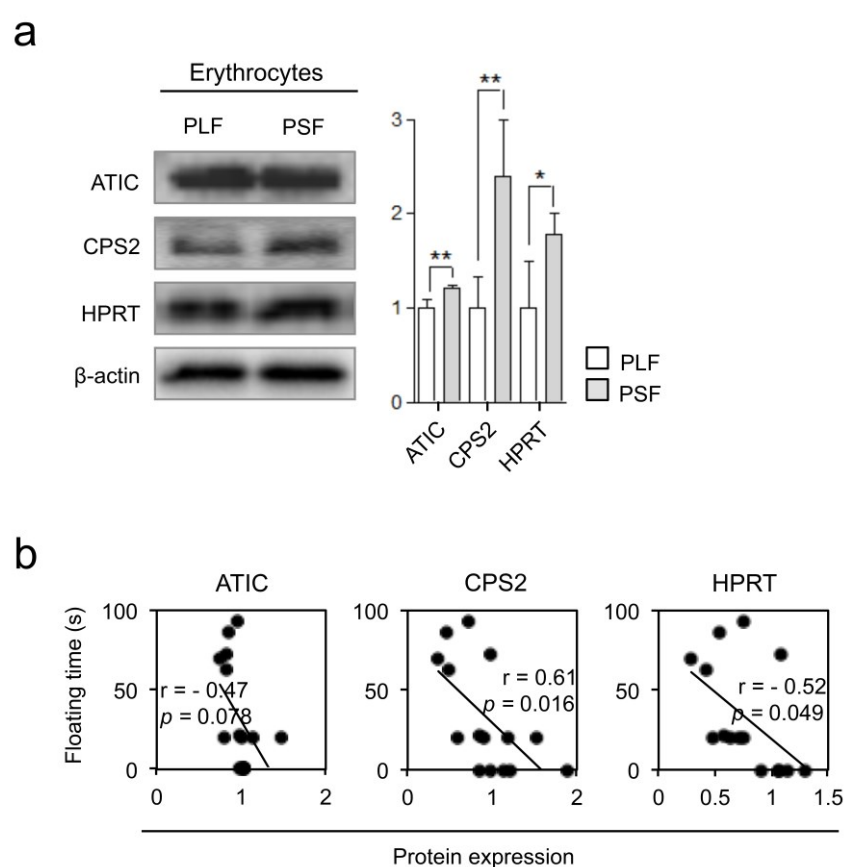


**Figure 29.** The effect of chronic paroxetine treatment on ATIC, CPS2 and HPRT protein expressions in the mouse erythrocytes. **(a)** Western blot and densitometry analyses of CPS2 and HPRT protein levels in the erythrocytes. Erythrocytic ATIC, CPS2 and HPRT proteins showed significant expression level differences between the PLF and PSF groups,  $n=5$ /group. **(b)** Correlation of the pathway protein levels with FST floating time. CPS2 and HPRT protein levels with FST floating time was significant. ATIC protein moderately correlated with FST floating time,  $n=15$ . Protein expression levels were normalized with  $\beta$ -actin. Data are expressed as the mean  $\pm$  SEM. \* $p < 0.05$ , \*\* $p < 0.01$ , \*\*\* $p < 0.001$  (two-tailed  $t$ -test). Pearson correlation coefficients ( $r$ ) with  $p$  values are indicated in the correlation graphs.

### 3.5. Analysis of peripheral patient specimens

Next, I sought to corroborate my findings on pyrimidine and purine metabolism in patients chronically treated with antidepressants. For this purpose I carried out experiments with PBMCs isolated from patients.

First, the same pyrimidine and purine pathway proteins analyzed in mice, ATIC, CPS2 and HPRT, were assessed in PBMCs obtained from antidepressant responder and non-responder patients of the MARS study. In PBMCs collected after 4-6 weeks of antidepressant treatment, ATIC and CPS2 protein levels were significantly correlated with clinical antidepressant treatment response (ATIC:  $r = 0.52$ ,  $p = 0.034$  CPS2:  $r = -0.69$ ,  $p = 0.002$  HPRT:  $r = -0.23$ ,  $p = 0.365$ ) (Figure 30a).

To further investigate pharmacological effects of paroxetine I also performed *ex vivo* experiments with patients' PBMCs. Cells collected from patients upon admittance were cultivated and treated with paroxetine for 2 days. As had been the case for the *in vivo* PBMCs analysis, ATIC and CPS2 protein levels also significantly correlated with patients' clinical antidepressant response when their cultured PBMCs were treated with paroxetine (ATIC:  $r = -0.37$ ,  $p = 0.048$  CPS2:  $r = -0.39$ ,  $p = 0.029$  HPRT:  $r = 0.05$ ,  $p = 0.789$ ) (Figure 30b).

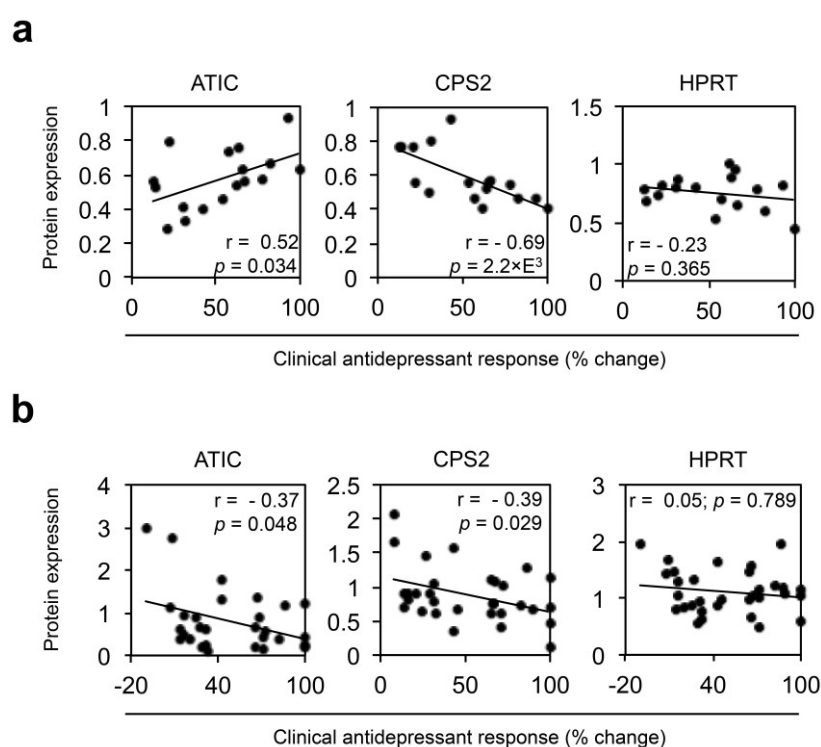


**Figure 30.** Correlation of ATIC, CPS2 and HPRT protein levels with clinical antidepressant treatment response. (a) Depression patients' PBMCs collected after 4-6 weeks of antidepressant

treatment were analyzed for ATIC, CPS2 and HPRT protein expression. ATIC and CPS2 protein levels significantly correlated with clinical antidepressant response,  $n=17$ . **(b)** PBMCs from inpatients with depression were collected at admission. Cells were *ex vivo* cultivated and treated with paroxetine for 2 days. After treatment, ATIC and CPS2 protein levels significantly correlated with clinical antidepressant response,  $n=32$ . Pearson correlation coefficients ( $r$ ) with  $p$  values are indicated in the correlation graphs.

### 3.6. Identification of glutamatergic and ubiquitin proteasome system (UPS) pathways

Mice were treated with paroxetine (5 mg/kg, twice a day) for 28 days. Three animal sub-groups, paroxetine-treated long floating (PLF), paroxetine-treated intermediate floating (PIF) and paroxetine-treated short floating (PSF) groups were identified according to FST floating time ( $F_{(3,141)} = 132.1, p < 0.0001$ ) (Figure 31).

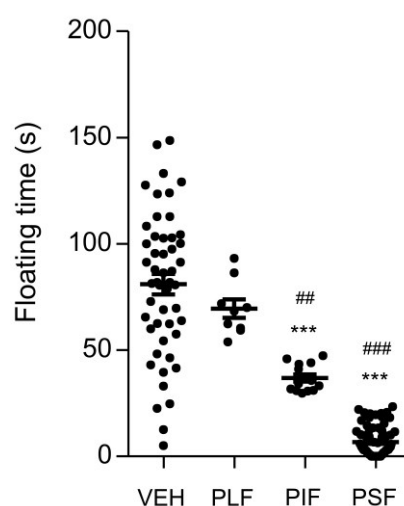


**Figure 31.** Sub-grouping of mice treated with paroxetine. Paroxetine-treated mice were categorized into PLF, PIF and PSF groups based on FST floating time,  $n(\text{VEH/PLF/PIF/PSF})=50/9/14/72$ . Data are expressed as the mean  $\pm$  SEM. \*\*\* $p < 0.001$  (two-tailed  $t$ -test). ## $p < 0.01$  vs. PLF, ### $p < 0.001$  vs. PLF and PIF (one-way ANOVA with Tukey's test).

To investigate the systemic effect of chronic paroxetine treatment on hippocampal molecular pathways, proteomic analyses were performed of the two extreme groups (PLF and PSF groups), which resulted in significant protein expression differences. Significantly affected pathways related to Amyotrophic lateral sclerosis (ALS), Alzheimer's disease, Huntington's disease and long-term potentiation commonly enriched NR1, NR2A and NR2B proteins. Based on the common protein signatures,

glutamate receptors, glutamate metabolism and transport, and synapse and vesicle trafficking pathways were also altered (Figure 32).

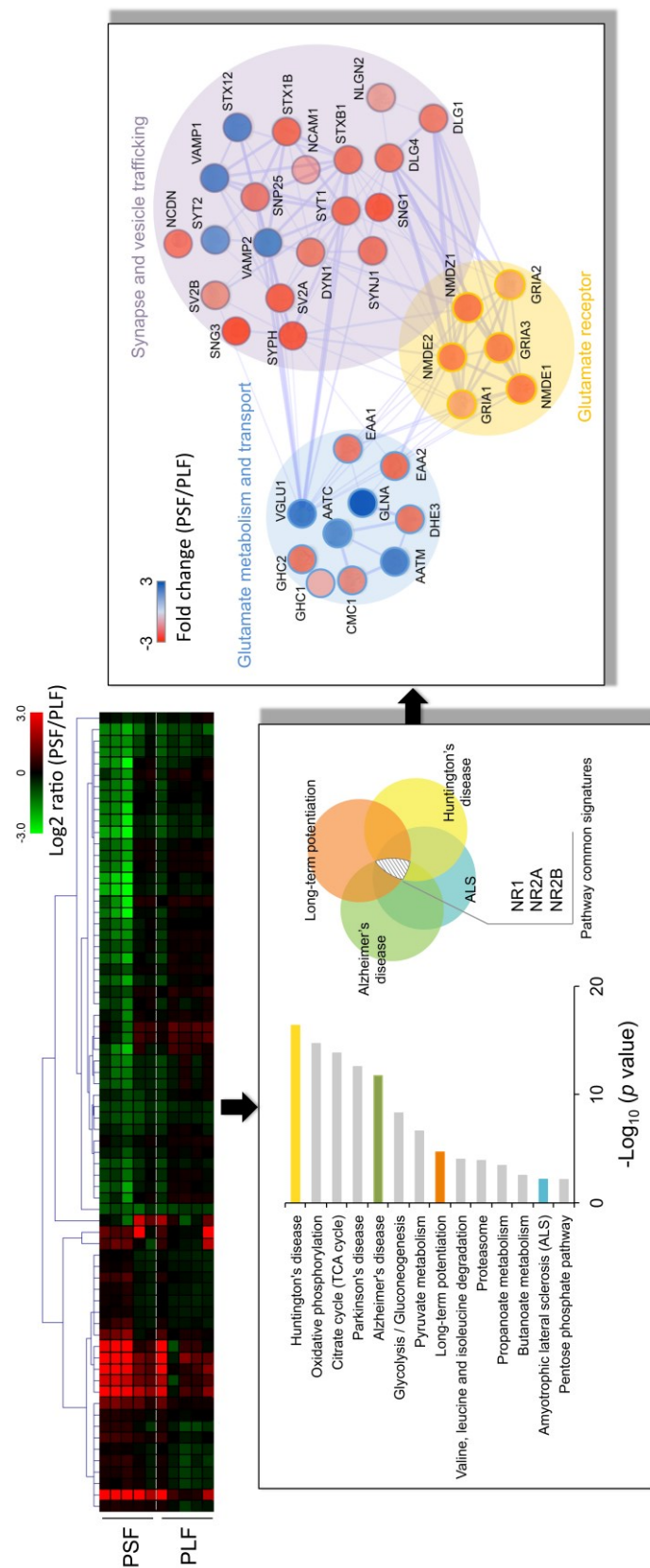


**Figure 32.** Proteomics profiles and enriched pathways between the PLF and PSF groups. The

common protein signatures among pathways were obtained using Venn diagram analysis and further subjected to protein interaction network analysis. In the heatmap, colors denote  $\log_2$  ratio. In the interaction pathway map, colors denote fold difference between the two groups. Proteins with  $|\log_2FC| > 0.3$  and adjusted  $p$  value  $< 0.05$  were considered significant,  $n=5/\text{group}$ .

Hippocampal metabolite profiling data showed altered levels of relevant NMDA receptor modulators and metabolites that are part of the glutamate metabolism pathway (Figure 33). All metabolites were at significantly higher levels in PSF compared to PLF mice (Figure 34).

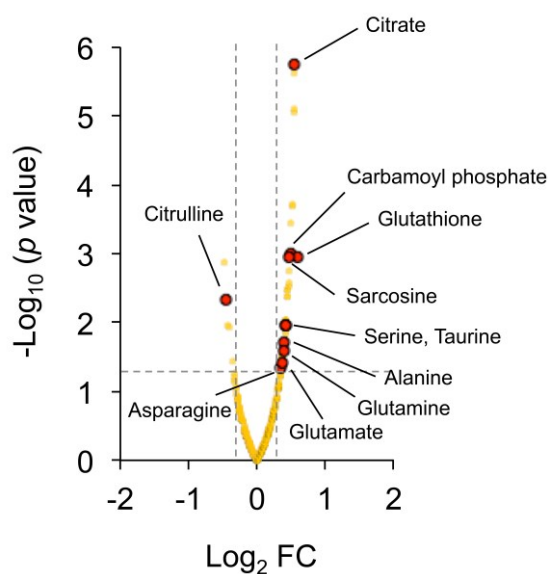


**Figure 33.** A volcano plot comparing PLF and PSF metabolites. Metabolites with  $|\log_2FC| > 0.3$  and  $-\log_{10}(p \text{ value}) > 1.3$  were considered significant,  $n=5/\text{group}$ .

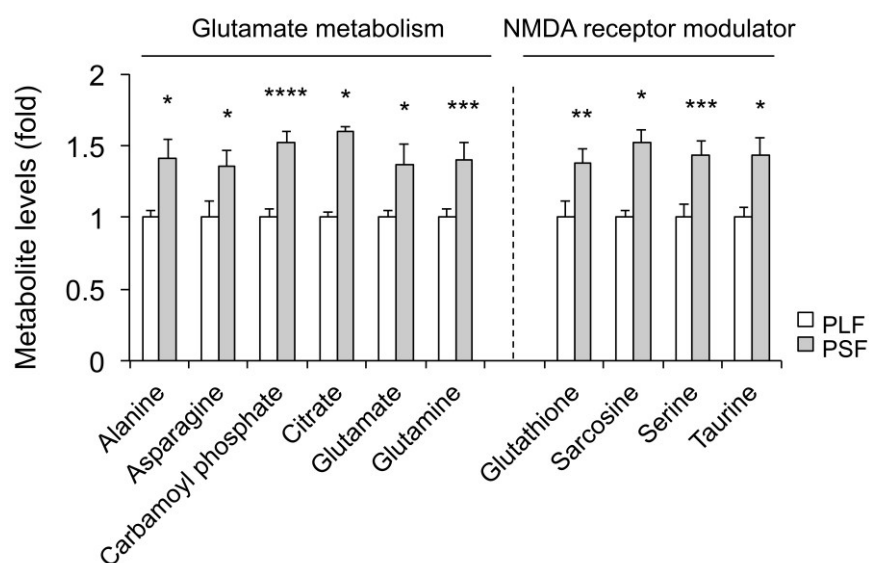


**Figure 34.** Glutamate-related metabolite differences between PLF and PSF mice,  $n=5/\text{group}$ .

Data are expressed as the mean  $\pm$  SEM. \* $p < 0.05$ , \*\* $p < 0.01$ , \*\*\* $p < 0.001$ , \*\*\*\* $p < 0.0001$  (two-tailed  $t$ -test).

Altered levels of citrulline whose conversion from arginine is catalyzed by nNOS protein were detected as well (Figure 35). Integration of proteomic and metabolomic data sets identified systemic metabolite-protein network differences between the PLF and PSF groups (Figure 36).

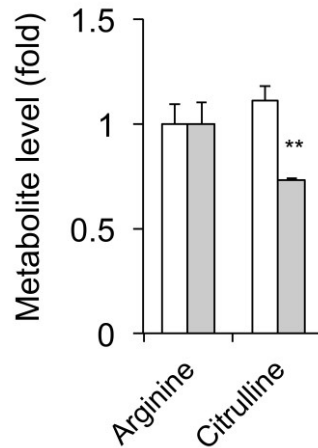


**Figure 35.** Arginine and citrulline levels in PLF and PSF mice,  $n=5$ /group. Data are expressed as the mean  $\pm$  SEM. \*\* $p < 0.01$  (two-tailed  $t$ -test).

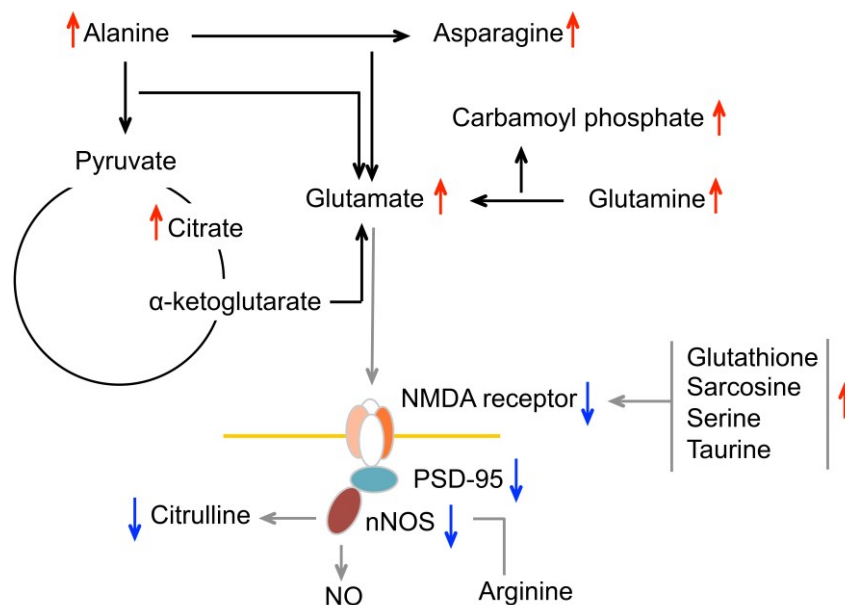


**Figure 36.** Affected protein-metabolite network following chronic paroxetine treatment. Upward-pointing red arrow indicates higher biosignature level in PSF compared to PLF mice. Downward-pointing blue arrow indicates lower biosignature level in PSF compared to PLF mice.

### 3.7. Validation of glutamatergic and UPS pathways

Hippocampal NRs and their phosphorylation levels were compared between PLF and PSF mice. Except for P-NR1/NR1 and P-NR2B/NR2B ratios, all NRs and P-NRs levels were significantly different between the two groups (Figure 37). In addition, NR levels were significantly correlated with FST floating time (Figure 38).

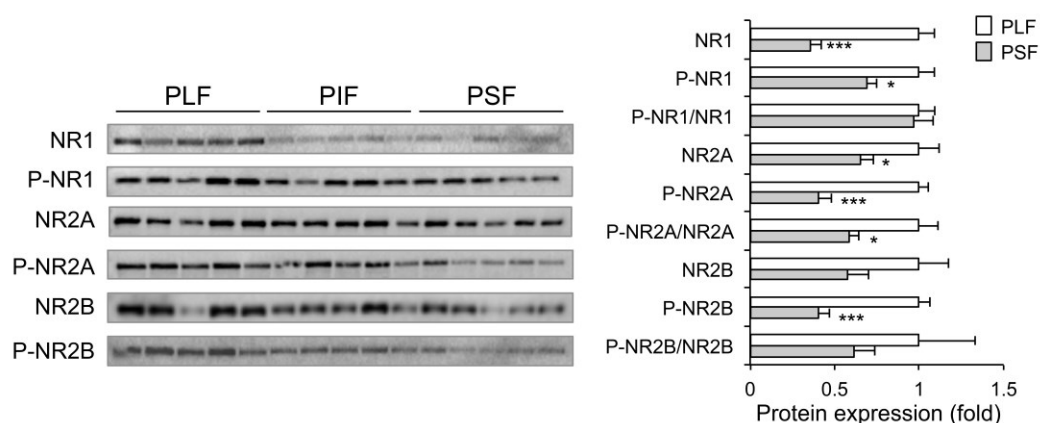


**Figure 37.** NR protein level differences between the sub-groups,  $n=5$ /group. Data are expressed as the mean  $\pm$  SEM. \* $p < 0.05$ , \*\*\* $p < 0.001$  vs. PLF (two-tailed  $t$ -test).

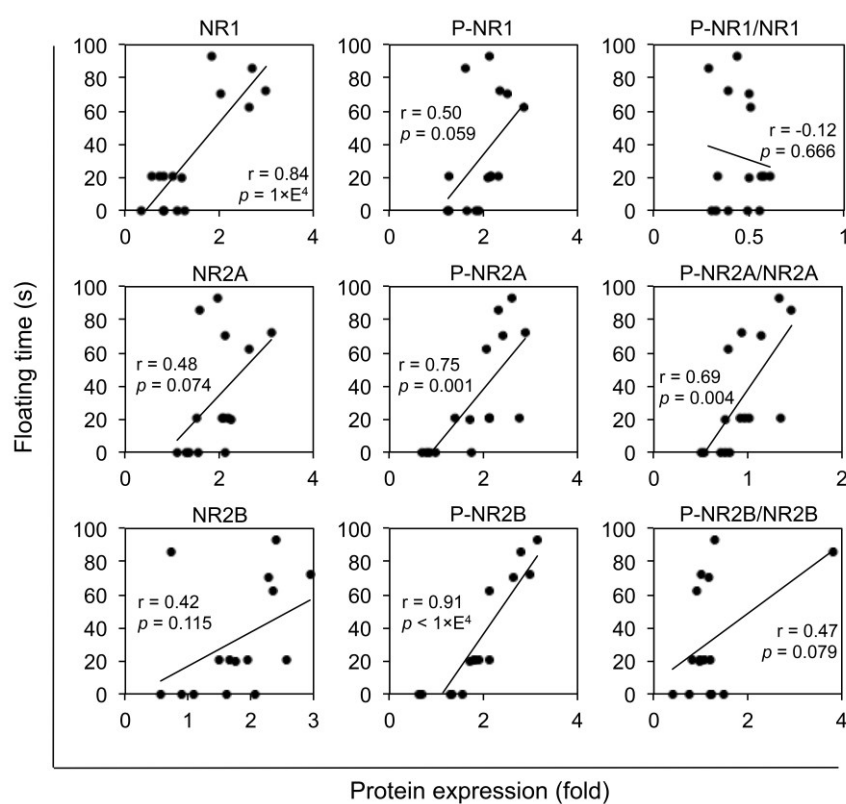


**Figure 38.** Correlation of NR protein levels with FST floating time,  $n=15$ . Pearson correlation coefficients ( $r$ ) with  $p$  values are indicated in the correlation graphs.

Hippocampal NMDA receptor signaling proteins and their phosphorylation status were also investigated between PLF and PSF groups. Especially, P-ERK, CaMK2 and GSK3 $\beta$  levels were significantly different between the two groups (Figure 39) and correlated with FST floating time (Figure 40).

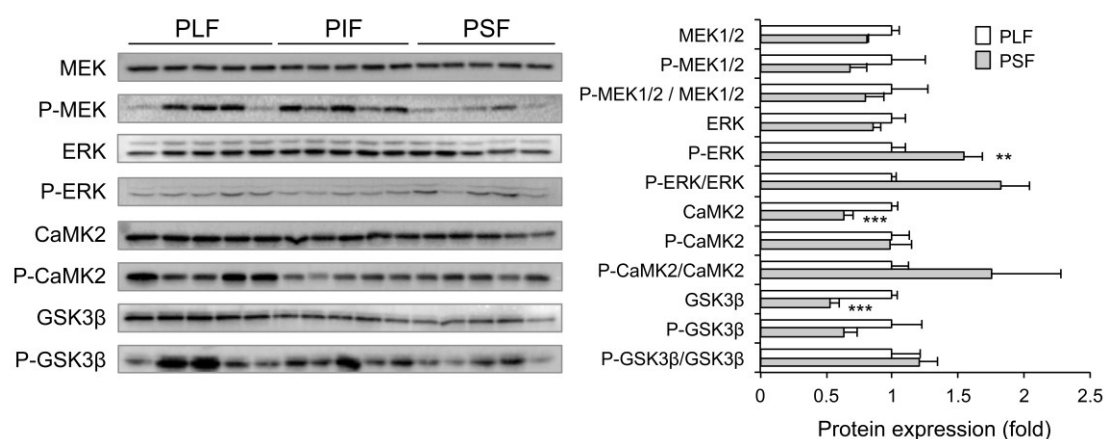


**Figure 39.** NMDA receptor signaling protein level differences between the sub-groups,  $n=5$ /group. Data are expressed as the mean  $\pm$  SEM. \* $p < 0.05$ , \*\*\* $p < 0.001$  vs. PLF (two-tailed  $t$ -test).

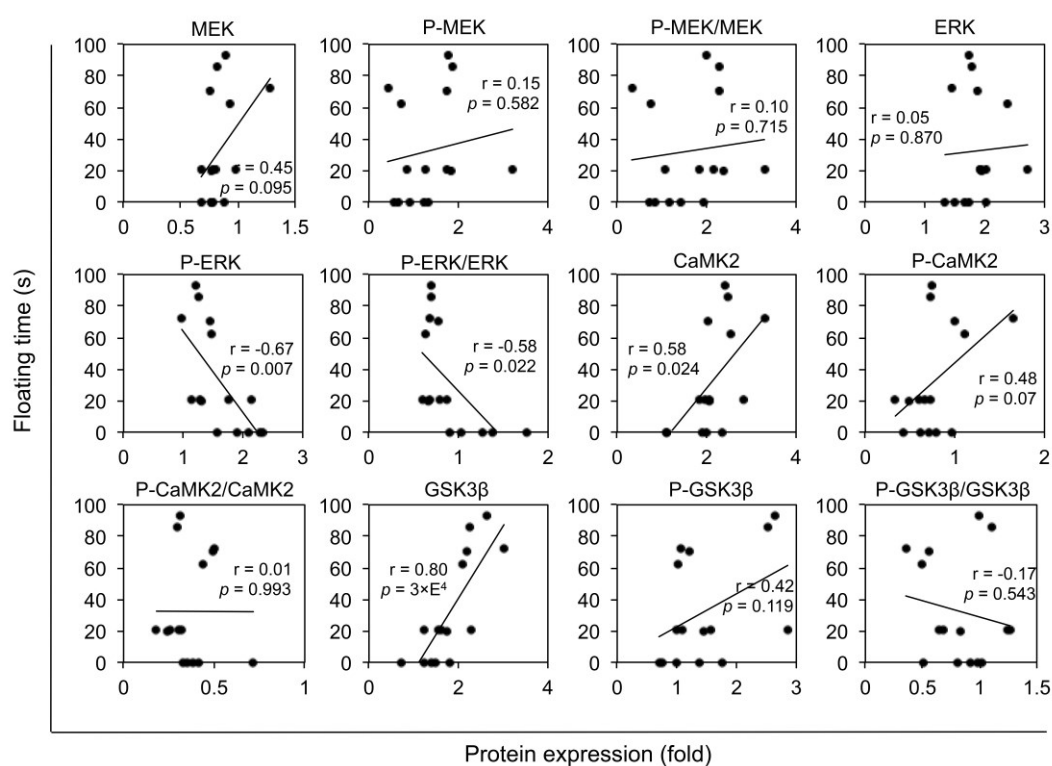


**Figure 40.** Correlation of NMDA receptor signaling protein levels with FST floating time,  $n=15$ . Pearson correlation coefficients ( $r$ ) with  $p$  values are indicated in the correlation graphs.

Nitric oxide (NO) production-related proteins were also significantly different between PLF and PSF mice (Figure 41). PSD-95, nNOS and CAPON protein levels showed significant correlation with FST floating time (Figure 42).

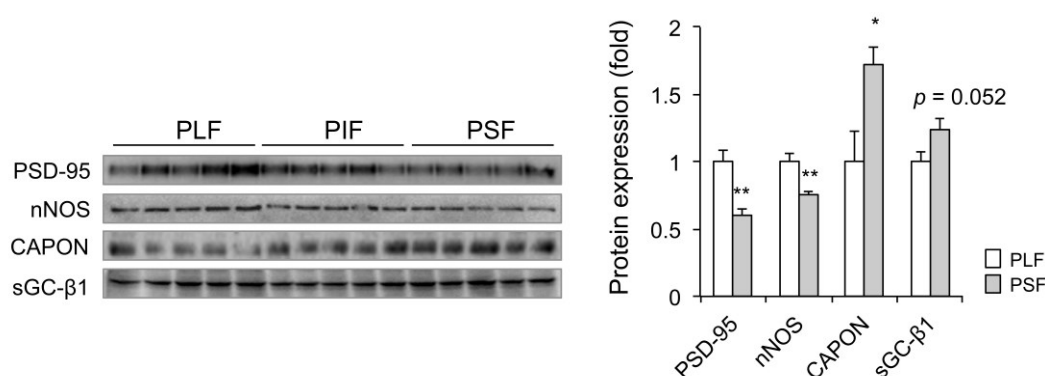


**Figure 41.** Differential effect of chronic paroxetine treatment on PSD-95/nNOS complex. PSD-95, nNOS, CAPON and sGC-β1 protein level differences between PLF and PSF mice,  $n=5$ /group. Data are expressed as the mean  $\pm$  SEM. \* $p < 0.05$ , \*\* $p < 0.01$  vs. PLF (two-tailed  $t$ -test).

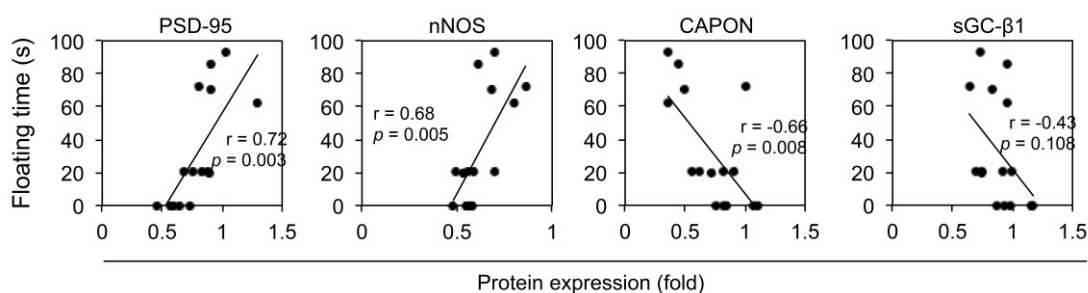


**Figure 42.** Correlation of PSD-95/nNOS complex with FST floating time. PSD-95, nNOS, CAPON and sGC-β1 protein levels with FST floating time,  $n=15$ . Pearson correlation coefficients ( $r$ ) with  $p$  values are indicated in the correlation graphs.

Glutamate metabolism-related protein levels between PLF and PSF mice were further investigated in the hippocampus. Particularly GDH1 showed significant level differences between the two groups and correlated with FST floating time (Figures 43 and 44).

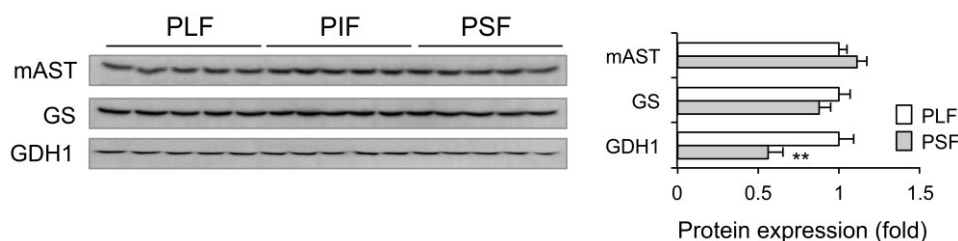


**Figure 43.** Glutamate metabolism protein level differences between PLF and PSF mice,  $n=5$ /group. Data are expressed as the mean  $\pm$  SEM.  $**p < 0.01$  vs. PLF (two-tailed  $t$ -test).

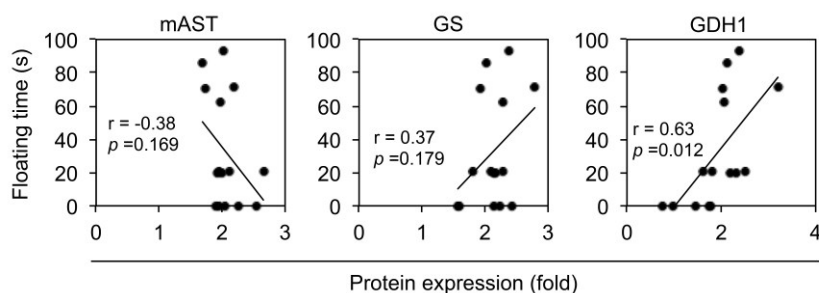


**Figure 44.** Correlation of glutamate metabolism protein levels of FST floating time,  $n=15$ . Pearson correlation coefficients ( $r$ ) with  $p$  values are indicated in the correlation graphs.

Synapse and vesicle trafficking-associated protein level differences were also assessed. Only SYNJ1 protein was found to be significantly different between the groups, and correlated with FST floating time (Figures 45 and 46).

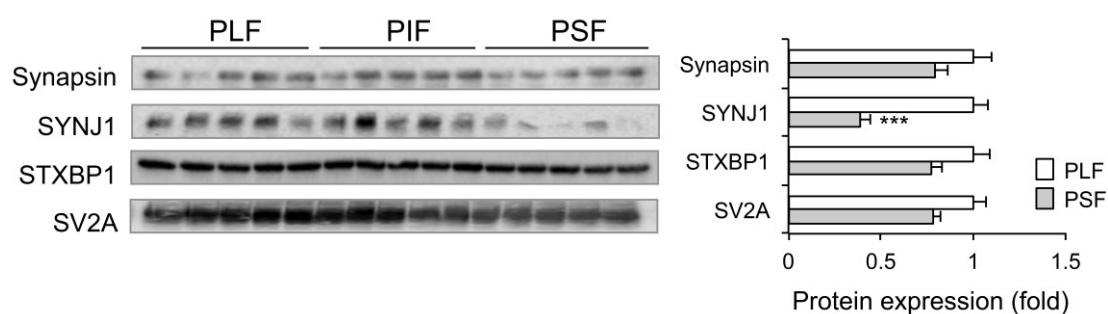


**Figure 45.** Synapse and vesicle trafficking-associated protein level differences between PLF and PSF mice,  $n=5$ /group. Data are expressed as the mean  $\pm$  SEM.  $***p < 0.001$  vs. PLF (two-tailed  $t$ -test).

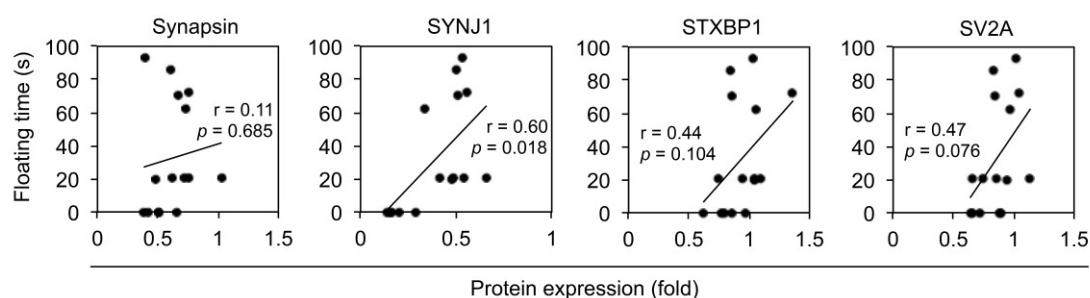


**Figure 46.** Correlation of Synapse and vesicle trafficking-associated protein levels with FST floating time,  $n=15$ . Pearson correlation coefficients ( $r$ ) with  $p$  values are indicated in the correlation graphs.

Since I did not see any NRs, PSD-95 and nNOS transcript level differences between PLF and PSF groups (Figure 47) I next examined the possible involvement of the UPS protein degradation pathway in the observed protein expression differences. Whereas no ubiquitinated NR1, NR2A and PSD-95 differences were detected (Figure 48), PSF mice showed greater PM2A and ubiquitination levels compared to PLF mice (Figure 49), which correlated with FST floating time (Figure 50).

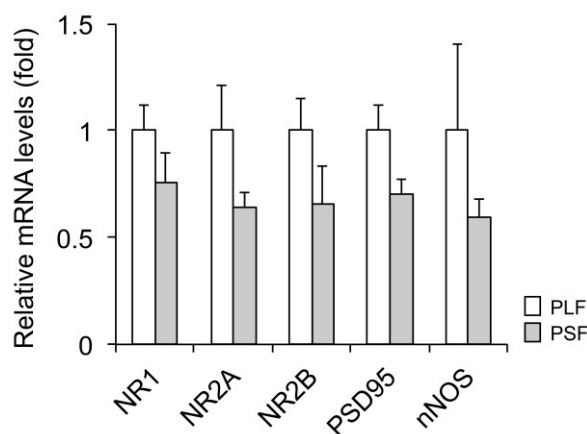


**Figure 47.** qRT-PCR data of NRs, PSD95 and nNOS. No transcription differences were found between PLF and PSF groups,  $n=6$ /group. Data are expressed as the mean  $\pm$  SEM.

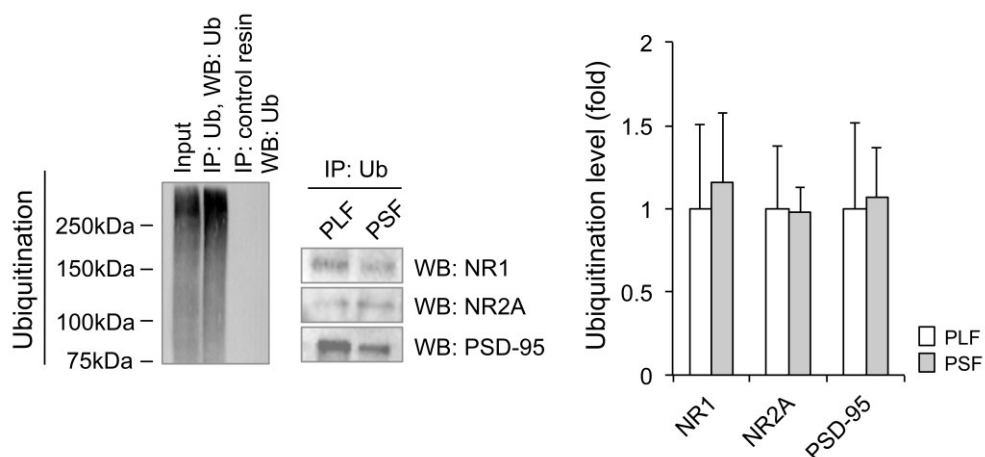


**Figure 48.** Ubiquitinated NR1, NR2A and PSD-95 protein level differences between PLF and PSF groups. No differences were found between PLF and PSF groups,  $n=3$ /group. Data are expressed as the mean  $\pm$  SEM.

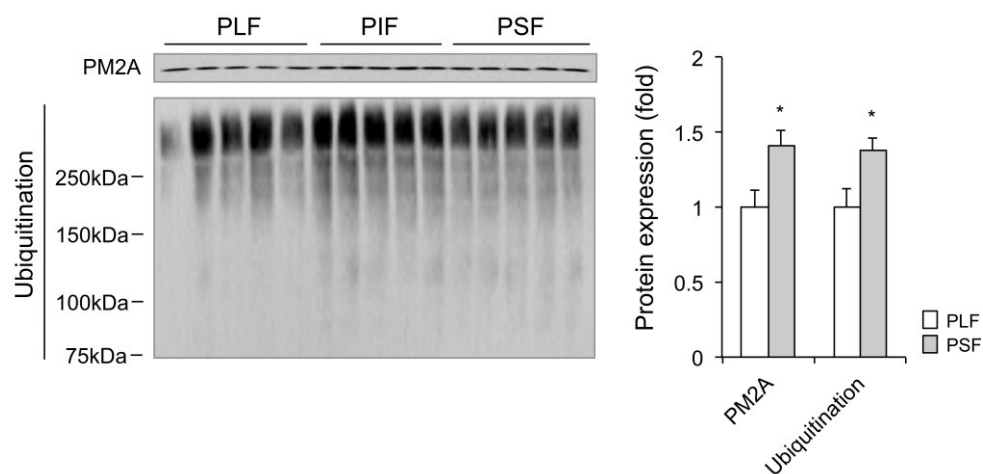


**Figure 49.** PM2A and ubiquitination level differences between PLF and PSF mice,  $n=5$ /group. Data are expressed as the mean  $\pm$  SEM. \* $p < 0.05$  vs. PLF (two-tailed  $t$ -test).

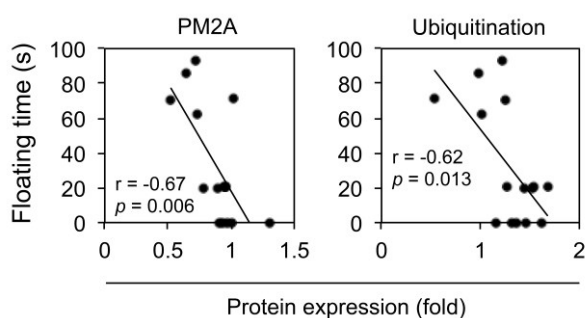


**Figure 50.** Correlation of PM2A and ubiquitination levels with FST floating time,  $n=15$ . Pearson correlation coefficients ( $r$ ) with  $p$  values are indicated in the correlation graphs.

### 3.8. Candidate biomarker validation in human PBMCs from MDD patients

To investigate the relevance of the identified biosignatures, sGC- $\beta$ 1, PM2A and ubiquitination levels were analyzed in MDD patients' PBMCs (Figures 51 and 52). All three proteins were differentially expressed between the antidepressant responder and non-responder patient groups, especially 6 weeks after admission (T6) (Figure 52a). Whereas sGC- $\beta$ 1 protein levels were significantly reduced in both groups at T6, PM2A protein levels were significantly reduced only in responder patients' PBMCs at T6. Ubiquitination levels were not altered by chronic antidepressant treatment in either group. However, they were lower in responder compared to non-responder patients. All three protein levels significantly correlated with clinical antidepressant response at T6 (Figure 52b). Only PM2A protein level changes between baseline (T0) and T6 samples significantly correlated with the clinical antidepressant treatment response (Figure 52c).

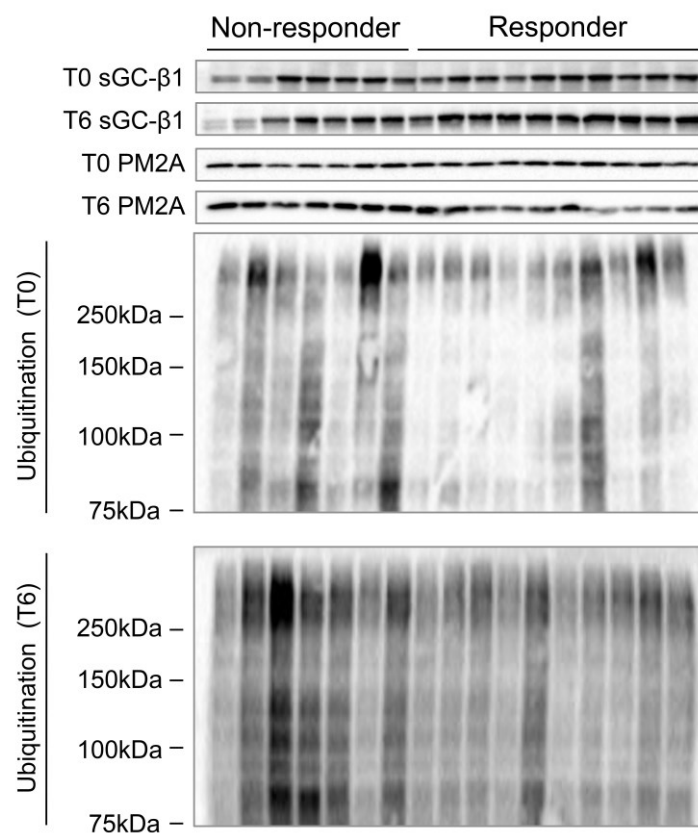


**Figure 51.** Western blot analysis in MDD patient's PBMCs.

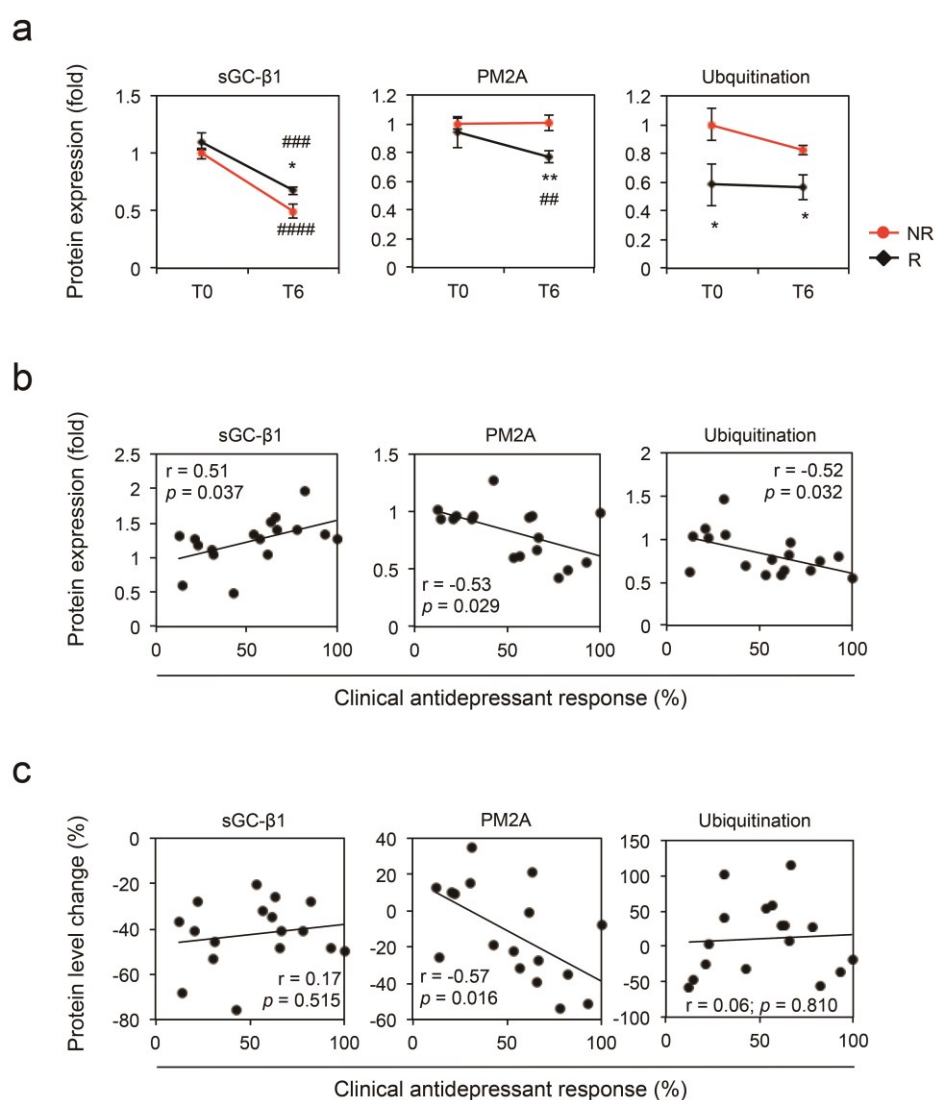


**Figure 52.** sGC-β1, PM2A and ubiquitination levels in human PBMCs from antidepressant responder and non-responder patients. **(a)** sGC-β1, PM2A and ubiquitination level differences between antidepressant non-responder (NR) and responder patients (R) at baseline (T0) and after 6-weeks treatment (T6),  $n=17$ . **(b)** Correlation of protein levels at T6 with clinical antidepressant treatment response,  $n=17$ . **(c)** Correlation of protein level changes (between T0 and T6) with clinical antidepressant treatment response,  $n=17$ . \* $p < 0.05$ , \*\* $p < 0.01$  vs. NR (two-tailed  $t$ -test). ## $p < 0.01$ , ### $p < 0.001$ , #### $p < 0.0001$  vs. T0 (two-tailed paired  $t$ -test). Data are expressed as the mean  $\pm$  SEM. Pearson correlation coefficients ( $r$ ) with  $p$  values are indicated in the correlation graphs.

## 4. Discussion

### 4.1. Purine and pyrimidine metabolism pathway

In my thesis project I have attempted to integrate quantitative proteomics and metabolomics data to improve our understanding of biological pathway changes relevant for the antidepressant treatment response. Integrated -omics data coupled with *in silico* analysis has delineated several molecular pathways and biomarker candidates involved in the differential antidepressant treatment response in mice, which were further validated in human MDD patients' PBMCs.

Using an inbred mouse strain I was able to stratify paroxetine response sub-groups based on animals' behavioral phenotype. For the unbiased separation of paroxetine responder and non-responder mice, I carried out HCA based on FST floating time. The HCA has been a method to build and split different hierarchies of clusters. It has been applied to identify sub-groups of cells and animals based on marker protein expression or behavioral parameters (Droy-Dupré et al., 2015; Muehlmann et al., 2015).

The FST is a behavioral test commonly used to evaluate antidepressant-like effects in mice (Webhofer et al., 2011; Doucet et al., 2013; Kaster et al., 2013; Weckmann et al., 2014). I submit that paroxetine-treated mice that exhibit no FST floating time difference compared with vehicle-treated mice are drug non-responders. My results indicate that 15-40% of the mice are antidepressant non-responders, similar to what is observed for MDD patients.

To further characterize the PLF and PSF sub-groups I also assessed female urine sniffing time, a behavioral parameter pertinent to evaluate SSRI treatment effect in mice (Malkesman et al., 2010; Wagner et al., 2012). While the PLF and PSF groups did not show any difference of female urine sniffing time prior to being treated with paroxetine, chronic paroxetine treatment induced a differential behavioral effect between the groups. This finding indicates that the different behavior between mice is not inherent, but is the result of chronic paroxetine treatment.

Stratification of sub-groups and tailored treatment has been suggested to result in a more favorable outcome and increased treatment efficiency (O'Donnell, 2013; Landeck et al., 2016). Sub-group stratification of patients with multifactorial diseases

like psychiatric and neurodegenerative disorders need to be assessed for molecular and phenotypic signatures. In the current study I only took FST floating time into account for the stratification to simplify data processing and interpretation. Including other behavioral parameters such as FST swimming and struggling time may add further information with regard to the heterogeneous individual response to chronic antidepressant treatment. Associated physiological signatures can also be used towards this goal. ACTH, corticosterone, CRH and other biomolecules associated with psychiatric disorders and treatment, as well as phenotypic markers including cognitive function, specific brain region activity and body mass index (BMI) would qualify in this regard. Integration of other biological dimensions such as the microbiome, lipidome and glycome can also be informative to enhance the systemic understanding of depressive disorders and determine sub-groups more precisely.

To examine the relevance of covariates, drug levels, age and body weight gain were assessed. Paroxetine concentrations in whole brain and plasma were analyzed to check for a possible association of drug levels with antidepressant-like activity. Previous studies have reported a significant relationship between plasma levels and therapeutic response towards paroxetine (Yoshimura and Nakano, 2009). An association of genetic variants of CYP2D6 and ABCB1, which are involved in drug metabolism and permeability, with heterogeneous paroxetine treatment response has been suggested previously (Gex-Fabry et al., 2008; Preskorn, 2014). In my study I did not find any paroxetine concentration differences between PLF and PSF mice in either whole brain or plasma and drug levels did not correlate with FST floating time. This suggests that paroxetine levels in whole brain and plasma are irrelevant for the observed differential drug treatment response in our long-term treatment setting. I also considered animal age and its relationship with paroxetine response. Age-dependent outcome of SSRI treatment has been assessed with regard to adverse effects of drug treatment by comparing antidepressant-induced behavioral response of juvenile or adolescent and adult rodents (Olivier et al., 2011; Mitchell et al., 2013). In the current study all mice reached adulthood prior to being subjected to experiments (> 8 weeks). Although significant FST floating time differences were observed for mice between 18 and 20 weeks of age, no general age effect on FST floating time was detected. The relationship between body weight gain and chronic paroxetine treatment response was also investigated. Chronic paroxetine treatment induced a significant

increase of body weight. However, body weight gain and drug treatment response for each group did not correlate significantly.

My integrated metabolomics and proteomics data showed a differential effect of chronic paroxetine treatment on mouse hippocampal purine and pyrimidine metabolism. Purine and pyrimidine metabolites and their receptors have previously been shown to be associated with various neuropsychiatric disorders. The anti-purinerbic drug suramin was found to reverse autism-like behaviors and metabolism in mice (Naviaux et al., 2014). Polymorphisms of the P2RX7 gene, which encodes a purinerbic ion channel, have been associated with the development of MDD (Lucae et al., 2006). In addition, low brain purine levels were found in female depressed patients responding to treatment with the SSRI fluoxetine (Renshaw et al., 2001). Pyrimidines such as cytidine and uridine have been shown to have antidepressant-like activities in mice (Carlezon et al., 2002; 2005).

Hippocampal metabolome profiling also implicated other metabolites with elevated levels in PSF mice that have antidepressant-like activity. Folate has been shown to have an antidepressant-like effect in mice (Brocardo et al., 2008) and low folate levels were found to be associated with MDD (Gilbody et al., 2007). L-Methylfolate, the active metabolite of folate is used for patients with MDD who partially respond or do not respond to SSRIs (Papakostas et al., 2012). Myo-inositol has been identified as a potential biomarker of SSRI treatment response and innate anxiety disorder (Zhang et al., 2011a; Webhofer et al., 2013; Zhao et al., 2015) and has been shown to have anxiolytic and antidepressant-like effects in both animals and humans (Wurglics and Schubert-Zsilavecz, 2006; Herrera-Ruiz et al., 2011) Flavones are also known to have an antidepressant-like effect (Wurglics and Schubert-Zsilavecz, 2006; Herrera-Ruiz et al., 2011). The elevated levels of folate, myo-inositol and flavones that I found in the hippocampus of PSF mice might be of relevance for the favorable paroxetine response.

I also compared the plasma metabolome of the two mouse sub-groups, PLF and PSF, at baseline and after 28 days of treatment (T0 and T4) with the aim of identifying differentially affected pathways and potential biomarker candidates in the periphery. Plasma metabolome changes over time resulted in group-specific profiles. Major metabolite level alterations and elevation of purine and pyrimidine metabolites were observed in the PSF group. In contrast, the plasma metabolome was minimally affected by chronic paroxetine treatment in the PLF group. Despite the fact that the

glycine, serine and threonine metabolism pathway was specifically enriched as a sub-pathway of PLF group, significant metabolite level changes were observed in both sub-groups. I also found plasma metabolite biosignatures commonly regulated between the PLF and PSF groups. In particular, levels of choline and threonine that are part of the glycine, serine and threonine metabolism pathway were significantly changed both in the PLF and PSF groups after chronic paroxetine treatment. Metabolites of glycine, serine and threonine metabolism may thus constitute confounding biosignatures.

In contrast to hippocampal purine/pyrimidine metabolites, plasma metabolite level changes were not correlated with FST floating time. Small plasma metabolite level differences between the PLF and PSF groups might be responsible for non-significant correlation. Despite non-significant correlation between plasma metabolite level changes and chronic paroxetine treatment response, group-specific analysis showed PSF-group specific pathway enrichment and significant metabolite changes.

Based on my integrated -omics data that implicate purine and pyrimidine metabolism pathways to be involved in paroxetine response I next wanted to corroborate these findings through the analysis of proteins that are part of these pathways. Based on the observed differences of carbamoyl phosphate and IMP levels between the PLF and PSF groups, ATIC, CPS2 and HPRT protein levels were analyzed. CPS2 catalyzes early steps of carbamoyl phosphate synthesis in the pyrimidine biosynthesis pathway. ATIC and HPRT play a central role in synthesis and conversion of inosine monophosphate (IMP), the end product of the purine biosynthesis pathway. For pathway validation I chose hippocampus, prefrontal cortex and erythrocytes and compared ATIC, CPS2 and HPRT protein levels between the PLF and PSF groups. Western blot analyses revealed that hippocampal and erythrocytic ATIC, CPS2 and HPRT proteins were differentially expressed between the two groups while prefrontal cortex protein expression showed no difference. Hippocampal and erythrocytic ATIC, CPS2 and HPRT protein levels were also highly correlated with FST floating time while no significant correlation was observed in the prefrontal cortex. This indicates that different purine and pyrimidine metabolism pathway activities between PLF and PSF groups might be specific for the hippocampus.

Interestingly, I observed an inverse relationship between hippocampal and erythrocytic protein expression for the three proteins. Inconsistent biosignature expression patterns in brain and peripheral tissues have been found in other cases

related to psychiatric disorders. Brain and blood BDNF levels were inversely correlated in a genetic rat model of depression (Elfving et al., 2010). Brain and white blood cell p11 protein levels also showed an inverse relationship (Svenningsson et al., 2014). Inverse myo-inositol levels between hippocampus and plasma were also reported previously in mice chronically treated with paroxetine (Webhofer et al., 2013). In the current study we found that carbamoyl phosphate and IMP levels have an inverse correlation between hippocampus and plasma. This might be caused by the observed inverse relationship of ATIC, CPS2 and HPRT enzyme expression levels between hippocampus and erythrocytes (Figure 53).

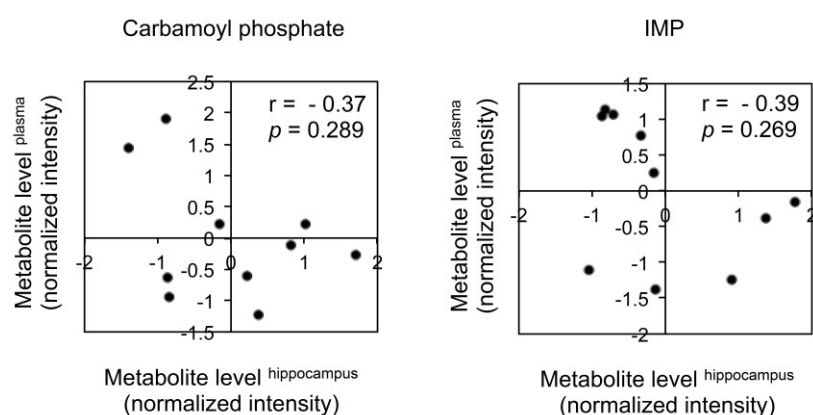


**Figure 53.** Correlation between hippocampus and plasma metabolite levels. Carbamoyl phosphate and IMP metabolite levels showed inverse relationships between hippocampus and plasma. Pearson correlation coefficients ( $r$ ) with  $P$  values are indicated in the correlation graphs.

Lower expression of hippocampal ATIC, CPS2 and HPRT in the PSF group might be caused by negative feedback regulation in response to elevated pathway metabolite levels. Higher erythrocytic protein levels in the PSF mice might reflect PSF group-specific activation of purine and pyrimidine metabolisms.

To address the question whether the pathways for antidepressant response identified in the mouse are also relevant for patients' response, PBMCs from antidepressant responder and non-responder patients were analyzed for ATIC, CPS2 and HPRT protein expressions. PBMCs collected after 4-6 weeks of antidepressant treatment showed significant correlation between ATIC and CPS2 protein expression levels and HDRS score change between baseline and following chronic antidepressant treatment. Whereas PBMCs ATIC protein expression showed a similar pattern as the one

observed in mouse erythrocytes, PBMCs CPS2 protein expression resembled that of mouse hippocampus.

In *ex vivo* experiments, PBMCs ATIC protein levels were negatively correlated with clinical antidepressant response. The observed discrepancy between *in vivo* and *ex vivo* PBMCs ATIC protein expression could be due to different treatment conditions (chronic vs. subchronic) and exposure to multiple types of drugs. PBMCs' CPS2 protein expression consistently showed negative correlation with mouse hippocampal protein expression both in *in vivo* and *ex vivo*. ATIC and CPS2 proteins may thus represent candidate biomarkers to determine clinical antidepressant treatment response. For HPRT protein, I failed to determine a significant correlation between clinical antidepressant response and PBMCs protein levels both *in vivo* and *ex vivo*.

Previously obtained data by Webhofer et al. revealed altered energy metabolism upon chronic paroxetine treatment in DBA/2OlaHsd mice when compared to vehicle-treated control mice (Webhofer et al., 2011; 2013). The previous and current studies are not directly comparable since the studies were performed under different conditions (groups, dosage and route of paroxetine administration, mouse strain). In the current study, energy metabolism-related pathways including glycolysis, Krebs cycle and glycogen metabolism that came up in the previous study were not enriched when PLF and PSF groups were compared. The current -omics analyses were performed to compare PLF and PSF mouse groups and identified purine and pyrimidine metabolisms as the main distinguishing pathways. However, based on ATP/ADP and NAD<sup>+</sup>/NADH ratios found in the current study I can not exclude that energy metabolism might also distinguish the PLF and PSF groups (Figure 54).

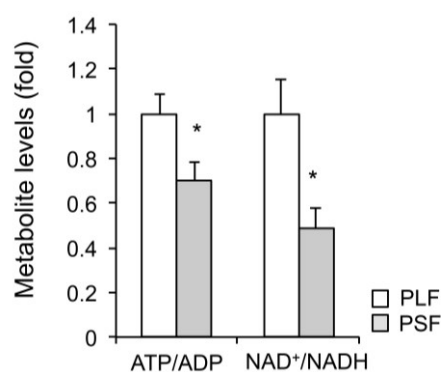


**Figure 54.** Energy-related metabolite ratios in the hippocampus. ATP/ADP and NAD<sup>+</sup>/NADH ratios in the hippocampus in the PLF and PSF group ( $n = 5/\text{group}$ ). Bars represent mean  $\pm$  SEM. \* $p < 0.05$  (two-tailed  $t$ -test).

Hippocampal neurogenesis is known to be caused by the action of antidepressants (Malberg et al., 2000, Santarelli et al., 2003, Gundersen et al., 2013). Since purine and pyrimidine metabolites are critical for cell proliferation, increased purine/pyrimidine metabolism activity in PSF mice may also result in neurogenesis in these animals.

Based on evidence from the literature microRNAs (miRNAs) may be also relevant for the distinct regulation of purine/pyrimidine metabolisms in the PLF and PSF mouse groups. Feng et al have shown that miR-1 and miR-133a-3p regulate purine and pyrimidine metabolic pathways (Feng et al., 2015) and the purine metabolism gene *GART* is regulated by 16 miRNAs (Li et al., 2014). Since SSRIs impact miRNA levels (Hansen and Obrietan, 2013) this may explain the observed differences in the purine and pyrimidine metabolisms upon chronic paroxetine treatment.

Based on these data a pharmacological study with an inhibitor of the folate pathway that also regulates purine and pyrimidine metabolism could shed light on the functional relevance of the pathways in chronic antidepressant treatment response.

The current study used wild-type stress naïve DBA/2J mice to investigate the pharmacological heterogeneity of the antidepressant response. Wild-type stress naïve rodents have been used previously to evaluate antidepressant-like effects (Guzzetti et al., 2008; Gurbuz Ozgur et al., 2015; Taguchi et al., 2016). An extension of our studies using an animal model with a depression-like phenotype would further validate the identified pathways affected by the antidepressant treatment response and add relevant information for the antidepressant treatment of patients.

## 4.2. Glutamatergic pathway

My results also suggest that proteins and metabolites associated with the glutamatergic pathway are affected by chronic antidepressant treatment which became apparent with the categorization of a paroxetine-treated intermediate floating (PIF) group.

The glutamatergic pathway has previously been associated with MDD pathobiology and antidepressant response. In depressed patients, significantly elevated serum, plasma and cerebrospinal fluid glutamate levels were found (Kim et al., 1982; Altamura et al., 1993; Mauri et al., 1998; Levine et al., 2000; Mitani et al., 2006). A single nucleotide polymorphism (SNP) in metabotropic 7 glutamate receptor was shown to be involved in the onset of the clinical antidepressant effect (Fabbri et al.,

2013). Glutamate release decreases with chronic fluoxetine, desipramine, reboxetine, venlafaxine or agomelatine treatment (Bonanno et al., 2005; Musazzi et al., 2010). Numerous studies have shown that chronic antidepressant treatment regulates glutamatergic receptor expression in rodent hippocampus (Boyer et al., 1998; Skolnick, 1999; Martinez-Turrillas et al., 2002; Barbon et al., 2006; Pittaluga et al., 2007; Wieronska et al., 2007; Ryan et al., 2009; Calabrese et al., 2012; O' Connor et al., 2013). The current study also indicates that NRs and P-NRs expression levels were differentially affected in paroxetine-treated sub-groups.

We also observed different levels of proteins downstream of the glutamate receptor (CaMKII, GSK-3 $\beta$ , P-ERK), which might be a reflection of differential NMDA receptor activity. CaMKII has been linked to neurotransmitter release and synaptic plasticity (Lotrich and Pollock, 2005), which has been associated with neuropsychiatric disorders and antidepressant treatment effects (Pavlidis et al., 2002; Holderbach et al., 2007; Wang et al., 2008). Our observation of a lower CaMKII expression level in PSF mice suggests a regulatory mechanism that prevents synaptic connections becoming too strong as has been suggested by Robison et al (Robison et al., 2014).

Accumulating evidence has implicated GSK-3 in the pathogenesis of bipolar disorder and major depressive disorder (Gould et al., 2004; Lovestone et al., 2007) as well as the antidepressant treatment response. Tsai et al., reported that polymorphisms in GSK-3 $\beta$  gene were associated SSRI treatment response (Tsai et al., 2008). Paroxetine and lithium treatments were shown to regulate GSK-3 $\beta$  phosphorylation which also predicts clinical improvement of depressive patients (Gassen et al., 2016). Joaquim et al. showed that long-term treatment with sertraline induces increased expression and decreased phosphorylation of GSK-3 $\beta$  in MDD patient platelets (Joaquim et al., 2012). Our chronic paroxetine treatment did not induce significantly different inhibition of GSK-3 $\beta$  activity, which is evident from Ser9-P-GSK-3 $\beta$  protein levels. As GSK-3 protein suppresses Ca<sup>2+</sup>-current and neurotransmitter release by inhibiting calcium channels and soluble NSF attachment protein receptor (SNARE) complex interaction (Wildburger and Laezza, 2012), low levels of GSK-3 $\beta$  total protein in PSF mice might result in greater synaptic transmission and a more favourable antidepressant treatment outcome.

Several lines of evidence have also associated ERK with MDD and the antidepressant treatment response. *Post-mortem* brains of depressed suicide subjects showed reduced

ERK expression suggesting a role of the protein in MDD pathophysiology (Dwivedi et al., 2001). Antidepressant treatment increases ERK phosphorylation levels in rodent hippocampus (Gourley et al., 2008; Qi et al., 2008). Different P-ERK levels between PLF and PSF mice implicate a potential role in the heterogeneous antidepressant treatment response.

We also observed significantly different GDH1 and SYNJ1 protein levels between PLF and PSF groups. GDH1 has been associated with glutamatergic transmission and synaptic activity in the hippocampus (Bao et al., 2009; Michaelis et al., 2011). In addition, SYNJ1 gene expression, which is required for vesicle recycling and synaptic transmission (Cremona et al., 1999; Lüthi et al., 2001; Kim et al., 2002; Mani et al., 2007) was reported to be significantly altered by imipramine and St John's wort, an herbal product with antidepressant activities (Wong et al., 2004). GDH1 and SYNJ1 protein level alterations may indicate different synaptic transmission activity between PLF and PSF groups.

My results were further corroborated by metabolite profiling data. GDH1 catabolizes glutamate and its elevated levels may be caused by the low GDH1 protein expression I found in PSF mice. Alternatively, high glutamate levels might induce a compensatory feedback regulation of GDH1 protein expression to prevent pathway over-activation. Altered NR levels are consistent with the observed glutamate levels in the PLF and PSF mice. More glutamate and other NMDA receptor modulators could result in reduced NMDA receptor expression as previously reported in studies with L-trans-pyrrolidine-2,4-dicarboxylate, a high-affinity glutamate reuptake inhibitor (Cebers et al., 1999; 2001).

In particular PSD-95 and nNOS, which functionally interact with NMDA receptor (Bredt and Snyder, 1989; Vallebuona and Raiteri, 1994; Fedele et al., 2001) and produce NO, are of great interest with regard to the heterogeneous antidepressant response. Hippocampal nNOS was found to mediate glucocorticoid-induced depressive behavior in mice (Zhou et al., 2011) and the number of nNOS-immunoreactive neurons in *post-mortem* hippocampus samples was higher in MDD and bipolar disorder patients compared to the control group (Oliveira et al., 2008). Plasma NO metabolite levels were higher in MDD patients compared to healthy controls, which was reversed by 8 week paroxetine treatment (Chrapko et al., 2006). NO has also been implicated to play a role for the function of antidepressant-like agents tramadol, bupropion and lithium (Dhir and Kulkarni, 2007; Ghasemi et al.,

2008; Jesse et al., 2008). Serotonergic antidepressants including citalopram, imipramine, paroxetine and tianeptine have been shown to decrease hippocampal NOS activity *in vitro and in vivo* (Finkel et al., 1996; Wegener et al., 2003). Based on these findings targeting the NO system is a potential therapeutic strategy for major depressive disorders. Doucet et al., reported that a single administration of PSD-95/nNOS interface inhibitors, IC87201 and ZL006, produced an antidepressant-like effect in the FST and tail suspension test (TST) (Doucet et al., 2013). In addition, nNOS inhibitors like *N $\omega$ -Propyl-L-Arginine*, *7-nitroindazole* and *aminoguanidine* have been shown to produce antidepressant-like effects (Joca and Guimarães, 2006; Zhou et al., 2007; Hiroaki-Sato et al., 2014; Tomaz et al., 2014). I found that the hippocampal NMDA receptor/PSD-95/nNOS protein complex was expressed at significantly different levels between PLF and PSF mice, implying that it has an important role in the chronic antidepressant treatment response.

We also investigated CAPON and sGC- $\beta$ 1, proteins associated with the NO pathway, to further corroborate the differential activity of the NMDA receptor/PSD-95/nNOS protein complex between PLF and PSF groups. CAPON has been shown to disrupt the interaction between nNOS and postsynaptic proteins including PSD-95, which prevents NMDA receptor-mediated NO release (Xu et al., 2005). I found high levels of hippocampal CAPON protein in PSF mice which may contribute to a favorable antidepressant treatment response, possibly by suppressing nNOS activity.

sGC- $\beta$ 1 protein levels between PLF and PSF mice were not significantly different, which is in line with results from Reiersen et al. who reported that 8-weeks of SSRI fluoxetine treatment did not change sGC- $\beta$ 1mRNA levels in rat hippocampus (Reiersen et al., 2009). It has been also shown that sGC- $\beta$ 1mRNA levels were not affected in human schizophrenic prefrontal cortex *post-mortem* samples that had higher nNOS mRNA levels compared to controls (Baba et al., 2004). Although I did not find sGC- $\beta$ 1protein expression level differences, I cannot exclude the possibility that sGC enzymatic activity might be different between PLF and PSF groups.

Consistent with nNOS protein levels, citrulline levels between PLF and PSF mice were also altered after 28 days of paroxetine treatment. Since nNOS catalyzes the production of NO and citrulline from arginine, lower levels of citrulline in PSF mouse hippocampus may indicate lower enzymatic nNOS activity.

Hippocampal metabolome profiling also supported differential NMDA receptor activity between the two groups. Alanine and citrate are known to regulate NMDA

receptor activity. (Westergaard et al., 1995; Popescu et al., 2010) Glutathione is an NMDA receptor agonist (CHUEH, 2006; Rosa et al., 2013) and sarcosine is an NMDA receptor co-agonist (Zhang et al., 2009; Huang et al., 2013). The role of serine as a potent co-agonist of NMDA receptor has been demonstrated. (Mothet et al., 2000; Panatier et al., 2006) In addition, taurine is suggested to interact directly with NMDA receptor and regulates its function (Suárez and Solís, 2006).

Maes et al. found that low serum levels of asparagine, serine and taurine levels characterized non-responder patients after 5-weeks of antidepressants treatment (Maes et al., 1998). In addition, glutathione, sarcosine and taurine administration have antidepressant-like effects suggesting the here found elevated levels might be relevant for the favorable paroxetine response (Huang et al., 2013; Rosa et al., 2013; Toyoda and Iio, 2013).

The different glutamatergic pathway activity is also reflected in MDD patients' PBMCs by the observed sGC- $\beta$ 1 protein levels, which is downstream of the glutamatergic pathway.

Taken together, my study suggests that monitoring glutamatergic pathway protein and metabolite levels can be used to determine whether paroxetine-treated patients with depressive disorders are responding to the drug.

### 4.3. Ubiquitin-proteasome system pathway

No significant mRNA level differences for NRs, PSD-95 and nNOS were found between PLF and PSF groups suggesting that post-translational modifications might be relevant instead. Supporting this notion I found proteomics signatures involved in the UPS pathway that significantly differed between the two groups. While my data indicate that ubiquitination is not associated with differential protein expression levels in paroxetine-treated mice, PM2A protein and total ubiquitination level differences suggest potential roles in the antidepressant treatment response.

Protein analyses of PBMCs showed that UBS pathway components including PM2A and ubiquitination can separate antidepressant treatment responder/non-responder patients. Especially PM2A levels were significantly lower at T6 only in antidepressant responder patients and could be used to monitor and determine the antidepressant treatment response. In addition, ubiquitination at baseline may be used

to predict the response to antidepressant treatment, as its levels stayed low in antidepressant responder patients at T0 and T6 compared to non-responder patients. Evidence from other studies suggests that the UPS may be linked to MDD treatment. In this regard, it has been shown that SNPs in proteasome subunit  $\alpha 7$  (PSMA7), proteasome 26S non-ATPase subunit 9 (PSMD9) and proteasome 26S non-ATPase subunit 13 (PSMD13) are associated with clinical antidepressant response (Wong et al., 2008; Gragnoli, 2014). Data from my thesis project suggest that UPS protein signatures such as PM2A and ubiquitination levels could be used to assess antidepressant treatment outcome. Especially ubiquitination levels at baseline may be able to predict the response to antidepressant treatment. As stressful events are known to alter the UPS pathway (Ryan et al., 2006; Karssen et al., 2007; Minelli et al., 2015), higher ubiquitination levels in antidepressant non-responder patients might be a reflection of that. Despite the fact that data from the present study failed to show a significant correlation between baseline ubiquitination levels and clinical antidepressant treatment response (Figure 55), the inclusion of larger sample size may increase predictability power of the analysis.

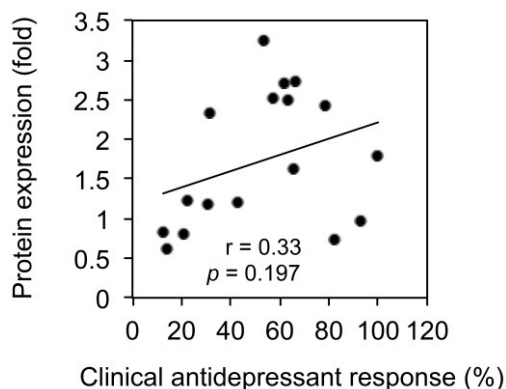


**Figure 55.** Correlation between baseline ubiquitination levels and clinical antidepressant response. Baseline ubiquitination levels did not show significant correlation with HDRS score changes after treatment. Pearson correlation coefficients ( $r$ ) with  $P$  values are indicated in the correlation graphs.

UPS was shown to be involved in the regulation of various neuronal pathways including synaptic formation and function (Yi and Ehlers, 2007). In light of this, significant differences of PM2A and ubiquitination levels between antidepressant responder and non-responder mice and humans implicate a potential involvement of systemic molecular pathways. For example, UPS has been shown to mediate NMDA

receptor degradation (Kato et al., 2005; Yi and Ehlers, 2007; Tsai, 2014). Tai *et al.* reported that NMDA treatment of cultured hippocampal neurons decreases UPS activity, suggesting an interaction between glutamatergic and proteasome pathways (Tai et al., 2010). This is in agreement with my data, which also point towards an involvement of both pathways in the different response of the PLF and PSF mouse groups. Although my results indicate that ubiquitination does not seem to be associated with the regulation of NMDA receptor/PSD-95 protein levels in the paroxetine-treated mice, my proteomics analysis significantly enriched the UPS pathway (Figure 56). The relationship of UPS and glutamatergic pathways is of interest and should be further explored in the future.

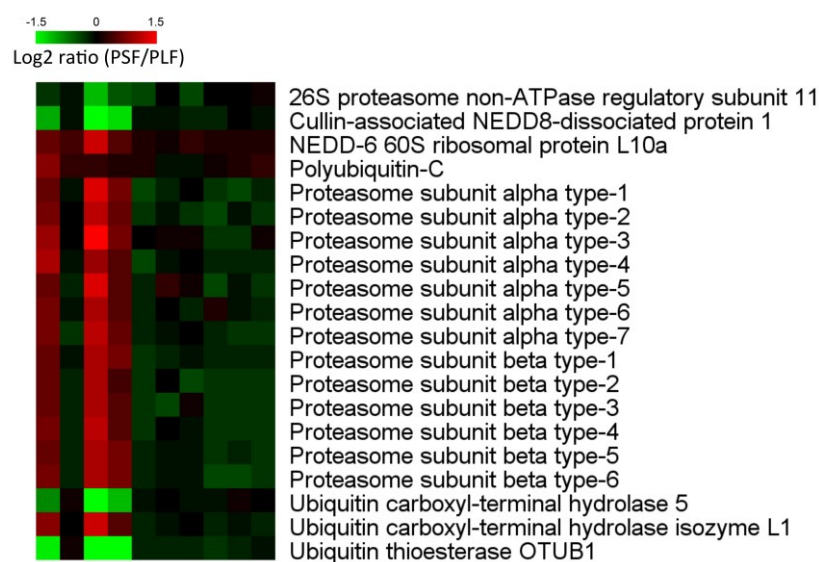


**Figure 56.** A heatmap of hippocampal UPS pathway proteins comparing PLF and PSF groups. In the heatmap, colors denote  $\log_2$  ratio. Proteins with adjusted  $p$  value  $< 0.05$  were considered significant,  $n=5/\text{group}$ .

Kaminsky and Kosenko showed that MK-801, an NMDA receptor blocker, and sodium nitroprusside, an NO donor, were able to modulate brain purine metabolism activity suggesting a functional involvement of NMDA receptor and nitric oxide in purine metabolism pathway (Kaminsky and Kosenko, 2009). GDA, which catalyzes conversion of guanine to xanthine in the purine metabolism pathway (Yuan et al., 1999; Paletzki, 2002), was found to be important for neuronal dendrite branching by regulating postsynaptic trafficking of PSD-95 protein, a major component of the glutamatergic synapse (Firestein et al., 1999). Antidepressant-like and neuroprotective effects of pyrimidines including cytidine and uridine have been linked to the

regulation of glutamatergic neurotransmission (Mir et al., 2003; Hurtado et al., 2005; Radad et al., 2007; Yoon et al., 2009). In this context, illuminating the crosstalk between purine/pyrimidine metabolism and glutamatergic pathways may aid in an improved understanding of their functions in the pathobiology of MDD and its treatment.

Whether the pathways I have identified in the mouse will qualify as predictive biosignatures for the antidepressant treatment response in patients and routine use in the clinic remains to be further investigated. Eventually biomarkers for the antidepressant treatment response will enable patient sub-group stratification and will render clinical decision making more objective to realize a personalized psychiatry approach.

#### 4.4. Outlook

This study aimed at the molecular delineation of the chronic antidepressant treatment response in mice, and validation in MDD patients' PBMCs. While my integrated -omics analyses of the hippocampus revealed novel pathways and biomarker candidates, additional analyses of other brain regions that are implicated in neuropsychiatric disorders may provide a more systemic understanding related to the antidepressant response heterogeneity.

As shown in previous reports several metabolites seem to play a role in the regulation of mood status and have potential to be used as supplements in treating psychiatric disorders (Papakostas et al., 2012; Foster and McVey Neufeld, 2013; Slyepchenko et al., 2014). Based on the dynamic changes of the metabolome in response to antidepressant treatment, the effect of nutritional supplements are also of great interest.

Conventional mental disorder diagnosis systems may benefit from Research Domain Criteria (RDoC), a new research framework initiated by the *U.S. National Institute of Mental Health*. Integration of multi-dimensional data from genomics to clinical reports can reduce the gap between molecular research and clinical practice, and therefore is expected to provide new evidence and perspectives on classification and treatment decision of neuropsychiatric disorders.

## Appendix

### References

Alexander, B., Warner-Schmidt, J., Eriksson, T., Tamminga, C., Arango-Lievano, M., Arango-Llievano, M., Ghose, S., Vernov, M., Stavarache, M., Stavarache, M., et al. (2010). Reversal of depressed behaviors in mice by p11 gene therapy in the nucleus accumbens. *Sci Transl Med* 2, 54ra76.

Altamura, C.A., Mauri, M.C., Ferrara, A., Moro, A.R., D'Andrea, G., and Zamberlan, F. (1993). Plasma and platelet excitatory amino acids in psychiatric disorders. *Am J Psychiatry* 150, 1731–1733.

Anacker, C., Zunszain, P.A., Cattaneo, A., Carvalho, L.A., Garabedian, M.J., Thuret, S., Price, J., and Pariante, C.M. (2011). Antidepressants increase human hippocampal neurogenesis by activating the glucocorticoid receptor. *Mol. Psychiatry* 16, 738–750.

Anisman, H., Du, L., Palkovits, M., Faludi, G., Kovacs, G.G., Szontagh-Kishazi, P., Merali, Z., and Poulter, M.O. (2008). Serotonin receptor subtype and p11 mRNA expression in stress-relevant brain regions of suicide and control subjects. *J Psychiatry Neurosci* 33, 131–141.

Appel, K., Schwahn, C., Mahler, J., Schulz, A., Spitzer, C., Fenske, K., Stender, J., Barnow, S., John, U., Teumer, A., et al. (2011). Moderation of adult depression by a polymorphism in the FKBP5 gene and childhood physical abuse in the general population. *Neuropsychopharmacology* 36, 1982–1991.

Arias, B., Catalán, R., Gastó, C., Gutiérrez, B., and Fañanás, L. (2003). 5-HTTLPR polymorphism of the serotonin transporter gene predicts non-remission in major depression patients treated with citalopram in a 12-weeks follow up study. *J Clin Psychopharmacol* 23, 563–567.

Armitage, E.G., and Barbas, C. (2014). Metabolomics in cancer biomarker discovery: current trends and future perspectives. *J Pharm Biomed Anal* 87, 1–11.

Baba, H., Suzuki, T., Arai, H., and Emson, P.C. (2004). Expression of nNOS and soluble guanylate cyclase in schizophrenic brain. *Neuroreport* 15, 677–680.

Banasr, M., Valentine, G.W., Li, X.-Y., Gourley, S.L., Taylor, J.R., and Duman, R.S. (2007). Chronic unpredictable stress decreases cell proliferation in the cerebral cortex of the adult rat. *Biol. Psychiatry* 62, 496–504.

Bao, X., Pal, R., Hascup, K.N., Wang, Y., Wang, W.-T., Xu, W., Hui, D., Agbas, A., Wang, X., Michaelis, M.L., et al. (2009). Transgenic expression of Glud1 (glutamate

dehydrogenase 1) in neurons: in vivo model of enhanced glutamate release, altered synaptic plasticity, and selective neuronal vulnerability. *J. Neurosci.* *29*, 13929–13944.

Barbon, A., Popoli, M., La Via, L., Moraschi, S., Vallini, I., Tardito, D., Tiraboschi, E., Musazzi, L., Giambelli, R., Gennarelli, M., et al. (2006). Regulation of editing and expression of glutamate alpha-amino-propionic-acid (AMPA)/kainate receptors by antidepressant drugs. *Biol. Psychiatry* *59*, 713–720.

Bares, M., Brunovsky, M., Kopecek, M., Stopkova, P., Novak, T., Kozeny, J., and Hoschl, C. (2007). Changes in QEEG prefrontal cordance as a predictor of response to antidepressants in patients with treatment resistant depressive disorder: a pilot study. *J Psychiatr Res* *41*, 319–325.

Baumann, B., Danos, P., Krell, D., Diekmann, S., Leschinger, A., Stauch, R., Wurthmann, C., Bernstein, H.G., and Bogerts, B. (1999). Reduced volume of limbic system-affiliated basal ganglia in mood disorders: preliminary data from a postmortem study. *J Neuropsychiatry Clin Neurosci* *11*, 71–78.

Beautrais, A.L., Joyce, P.R., Mulder, R.T., Fergusson, D.M., Deavoll, B.J., and Nightingale, S.K. (1996). Prevalence and comorbidity of mental disorders in persons making serious suicide attempts: a case-control study. *Am J Psychiatry* *153*, 1009–1014.

Binder, E.B. (2009). The role of FKBP5, a co-chaperone of the glucocorticoid receptor in the pathogenesis and therapy of affective and anxiety disorders. *Psychoneuroendocrinology* *34 Suppl 1*, S186–S195.

Binder, E.B., Künzel, H.E., Nickel, T., Kern, N., Pfennig, A., Majer, M., Uhr, M., Ising, M., and Holsboer, F. (2008). HPA-axis regulation at in-patient admission is associated with antidepressant therapy outcome in male but not in female depressed patients. *Psychoneuroendocrinology* *34*, 99–109.

Bonanno, G., Giambelli, R., Raiteri, L., Tiraboschi, E., Zappettini, S., Musazzi, L., Raiteri, M., Racagni, G., and Popoli, M. (2005). Chronic antidepressants reduce depolarization-evoked glutamate release and protein interactions favoring formation of SNARE complex in hippocampus. *J. Neurosci.* *25*, 3270–3279.

Boyer, P.A., Skolnick, P., and Fossom, L.H. (1998). Chronic administration of imipramine and citalopram alters the expression of NMDA receptor subunit mRNAs in mouse brain. A quantitative in situ hybridization study. *J. Mol. Neurosci.* *10*, 219–233.

Bredt, D.S., and Snyder, S.H. (1989). Nitric oxide mediates glutamate-linked enhancement of cGMP levels in the cerebellum. *Proc. Natl. Acad. Sci. U.S.A.* *86*, 9030–9033.

Bremner, J.D., Vythilingam, M., Vermetten, E., Nazeer, A., Adil, J., Khan, S., Staib, L.H., and Charney, D.S. (2002). Reduced volume of orbitofrontal cortex in major depression. *Biol. Psychiatry* *51*, 273–279.

Brocardo, P.S., Budni, J., Kaster, M.P., Santos, A.R.S., and Rodrigues, A.L.S. (2008). Folic acid administration produces an antidepressant-like effect in mice: evidence for

the involvement of the serotonergic and noradrenergic systems. *Neuropharmacology* 54, 464–473.

Calabrese, F., Guidotti, G., Molteni, R., Racagni, G., Mancini, M., and Riva, M.A. (2012). Stress-induced changes of hippocampal NMDA receptors: modulation by duloxetine treatment. *PLoS ONE* 7, e37916.

Campbell, S., Marriott, M., Nahmias, C., and MacQueen, G.M. (2004). Lower hippocampal volume in patients suffering from depression: a meta-analysis. *Am J Psychiatry* 161, 598–607.

Carlezon, W.A., Mague, S.D., Parow, A.M., Stoll, A.L., Cohen, B.M., and Renshaw, P.F. (2005). Antidepressant-like effects of uridine and omega-3 fatty acids are potentiated by combined treatment in rats. *Biol. Psychiatry* 57, 343–350.

Carlezon, W.A., Pliakas, A.M., Parow, A.M., Detke, M.J., Cohen, B.M., and Renshaw, P.F. (2002). Antidepressant-like effects of cytidine in the forced swim test in rats. *Biol. Psychiatry* 51, 882–889.

Carpenter, L.L., Jovic, Z., Hall, J.M., Rasmussen, S.A., and Price, L.H. (1998). Mirtazapine augmentation in the treatment of refractory depression. *J Clin Psychiatry* 60, 45–49.

Cebers, G., Cebere, A., Kovács, A.D., Högberg, H., Moreira, T., and Liljequist, S. (2001). Increased ambient glutamate concentration alters the expression of NMDA receptor subunits in cerebellar granule neurons. *Neurochem. Int.* 39, 151–160.

Cebers, G., Cebere, A., Wägner, A., and Liljequist, S. (1999). Prolonged inhibition of glutamate reuptake down-regulates NMDA receptor functions in cultured cerebellar granule cells. *J. Neurochem.* 72, 2181–2190.

Chen, Z.-Y., Jing, D., Bath, K.G., Ieraci, A., Khan, T., Siao, C.-J., Herrera, D.G., Toth, M., Yang, C., McEwen, B.S., et al. (2006). Genetic variant BDNF (Val66Met) polymorphism alters anxiety-related behavior. *Science* 314, 140–143.

Chrapko, W., Jurasz, P., Radomski, M.W., Archer, S.L., Newman, S.C., Baker, G., Lara, N., and Le Mellédo, J.-M. (2006). Alteration of decreased plasma NO metabolites and platelet NO synthase activity by paroxetine in depressed patients. *Neuropsychopharmacology* 31, 1286–1293.

CHUEH, S. (2006). S-Nitrosoglutathione and glutathione act as NMDA receptor agonists in cultured hippocampal neurons. *Acta Pharmacol. Sin.*

Cook, I.A., Leuchter, A.F., Morgan, M., Witte, E., Stubbeman, W.F., Abrams, M., Rosenberg, S., and Uijtdehaage, S.H.J. (2002). Early changes in prefrontal activity characterize clinical responders to antidepressants. *Neuropsychopharmacology* 27, 120–131.

Cook, I.A., Leuchter, A.F., Morgan, M.L., Stubbeman, W., Siegman, B., and Abrams, M. (2005). Changes in prefrontal activity characterize clinical response in SSRI nonresponders: a pilot study. *J Psychiatr Res* 39, 461–466.

- Cook, S.C., and Wellman, C.L. (2004). Chronic stress alters dendritic morphology in rat medial prefrontal cortex. *J. Neurobiol.* *60*, 236–248.
- Cremona, O., Di Paolo, G., Wenk, M.R., Lüthi, A., Kim, W.T., Takei, K., Daniell, L., Nemoto, Y., Shears, S.B., Flavell, R.A., et al. (1999). Essential role of phosphoinositide metabolism in synaptic vesicle recycling. *Cell* *99*, 179–188.
- D'Aquila, P.S., Collu, M., Gessa, G.L., and Serra, G. (2000). The role of dopamine in the mechanism of action of antidepressant drugs. *Eur. J. Pharmacol.* *405*, 365–373.
- Dam, H., Møllerup, E.T., and Rafaelsen, O.J. (1985). The dexamethasone suppression test in depression. *J Affect Disord* *8*, 95–103.
- De Kloet, E.R. (2004). Hormones and the stressed brain. *Ann N Y Acad Sci* *1018*, 1–15.
- de Montigny, C., Cournoyer, G., Morissette, R., Langlois, R., and Caillé, G. (1983). Lithium carbonate addition in tricyclic antidepressant-resistant unipolar depression. Correlations with the neurobiologic actions of tricyclic antidepressant drugs and lithium ion on the serotonin system. *Arch. Gen. Psychiatry* *40*, 1327–1334.
- Dell'Osso, B., Palazzo, M.C., Oldani, L., and Altamura, A.C. (2011). The noradrenergic action in antidepressant treatments: pharmacological and clinical aspects. *CNS Neurosci Ther* *17*, 723–732.
- Dhir, A., and Kulkarni, S. (2007). Involvement of nitric oxide (NO) signaling pathway in the antidepressant action of bupropion, a dopamine reuptake inhibitor. *Eur. J. Pharmacol.*
- Dierckx, B., Heijnen, W.T., van den Broek, W.W., and Birkenhäger, T.K. (2012). Efficacy of electroconvulsive therapy in bipolar versus unipolar major depression: a meta-analysis. *Bipolar Disord* *14*, 146–150.
- Domon, B., and Aebersold, R. (2010). Options and considerations when selecting a quantitative proteomics strategy. *Nat Biotechnol* *28*, 710–721.
- Doucet, M.V., Levine, H., Dev, K.K., and Harkin, A. (2013). Small-molecule inhibitors at the PSD-95/nNOS interface have antidepressant-like properties in mice. *Neuropsychopharmacology* *38*, 1575–1584.
- Drevets, W.C., Price, J.L., Simpson, J.R., Todd, R.D., Reich, T., Vannier, M., and Raichle, M.E. (1997). Subgenual prefrontal cortex abnormalities in mood disorders. *Nature* *386*, 824–827.
- Drevets, W.C., Videen, T.O., Price, J.L., Preskorn, S.H., Carmichael, S.T., and Raichle, M.E. (1992). A functional anatomical study of unipolar depression. *J. Neurosci.* *12*, 3628–3641.
- Drevets, W.C., Zarate, C.A., and Furey, M.L. (2013). Antidepressant effects of the muscarinic cholinergic receptor antagonist scopolamine: a review. *Biol. Psychiatry* *73*, 1156–1163.

- Droy-Dupré, L., Bossard, C., Volteau, C., Bezieau, S., Laboisse, C.L., and Mosnier, J.-F. (2015). Hierarchical clustering identifies a subgroup of colonic adenocarcinomas expressing crypt-like differentiation markers, associated with MSS status and better prognosis. *Virchows Arch.* *466*, 383–391.
- Dwivedi, Y. (2009). Brain-derived neurotrophic factor: role in depression and suicide. *Neuropsychiatr Dis Treat* *5*, 433–449.
- Dwivedi, Y., Rizavi, H.S., Roberts, R.C., Conley, R.C., Tamminga, C.A., and Pandey, G.N. (2001). Reduced activation and expression of ERK1/2 MAP kinase in the post-mortem brain of depressed suicide subjects. *J. Neurochem.* *77*, 916–928.
- Elfving, B., Plougmann, P.H., Müller, H.K., Mathé, A.A., Rosenberg, R., and Wegener, G. (2010). Inverse correlation of brain and blood BDNF levels in a genetic rat model of depression. *Int. J. Neuropsychopharmacol.* *13*, 563–572.
- Elovainio, M., Aalto, A.-M., Kivimäki, M., Pirkola, S., Sundvall, J., Lönnqvist, J., and Reunanen, A. (2009). Depression and C-reactive protein: population-based Health 2000 Study. *Psychosom Med* *71*, 423–430.
- Fabbri, C., Drago, A., and Serretti, A. (2013). Early antidepressant efficacy modulation by glutamatergic gene variants in the STAR\*D. *Eur Neuropsychopharmacol* *23*, 612–621.
- Fava, M., Rosenbaum, J.F., McGrath, P.J., Stewart, J.W., Amsterdam, J.D., and Quitkin, F.M. (1994). Lithium and tricyclic augmentation of fluoxetine treatment for resistant major depression: a double-blind, controlled study. *Am J Psychiatry* *151*, 1372–1374.
- Fedele, E., Marchi, M., and Raiteri, M. (2001). In vivo NO/cGMP signalling in the hippocampus. *Neurochem. Res.* *26*, 1069–1078.
- Feng, L., Xu, Y., Zhang, Y., Sun, Z., Han, J., Zhang, C., Yang, H., Shang, D., Su, F., Shi, X., et al. (2015). Subpathway-GMir: identifying miRNA-mediated metabolic subpathways by integrating condition-specific genes, microRNAs, and pathway topologies. *Oncotarget* *6*, 39151–39164.
- Ferreri, M., Lavergne, F., Berlin, I., Payan, C., and Puech, A.J. (2001). Benefits from mianserin augmentation of fluoxetine in patients with major depression non-responders to fluoxetine alone. *Acta Psychiatr Scand* *103*, 66–72.
- Filiou, M.D., Zhang, Y., Teplytska, L., Reckow, S., Gormanns, P., Maccarrone, G., Frank, E., Kessler, M.S., Hamsch, B., Nussbaumer, M., et al. (2011). Proteomics and metabolomics analysis of a trait anxiety mouse model reveals divergent mitochondrial pathways. *Biol. Psychiatry* *70*, 1074–1082.
- Finkel, M.S., Laghrissi-Thode, F., Pollock, B.G., and Rong, J. (1996). Paroxetine is a novel nitric oxide synthase inhibitor. *Psychopharmacol Bull* *32*, 653–658.
- Firestein, B.L., Firestein, B.L., Brenman, J.E., Aoki, C., Sanchez-Perez, A.M., El-Husseini, A.E., and Bredt, D.S. (1999). Cypin: a cytosolic regulator of PSD-95 postsynaptic targeting. *Neuron* *24*, 659–672.

- Fitzgerald, P., O'Brien, S.M., Scully, P., Rijkers, K., Scott, L.V., and Dinan, T.G. (2006). Cutaneous glucocorticoid receptor sensitivity and pro-inflammatory cytokine levels in antidepressant-resistant depression. *Psychol Med* 36, 37–43.
- Ford, D.E., and Erlinger, T.P. (2004). Depression and C-reactive protein in US adults: data from the Third National Health and Nutrition Examination Survey. *Arch. Intern. Med.* 164, 1010–1014.
- Foster, J.A., and McVey Neufeld, K.-A. (2013). Gut-brain axis: how the microbiome influences anxiety and depression. *Trends Neurosci* 36, 305–312.
- Fountoulakis, K.N., Gonda, X., Rihmer, Z., Fokas, C., and Iacovides, A. (2008). Revisiting the Dexamethasone Suppression Test in unipolar major depression: an exploratory study. *Ann Gen Psychiatry* 7, 22.
- Furey, M.L., and Drevets, W.C. (2006). Antidepressant efficacy of the antimuscarinic drug scopolamine: a randomized, placebo-controlled clinical trial. *Arch. Gen. Psychiatry* 63, 1121–1129.
- Gassen, N.C., Hartmann, J., Zannas, A.S., Kretschmar, A., Zschocke, J., Maccarrone, G., Hafner, K., Zellner, A., Kollmannsberger, L.K., Wagner, K.V., et al. (2016). FKBP51 inhibits GSK3 $\beta$  and augments the effects of distinct psychotropic medications. *Mol. Psychiatry* 21, 277–289.
- Gassen, N.C., Hartmann, J., Zschocke, J., Stepan, J., Hafner, K., Zellner, A., Kirmeier, T., Kollmannsberger, L., Wagner, K.V., Dedic, N., et al. (2014). Association of FKBP51 with priming of autophagy pathways and mediation of antidepressant treatment response: evidence in cells, mice, and humans. *PLoS Med.* 11, e1001755.
- George, M.S., Wassermann, E.M., Williams, W.A., Callahan, A., Ketter, T.A., Basser, P., Hallett, M., and Post, R.M. (1995). Daily repetitive transcranial magnetic stimulation (rTMS) improves mood in depression. *Neuroreport* 6, 1853–1856.
- Gex-Fabry, M., Eap, C.B., Oneda, B., Gervasoni, N., Aubry, J.-M., Bondolfi, G., and Bertschy, G. (2008). CYP2D6 and ABCB1 genetic variability: influence on paroxetine plasma level and therapeutic response. *Ther Drug Monit* 30, 474–482.
- Ghasemi, M., Sadeghipour, H., Mosleh, A., Sadeghipour, H.R., Mani, A.R., and Dehpour, A.R. (2008). Nitric oxide involvement in the antidepressant-like effects of acute lithium administration in the mouse forced swimming test. *Eur Neuropsychopharmacol* 18, 323–332.
- Gilbody, S., Lewis, S., and Lightfoot, T. (2007). Methylene tetrahydrofolate reductase (MTHFR) genetic polymorphisms and psychiatric disorders: a HuGE review. *Am. J. Epidemiol.* 165, 1–13.
- Gould, T.D., Zarate, C.A., and Manji, H.K. (2004). Glycogen synthase kinase-3: a target for novel bipolar disorder treatments. *J Clin Psychiatry* 65, 10–21.
- Gourley, S., Wu, F., Kiraly, D., Ploski, J., and Kedves, A. (2008). Regionally specific regulation of ERK MAP kinase in a model of antidepressant-sensitive chronic depression. *Biological* ....

- Gragoli, C. (2014). Proteasome modulator 9 gene SNPs, responsible for anti-depressant response, are in linkage with generalized anxiety disorder. *J. Cell. Physiol.* 229, 1157–1159.
- Griffiths, W.J., Koal, T., Wang, Y., Kohl, M., Enot, D.P., and Deigner, H.-P. (2010). Targeted metabolomics for biomarker discovery. *Angew Chem Int Ed Engl* 49, 5426–5445.
- Guest, P.C., Martins-de-Souza, D., Schwarz, E., Rahmoune, H., Alsaif, M., Tomasik, J., Turck, C.W., and Bahn, S. (2013). Proteomic profiling in schizophrenia: enabling stratification for more effective treatment. *Genome Med* 5, 25.
- Gurbuz Ozgur, B., Aksu, H., Birincioglu, M., and Dost, T. (2015). Antidepressant-like effects of the xanthine oxidase enzyme inhibitor allopurinol in rats. A comparison with fluoxetine. *Pharmacol Biochem Behav* 138, 91–95.
- Guzzetti, S., Calcagno, E., Canetta, A., Sacchetti, G., Fracasso, C., Caccia, S., Cervo, L., and Invernizzi, R.W. (2008). Strain differences in paroxetine-induced reduction of immobility time in the forced swimming test in mice: role of serotonin. *Eur. J. Pharmacol.* 594, 117–124.
- Ham, B.-J., Lee, B.-C., Paik, J.-W., Kang, R.-H., Choi, M.-J., Choi, I.-G., and Lee, M.-S. (2007). Association between the tryptophan hydroxylase-1 gene A218C polymorphism and citalopram antidepressant response in a Korean population. *Prog. Neuropsychopharmacol. Biol. Psychiatry* 31, 104–107.
- Hamilton, J.P., Siemer, M., and Gotlib, I.H. (2008). Amygdala volume in major depressive disorder: a meta-analysis of magnetic resonance imaging studies. *Mol. Psychiatry* 13, 993–1000.
- Hansen, K.F., and Obrietan, K. (2013). MicroRNA as therapeutic targets for treatment of depression. *Neuropsychiatr Dis Treat* 9, 1011–1021.
- Hastings, R.S., Parsey, R.V., Oquendo, M.A., Arango, V., and Mann, J.J. (2004). Volumetric analysis of the prefrontal cortex, amygdala, and hippocampus in major depression. *Neuropsychopharmacology* 29, 952–959.
- Healy, D. (2000). The case for an individual approach to the treatment of depression. *J Clin Psychiatry* 61 Suppl 6, 18–23.
- Heller, A.S., Johnstone, T., Shackman, A.J., Light, S.N., Peterson, M.J., Kolden, G.G., Kalin, N.H., and Davidson, R.J. (2009). Reduced capacity to sustain positive emotion in major depression reflects diminished maintenance of fronto-striatal brain activation. *Proc. Natl. Acad. Sci. U.S.A.* 106, 22445–22450.
- Heninger, G.R., Charney, D.S., and Sternberg, D.E. (1983). Lithium carbonate augmentation of antidepressant treatment. An effective prescription for treatment-refractory depression. *Arch. Gen. Psychiatry* 40, 1335–1342.
- Herrera-Ruiz, M., Zamilpa, A., González-Cortazar, M., Reyes-Chilpa, R., León, E., García, M.P., Tortoriello, J., and Huerta-Reyes, M. (2011). Antidepressant effect and pharmacological evaluation of standardized extract of flavonoids from *Byrsonima*

- crassifolia. *Phytomedicine* 18, 1255–1261.
- Hickman, R., Khambaty, T., and Stewart, J. (2014a). C-reactive protein is elevated in atypical but not nonatypical depression: data from the National Health and Nutrition Examination Survey (NHANES) 1999–2004. *J Behav Med*.
- Hickman, R.J., Khambaty, T., and Stewart, J.C. (2014b). C-reactive protein is elevated in atypical but not nonatypical depression: data from the National Health and Nutrition Examination survey (NHANES) 1999–2004. *J Behav Med* 37, 621–629.
- Hiemke, C., Baumann, P., Bergemann, N., Conca, A., Dietmaier, O., Egberts, K., Fric, M., Gerlach, M., Greiner, C., Gründer, G., et al. (2011). AGNP consensus guidelines for therapeutic drug monitoring in psychiatry: update 2011. *Pharmacopsychiatry* 44, 195–235.
- Hiroaki-Sato, V.A., Sales, A.J., Biojone, C., and Joca, S.R.L. (2014). Hippocampal nNOS inhibition induces an antidepressant-like effect: involvement of 5HT1A receptors. *Behav Pharmacol* 25, 187–196.
- Holderbach, R., Clark, K., Moreau, J., and Bischofberger, J. (2007). Enhanced long-term synaptic depression in an animal model of depression. *Biological ....*
- Hori, H., Sasayama, D., Teraishi, T., Yamamoto, N., Nakamura, S., Ota, M., Hattori, K., Kim, Y., Higuchi, T., and Kunugi, H. (2016). Blood-based gene expression signatures of medication-free outpatients with major depressive disorder: integrative genome-wide and candidate gene analyses. *Sci Rep* 6, 18776.
- Howren, M.B., Lamkin, D.M., and Suls, J. (2009). Associations of depression with C-reactive protein, IL-1, and IL-6: a meta-analysis. *Psychosom Med* 71, 171–186.
- Huang, C.-C., Wei, I.-H., Huang, C.-L., Chen, K.-T., Tsai, M.-H., Tsai, P., Tun, R., Huang, K.-H., Chang, Y.-C., Lane, H.-Y., et al. (2013). Inhibition of glycine transporter-I as a novel mechanism for the treatment of depression. *Biol. Psychiatry* 74, 734–741.
- Huang, D.W., Sherman, B.T., Tan, Q., Kir, J., Liu, D., Bryant, D., Guo, Y., Stephens, R., Baseler, M.W., Lane, H.C., et al. (2007). DAVID Bioinformatics Resources: expanded annotation database and novel algorithms to better extract biology from large gene lists. *Nucleic Acids Res.* 35, W169–W175.
- Huezo-Diaz, P., Uher, R., Smith, R., Rietschel, M., Henigsberg, N., Marusic, A., Mors, O., Maier, W., Hauser, J., Souery, D., et al. (2009). Moderation of antidepressant response by the serotonin transporter gene. *Br J Psychiatry* 195, 30–38.
- Hurtado, O., Moro, M.A., Cárdenas, A., Sánchez, V., Fernández-Tomé, P., Leza, J.C., Lorenzo, P., Secades, J.J., Lozano, R., Dávalos, A., et al. (2005). Neuroprotection afforded by prior citicoline administration in experimental brain ischemia: effects on glutamate transport. *Neurobiol. Dis.* 18, 336–345.
- Inoue, K., Tsutsui, H., Akatsu, H., Hashizume, Y., Matsukawa, N., Yamamoto, T., and Toyo'oka, T. (2013). Metabolic profiling of Alzheimer's disease brains. *Sci Rep* 3, 2364.

- Jaffe, R.J., Novakovic, V., and Peselow, E.D. (2013). Scopolamine as an antidepressant: a systematic review. *Clin Neuropharmacol* 36, 24–26.
- Jesse, C., Bortolatto, C., and Savegnago, L. (2008). Involvement of l-arginine–nitric oxide–cyclic guanosine monophosphate pathway in the antidepressant-like effect of tramadol in the rat forced swimming test. *Progress in Neuro-* ....
- Joaquim, H.P.G., Talib, L.L., Forlenza, O.V., Diniz, B.S., and Gattaz, W.F. (2012). Long-term sertraline treatment increases expression and decreases phosphorylation of glycogen synthase kinase-3B in platelets of patients with late-life major depression. *J Psychiatr Res* 46, 1053–1058.
- Joca, S.R.L., and Guimarães, F.S. (2006). Inhibition of neuronal nitric oxide synthase in the rat hippocampus induces antidepressant-like effects. *Psychopharmacology (Berl.)* 185, 298–305.
- Joffe, R.T. (1997). Refractory depression: treatment strategies, with particular reference to the thyroid axis. *J Psychiatry Neurosci* 22, 327–331.
- Joffe, R.T., and Schuller, D.R. (1993). An open study of buspirone augmentation of serotonin reuptake inhibitors in refractory depression. *J Clin Psychiatry* 54, 269–271.
- Jun, H., Mohammed Qasim Hussaini, S., Rigby, M.J., and Jang, M.-H. (2012). Functional role of adult hippocampal neurogenesis as a therapeutic strategy for mental disorders. *Neural Plast.* 2012, 854285.
- Kaminsky, Y., and Kosenko, E. (2009). Brain purine metabolism and xanthine dehydrogenase/oxidase conversion in hyperammonemia are under control of NMDA receptors and nitric oxide. *Brain Res.* 1294, 193–201.
- Karege, F., Bondolfi, G., Gervasoni, N., Schwald, M., Aubry, J.-M., and Bertschy, G. (2005). Low brain-derived neurotrophic factor (BDNF) levels in serum of depressed patients probably results from lowered platelet BDNF release unrelated to platelet reactivity. *Biol. Psychiatry* 57, 1068–1072.
- Karege, F., Perret, G., Bondolfi, G., Schwald, M., Bertschy, G., and Aubry, J.-M. (2002). Decreased serum brain-derived neurotrophic factor levels in major depressed patients. *Psychiatry Res* 109, 143–148.
- Karssen, A.M., Her, S., Li, J.Z., Patel, P.D., Meng, F., Bunney, W.E., Jones, E.G., Watson, S.J., Akil, H., Myers, R.M., et al. (2007). Stress-induced changes in primate prefrontal profiles of gene expression. *Mol. Psychiatry* 12, 1089–1102.
- Kaster, M.P., Budni, J., Gazal, M., Cunha, M.P., Santos, A.R.S., and Rodrigues, A.L.S. (2013). The antidepressant-like effect of inosine in the FST is associated with both adenosine A1 and A 2A receptors. *Purinergic Signal.* 9, 481–486.
- Kato, A., Rouach, N., Nicoll, R.A., and Brecht, D.S. (2005). Activity-dependent NMDA receptor degradation mediated by retrotranslocation and ubiquitination. *Proc. Natl. Acad. Sci. U.S.A.* 102, 5600–5605.
- Kellner, C.H., Greenberg, R.M., Murrugh, J.W., Bryson, E.O., Briggs, M.C., and

- Pasculli, R.M. (2012). ECT in treatment-resistant depression. *Am J Psychiatry* *169*, 1238–1244.
- Kennedy, S.H., Giacobbe, P., Rizvi, S.J., Placenza, F.M., Nishikawa, Y., Mayberg, H.S., and Lozano, A.M. (2011). Deep brain stimulation for treatment-resistant depression: follow-up after 3 to 6 years. *Am J Psychiatry* *168*, 502–510.
- Khalid, N., Atkins, M., Tredget, J., Giles, M., Champney-Smith, K., and Kirov, G. (2008). The effectiveness of electroconvulsive therapy in treatment-resistant depression: a naturalistic study. *J Ect* *24*, 141–145.
- Kim, J.J., and Diamond, D.M. (2002). The stressed hippocampus, synaptic plasticity and lost memories. *Nat. Rev. Neurosci.* *3*, 453–462.
- Kim, J.S., Schmid-Burgk, W., Claus, D., and Kornhuber, H.H. (1982). Increased serum glutamate in depressed patients. *Arch Psychiatr Nervenkr* (1970) *232*, 299–304.
- Kim, W.T., Chang, S., Daniell, L., Cremona, O., Di Paolo, G., and De Camilli, P. (2002). Delayed reentry of recycling vesicles into the fusion-competent synaptic vesicle pool in synaptotagmin 1 knockout mice. *Proc. Natl. Acad. Sci. U.S.A.* *99*, 17143–17148.
- Kocabas, N.A., Antonijevic, I., Faghel, C., Forray, C., Kasper, S., Lecrubier, Y., Linotte, S., Massat, I., Mendlewicz, J., Noro, M., et al. (2011). Brain-derived neurotrophic factor gene polymorphisms: influence on treatment response phenotypes of major depressive disorder. *Int Clin Psychopharmacol* *26*, 1–10.
- Kruger, M., Moser, M., Ussar, S., Thievensen, I., Luber, C.A., Forner, F., Schmidt, S., Zanivan, S., Fassler, R., and Mann, M. (2008). SILAC mouse for quantitative proteomics uncovers kindlin-3 as an essential factor for red blood cell function. *Cell* *134*, 353–364.
- Lally, N., Nugent, A.C., Luckenbaugh, D.A., Ameli, R., Roiser, J.P., and Zarate, C.A. (2014). Anti-anhedonic effect of ketamine and its neural correlates in treatment-resistant bipolar depression. *Transl Psychiatry* *4*, e469.
- Landeck, L., Kneip, C., Reischl, J., and Asadullah, K. (2016). Biomarkers and personalized medicine: current status and further perspectives with special focus on dermatology. *Exp Dermatol* *25*, 333–339.
- Lanquillon, S., Krieg, J.C., Bening-Abu-Shach, U., and Vedder, H. (2000). Cytokine production and treatment response in major depressive disorder. *Neuropsychopharmacology* *22*, 370–379.
- Lee, B.-H., and Kim, Y.-K. (2010). The roles of BDNF in the pathophysiology of major depression and in antidepressant treatment. *Psychiatry Investig* *7*, 231–235.
- Lee, J.C., Blumberger, D.M., Fitzgerald, P.B., Daskalakis, Z.J., and Levinson, A.J. (2012). The role of transcranial magnetic stimulation in treatment-resistant depression: a review. *Curr. Pharm. Des.* *18*, 5846–5852.
- Lee, M.M., Reif, A., and Schmitt, A.G. (2013). Major depression: a role for

- hippocampal neurogenesis? *Curr Top Behav Neurosci* 14, 153–179.
- Lekman, M., Laje, G., Charney, D., Rush, A.J., Wilson, A.F., Sorant, A.J.M., Lipsky, R., Wisniewski, S.R., Manji, H., McMahon, F.J., et al. (2008). The FKBP5-gene in depression and treatment response--an association study in the Sequenced Treatment Alternatives to Relieve Depression (STAR\*D) Cohort. *Biol. Psychiatry* 63, 1103–1110.
- Levine, J., Panchalingam, K., Rapoport, A., Gershon, S., McClure, R.J., and Pettegrew, J.W. (2000). Increased cerebrospinal fluid glutamine levels in depressed patients. *Biol. Psychiatry* 47, 586–593.
- Li, J., Li, C., Han, J., Zhang, C., Shang, D., Yao, Q., Zhang, Y., Xu, Y., Liu, W., Zhou, M., et al. (2014). The detection of risk pathways, regulated by miRNAs, via the integration of sample-matched miRNA-mRNA profiles and pathway structure. *J Biomed Inform* 49, 187–197.
- Liukkonen, T., Silvennoinen-Kassinen, S., Jokelainen, J., Räsänen, P., Leinonen, M., Meyer-Rochow, V.B., and Timonen, M. (2006). The association between C-reactive protein levels and depression: Results from the northern Finland 1966 birth cohort study. *Biol. Psychiatry* 60, 825–830.
- Lotrich, F.E., and Pollock, B.G. (2005). Candidate genes for antidepressant response to selective serotonin reuptake inhibitors. *Neuropsychiatr Dis Treat* 1, 17–35.
- Lovestone, S., Killick, R., Di Forti, M., and Murray, R. (2007). Schizophrenia as a GSK-3 dysregulation disorder. *Trends Neurosci*.
- López-Muñoz, F., and Alamo, C. (2009). Monoaminergic neurotransmission: the history of the discovery of antidepressants from 1950s until today. *Curr. Pharm. Des.* 15, 1563–1586.
- Lucae, S., Salyakina, D., Barden, N., Harvey, M., Gagné, B., Labbé, M., Binder, E.B., Uhr, M., Paez-Pereda, M., Sillaber, I., et al. (2006). P2RX7, a gene coding for a purinergic ligand-gated ion channel, is associated with major depressive disorder. *Hum. Mol. Genet.* 15, 2438–2445.
- Lüthi, A., Di Paolo, G., Cremona, O., Daniell, L., De Camilli, P., and McCormick, D.A. (2001). Synaptotagmin 1 contributes to maintaining the stability of GABAergic transmission in primary cultures of cortical neurons. *J. Neurosci.* 21, 9101–9111.
- MacMaster, F.P., and Kusumakar, V. (2004). MRI study of the pituitary gland in adolescent depression. *J Psychiatr Res* 38, 231–236.
- MacMaster, F.P., Russell, A., Mirza, Y., Keshavan, M.S., Taormina, S.P., Bhandari, R., Boyd, C., Lynch, M., Rose, M., Ivey, J., et al. (2006). Pituitary volume in treatment-naïve pediatric major depressive disorder. *Biol. Psychiatry* 60, 862–866.
- Maes, M., Libbrecht, I., van Hunsel, F., Campens, D., and Meltzer, H.Y. (1999). Pindolol and mianserin augment the antidepressant activity of fluoxetine in hospitalized major depressed patients, including those with treatment resistance. *J Clin Psychopharmacol* 19, 177–182.

- Maes, M., Vandoolaeghe, E., and Desnyder, R. (1996). Efficacy of treatment with trazodone in combination with pindolol or fluoxetine in major depression. *J Affect Disord* *41*, 201–210.
- Maes, M., Verkerk, R., Vandoolaeghe, E., Lin, A., and Scharpé, S. (1998). Serum levels of excitatory amino acids, serine, glycine, histidine, threonine, taurine, alanine and arginine in treatment-resistant depression: modulation by treatment with antidepressants and prediction of clinical responsiveness. *Acta Psychiatr Scand* *97*, 302–308.
- Mahar, I., Bambico, F.R., Mechawar, N., and Nobrega, J.N. (2014). Stress, serotonin, and hippocampal neurogenesis in relation to depression and antidepressant effects. *Neurosci Biobehav Rev* *38*, 173–192.
- Malagié, I., Trillat, A.C., Bourin, M., Jacquot, C., Hen, R., and Gardier, A.M. (2001). 5-HT<sub>1B</sub> Autoreceptors limit the effects of selective serotonin re-uptake inhibitors in mouse hippocampus and frontal cortex. *J. Neurochem.* *76*, 865–871.
- Malberg, J.E., Eisch, A.J., Nestler, E.J., and Duman, R.S. (2000). Chronic antidepressant treatment increases neurogenesis in adult rat hippocampus. *J. Neurosci.* *20*, 9104–9110.
- Malhi, G.S., Parker, G.B., Crawford, J., Wilhelm, K., and Mitchell, P.B. (2005). Treatment-resistant depression: resistant to definition? *Acta Psychiatr Scand* *112*, 302–309.
- Malkesman, O., Scattoni, M.L., Paredes, D., Tragon, T., Pearson, B., Shaltiel, G., Chen, G., Crawley, J.N., and Manji, H.K. (2010). The female urine sniffing test: a novel approach for assessing reward-seeking behavior in rodents. *Biol. Psychiatry* *67*, 864–871.
- Mani, M., Lee, S.Y., Lucast, L., Cremona, O., Di Paolo, G., De Camilli, P., and Ryan, T.A. (2007). The dual phosphatase activity of synaptojanin1 is required for both efficient synaptic vesicle endocytosis and reavailability at nerve terminals. *Neuron* *56*, 1004–1018.
- Martinez, J.M., Garakani, A., Yehuda, R., and Gorman, J.M. (2012). Proinflammatory and “resiliency” proteins in the CSF of patients with major depression. *Depress Anxiety* *29*, 32–38.
- Martinez-Turrillas, R., Frechilla, D., and Del Río, J. (2002). Chronic antidepressant treatment increases the membrane expression of AMPA receptors in rat hippocampus. *Neuropharmacology* *43*, 1230–1237.
- Mauri, M.C., Ferrara, A., Boscati, L., Bravin, S., Zamberlan, F., Alecci, M., and Invernizzi, G. (1998). Plasma and platelet amino acid concentrations in patients affected by major depression and under fluvoxamine treatment. *Neuropsychobiology* *37*, 124–129.
- Mayberg, H.S., Brannan, S.K., Tekell, J.L., Silva, J.A., Mahurin, R.K., McGinnis, S., and Jerabek, P.A. (2000). Regional metabolic effects of fluoxetine in major depression: serial changes and relationship to clinical response. *Biol. Psychiatry* *48*,

830–843.

Mayberg, H.S., Lozano, A.M., Voon, V., McNeely, H.E., Seminowicz, D., Hamani, C., Schwab, J.M., and Kennedy, S.H. (2005). Deep brain stimulation for treatment-resistant depression. *Neuron* *45*, 651–660.

Mayberg, H.S., Silva, J.A., Brannan, S.K., Tekell, J.L., Mahurin, R.K., McGinnis, S., and Jerabek, P.A. (2002). The functional neuroanatomy of the placebo effect. *Am J Psychiatry* *159*, 728–737.

Meissner, F., and Mann, M. (2014). Quantitative shotgun proteomics: considerations for a high-quality workflow in immunology. *Nat. Immunol.* *15*, 112–117.

Merriam, E.P., Thase, M.E., Haas, G.L., Keshavan, M.S., and Sweeney, J.A. (1999). Prefrontal cortical dysfunction in depression determined by Wisconsin Card Sorting Test performance. *Am J Psychiatry* *156*, 780–782.

Michaelis, E.K., Wang, X., Pal, R., Bao, X., Hascup, K.N., Wang, Y., Wang, W.-T., Hui, D., Agbas, A., Choi, I.-Y., et al. (2011). Neuronal Glud1 (glutamate dehydrogenase 1) over-expressing mice: increased glutamate formation and synaptic release, loss of synaptic activity, and adaptive changes in genomic expression. *Neurochem. Int.* *59*, 473–481.

Minelli, A., Magri, C., Barbon, A., Bonvicini, C., Segala, M., Congiu, C., Bignotti, S., Milanesi, E., Trabucchi, L., Cattane, N., et al. (2015). Proteasome system dysregulation and treatment resistance mechanisms in major depressive disorder. *Transl Psychiatry* *5*, e687.

Mir, C., Clotet, J., Aledo, R., Durany, N., Argemí, J., Lozano, R., Cervós-Navarro, J., and Casals, N. (2003). CDP-choline prevents glutamate-mediated cell death in cerebellar granule neurons. *J. Mol. Neurosci.* *20*, 53–60.

Mitani, H., Shirayama, Y., Yamada, T., Maeda, K., Ashby, C.R., and Kawahara, R. (2006). Correlation between plasma levels of glutamate, alanine and serine with severity of depression. *Prog. Neuropsychopharmacol. Biol. Psychiatry* *30*, 1155–1158.

Mitchell, N.C., Gould, G.G., Smolik, C.M., Koek, W., and Daws, L.C. (2013). Antidepressant-like drug effects in juvenile and adolescent mice in the tail suspension test: Relationship with hippocampal serotonin and norepinephrine transporter expression and function. *Front Pharmacol* *4*, 131.

Mothet, J.P., Parent, A.T., Wolosker, H., Brady, R.O., Linden, D.J., Ferris, C.D., Rogawski, M.A., and Snyder, S.H. (2000). D-serine is an endogenous ligand for the glycine site of the N-methyl-D-aspartate receptor. *Proc. Natl. Acad. Sci. U.S.A.* *97*, 4926–4931.

Muehlmann, A.M., Bliznyuk, N., Duerr, I., and Lewis, M.H. (2015). Repetitive motor behavior: further characterization of development and temporal dynamics. *Dev Psychobiol* *57*, 201–211.

Murakami, S., Imbe, H., Morikawa, Y., Kubo, C., and Senba, E. (2005). Chronic stress, as well as acute stress, reduces BDNF mRNA expression in the rat

- hippocampus but less robustly. *Neurosci. Res.* 53, 129–139.
- Murray, C.J., and Lopez, A.D. (1997). Global mortality, disability, and the contribution of risk factors: Global Burden of Disease Study. *Lancet* 349, 1436–1442.
- Murray, E.A., Wise, S.P., and Drevets, W.C. (2011). Localization of dysfunction in major depressive disorder: prefrontal cortex and amygdala. *Biol. Psychiatry* 69, e43–e54.
- Murrough, J.W., Iosifescu, D.V., Chang, L.C., Jurdi, Al, R.K., Green, C.E., Perez, A.M., Iqbal, S., Pillemer, S., Foulkes, A., Shah, A., et al. (2013). Antidepressant efficacy of ketamine in treatment-resistant major depression: a two-site randomized controlled trial. *Am J Psychiatry* 170, 1134–1142.
- Musazzi, L., Milanese, M., Farisello, P., Zappettini, S., Tardito, D., Barbiero, V.S., Bonifacino, T., Mallei, A., Baldelli, P., Racagni, G., et al. (2010). Acute stress increases depolarization-evoked glutamate release in the rat prefrontal/frontal cortex: the dampening action of antidepressants. *PLoS ONE* 5, e8566.
- Naviaux, J.C., Schuchbauer, M.A., Li, K., Wang, L., Risbrough, V.B., Powell, S.B., and Naviaux, R.K. (2014). Reversal of autism-like behaviors and metabolism in adult mice with single-dose antipurinergic therapy. *Transl Psychiatry* 4, e400.
- Nelson, J.C. (1998). Overcoming treatment resistance in depression. *J Clin Psychiatry* 59 Suppl 16, 13–9–discussion40–2.
- Nemeroff, C.B., and Vale, W.W. (2005). The neurobiology of depression: inroads to treatment and new drug discovery. *J Clin Psychiatry* 66 Suppl 7, 5–13.
- Nemeroff, C.B., DeVane, C.L., and Pollock, B.G. (1996). Newer antidepressants and the cytochrome P450 system. *Am J Psychiatry* 153, 311–320.
- Nugent, A.C., Davis, R.M., Zarate, C.A., and Drevets, W.C. (2013). Reduced thalamic volumes in major depressive disorder. *Psychiatry Res* 213, 179–185.
- Núñez Galindo, A., Kussmann, M., and Dayon, L. (2015). Proteomics of Cerebrospinal Fluid: Throughput and Robustness Using a Scalable Automated Analysis Pipeline for Biomarker Discovery. *Anal. Chem.* 87, 10755–10761.
- O' Connor, R.M., Pusceddu, M.M., Dinan, T.G., and Cryan, J.F. (2013). Impact of early-life stress, on group III mGlu receptor levels in the rat hippocampus: effects of ketamine, electroconvulsive shock therapy and fluoxetine treatment. *Neuropharmacology* 66, 236–241.
- O'Donnell, J.C. (2013). Personalized medicine and the role of health economics and outcomes research: issues, applications, emerging trends, and future research. *Value Health* 16, S1–S3.
- Oliveira, R.M.W., Guimarães, F.S., and Deakin, J.F.W. (2008). Expression of neuronal nitric oxide synthase in the hippocampal formation in affective disorders. *Braz. J. Med. Biol. Res.* 41, 333–341.

- Olivier, J.D.A., Blom, T., Arentsen, T., and Homberg, J.R. (2011). The age-dependent effects of selective serotonin reuptake inhibitors in humans and rodents: A review. *Prog. Neuropsychopharmacol. Biol. Psychiatry* 35, 1400–1408.
- Ong, S.-E., Blagoev, B., Kratchmarova, I., Kristensen, D.B., Steen, H., Pandey, A., and Mann, M. (2002). Stable isotope labeling by amino acids in cell culture, SILAC, as a simple and accurate approach to expression proteomics. *Mol. Cell Proteomics* 1, 376–386.
- Opel, N., Redlich, R., Zwanzger, P., Grotegerd, D., Arolt, V., Heindel, W., Konrad, C., Kugel, H., and Dannlowski, U. (2014). Hippocampal atrophy in major depression: a function of childhood maltreatment rather than diagnosis? *Neuropsychopharmacology* 39, 2723–2731.
- Paletzki, R.F. (2002). Cloning and characterization of guanine deaminase from mouse and rat brain. *Neuroscience* 109, 15–26.
- Panatier, A., Theodosis, D.T., Mothet, J.-P., Touquet, B., Pollegioni, L., Poulain, D.A., and Oliet, S.H.R. (2006). Glia-derived D-serine controls NMDA receptor activity and synaptic memory. *Cell* 125, 775–784.
- Papakostas, G.I. (2009). Managing partial response or nonresponse: switching, augmentation, and combination strategies for major depressive disorder. *J Clin Psychiatry* 70 Suppl 6, 16–25.
- Papakostas, G.I., Shelton, R.C., Zajecka, J.M., Etemad, B., Rickels, K., Clain, A., Baer, L., Dalton, E.D., Sacco, G.R., Schoenfeld, D., et al. (2012). L-methylfolate as adjunctive therapy for SSRI-resistant major depression: results of two randomized, double-blind, parallel-sequential trials. *Am J Psychiatry* 169, 1267–1274.
- Papp, M., Klimek, V., and Willner, P. (1994). Parallel changes in dopamine D2 receptor binding in limbic forebrain associated with chronic mild stress-induced anhedonia and its reversal by imipramine. *Psychopharmacology (Berl.)* 115, 441–446.
- Pascual-Leone, A., Rubio, B., Pallardó, F., and Catalá, M.D. (1996). Rapid-rate transcranial magnetic stimulation of left dorsolateral prefrontal cortex in drug-resistant depression. *Lancet* 348, 233–237.
- Pavlidis, C., Nivón, L., and McEwen, B. (2002). Effects of chronic stress on hippocampal long-term potentiation. *Hippocampus*.
- Pfaffl, M.W. (2001). A new mathematical model for relative quantification in real-time RT-PCR. *Nucleic Acids Res.* 29, e45.
- Pittaluga, A., Raiteri, L., Longordo, F., Luccini, E., Barbiero, V.S., Racagni, G., Popoli, M., and Raiteri, M. (2007). Antidepressant treatments and function of glutamate ionotropic receptors mediating amine release in hippocampus. *Neuropharmacology* 53, 27–36.
- Pittenger, C., and Duman, R.S. (2008). Stress, depression, and neuroplasticity: a convergence of mechanisms. *Neuropsychopharmacology* 33, 88–109.

- Player, M.J., Taylor, J.L., Weickert, C.S., Alonzo, A., Sachdev, P., Martin, D., Mitchell, P.B., and Loo, C.K. (2013). Neuroplasticity in depressed individuals compared with healthy controls. *Neuropsychopharmacology* 38, 2101–2108.
- Pletscher, A. (1991). The discovery of antidepressants: a winding path. *Experientia* 47, 4–8.
- Popescu, G., Murthy, S., and Borschel, W. (2010). Allosteric inhibitors of NMDA receptor functions. *Pharmaceuticals*.
- Popik, P., Krawczyk, M., Golembiowska, K., Nowak, G., Janowsky, A., Skolnick, P., Lippa, A., and Basile, A.S. (2006). Pharmacological profile of the “triple” monoamine neurotransmitter uptake inhibitor, DOV 102,677. *Cell. Mol. Neurobiol.* 26, 857–873.
- Preskorn, S.H. (2014). Prediction of individual response to antidepressants and antipsychotics: an integrated concept. *Dialogues Clin Neurosci* 16, 545–554.
- Qi, X., Lin, W., Li, J., Li, H., Wang, W., Wang, D., and Sun, M. (2008). Fluoxetine increases the activity of the ERK-CREB signal system and alleviates the depressive-like behavior in rats exposed to chronic forced swim stress. *Neurobiol. Dis.* 31, 278–285.
- Qiao, H., Li, M.-X., Xu, C., Chen, H.-B., An, S.-C., and Ma, X.-M. (2016). Dendritic Spines in Depression: What We Learned from Animal Models. *Neural Plast.* 2016, 8056370.
- Radad, K., Gille, G., Xiaojing, J., Durany, N., and Rausch, W.-D. (2007). CDP-choline reduces dopaminergic cell loss induced by MPP(+) and glutamate in primary mesencephalic cell culture. *Int J Neurosci* 117, 985–998.
- Radley, J.J., Sisti, H.M., Hao, J., Rocher, A.B., McCall, T., Hof, P.R., McEwen, B.S., and Morrison, J.H. (2004). Chronic behavioral stress induces apical dendritic reorganization in pyramidal neurons of the medial prefrontal cortex. *Neuroscience* 125, 1–6.
- Reierson, G.W., Mastronardi, C.A., Licinio, J., and Wong, M.-L. (2009). Repeated antidepressant therapy increases cyclic GMP signaling in rat hippocampus. *Neurosci. Lett.* 466, 149–153.
- Renshaw, P.F., Parow, A.M., Hirashima, F., Ke, Y., Moore, C.M., Frederick, B. de B., Fava, M., Hennen, J., and Cohen, B.M. (2001). Multinuclear magnetic resonance spectroscopy studies of brain purines in major depression. *Am J Psychiatry* 158, 2048–2055.
- Robison, A.J., Vialou, V., Sun, H.-S., Labonte, B., Golden, S.A., Dias, C., Turecki, G., Tamminga, C., Russo, S., Mazei-Robison, M., et al. (2014). Fluoxetine epigenetically alters the CaMKII $\alpha$  promoter in nucleus accumbens to regulate  $\Delta$ FosB binding and antidepressant effects. *Neuropsychopharmacology* 39, 1178–1186.
- Rosa, J.M., Dafre, A.L., and Rodrigues, A.L.S. (2013). Antidepressant-like responses in the forced swimming test elicited by glutathione and redox modulation. *Behav.*

Brain Res. 253, 165–172.

Rotheneichner, P., Lange, S., O'Sullivan, A., Marschallinger, J., Zaunmair, P., Geretsegger, C., Aigner, L., and Couillard-Despres, S. (2014). Hippocampal neurogenesis and antidepressive therapy: shocking relations. *Neural Plast.* 2014, 723915.

Rubin, R.T., Phillips, J.J., Sadow, T.F., and McCracken, J.T. (1995). Adrenal gland volume in major depression. Increase during the depressive episode and decrease with successful treatment. *Arch. Gen. Psychiatry* 52, 213–218.

Ryan, B., Musazzi, L., Mallei, A., Tardito, D., Gruber, S.H.M., Houry, El, A., Anwyl, R., Racagni, G., Mathé, A.A., Rowan, M.J., et al. (2009). Remodelling by early-life stress of NMDA receptor-dependent synaptic plasticity in a gene-environment rat model of depression. *Int. J. Neuropsychopharmacol.* 12, 553–559.

Ryan, M.M., Lockstone, H.E., Huffaker, S.J., Wayland, M.T., Webster, M.J., and Bahn, S. (2006). Gene expression analysis of bipolar disorder reveals downregulation of the ubiquitin cycle and alterations in synaptic genes. *Mol. Psychiatry* 11, 965–978.

Samuels, B.A., Anacker, C., Hu, A., Levinstein, M.R., Pickenhagen, A., Tsetsenis, T., Madroñal, N., Donaldson, Z.R., Drew, L.J., Dranovsky, A., et al. (2015). 5-HT1A receptors on mature dentate gyrus granule cells are critical for the antidepressant response. *Nat. Neurosci.* 18, 1606–1616.

Sandi, C. (2004). Stress, cognitive impairment and cell adhesion molecules. *Nat. Rev. Neurosci.* 5, 917–930.

Sangkuhl, K., Klein, T.E., and Altman, R.B. (2009). Selective serotonin reuptake inhibitors pathway. *Pharmacogenet Genomics* 19, 907–909.

Sato, Y., Suzuki, I., Nakamura, T., Bernier, F., Aoshima, K., and Oda, Y. (2012). Identification of a new plasma biomarker of Alzheimer's disease using metabolomics technology. *J. Lipid Res.* 53, 567–576.

Schmidt, M.V., Scharf, S.H., Sterlemann, V., Ganea, K., Liebl, C., Holsboer, F., and Müller, M.B. (2010). High susceptibility to chronic social stress is associated with a depression-like phenotype. *Psychoneuroendocrinology* 35, 635–643.

Schmidt, W., and Reith, M. (2005). Dopamine and glutamate in psychiatric disorders.

Schöpf, J., Baumann, P., Lemarchand, T., and Rey, M. (1989). Treatment of endogenous depressions resistant to tricyclic antidepressants or related drugs by lithium addition. Results of a placebo-controlled double-blind study. *Pharmacopsychiatry* 22, 183–187.

Serretti, A., Cusin, C., Rausch, J.L., Bondy, B., and Smeraldi, E. (2006). Pooling pharmacogenetic studies on the serotonin transporter: a mega-analysis. *Psychiatry Res* 145, 61–65.

Serretti, A., Kato, M., De Ronchi, D., and Kinoshita, T. (2007). Meta-analysis of serotonin transporter gene promoter polymorphism (5-HTTLPR) association with

selective serotonin reuptake inhibitor efficacy in depressed patients. *Mol. Psychiatry* *12*, 247–257.

Serretti, A., Zanardi, R., Cusin, C., Rossini, D., Lorenzi, C., and Smeraldi, E. (2001). Tryptophan hydroxylase gene associated with paroxetine antidepressant activity. *Eur Neuropsychopharmacol* *11*, 375–380.

Sethi, S., and Brietzke, E. (2015). Omics-Based Biomarkers: Application of Metabolomics in Neuropsychiatric Disorders. *Int. J. Neuropsychopharmacol.* *19*.

Shah, S.H., Kraus, W.E., and Newgard, C.B. (2012). Metabolomic profiling for the identification of novel biomarkers and mechanisms related to common cardiovascular diseases: form and function. *Circulation* *126*, 1110–1120.

Sheline, Y.I., Sanghavi, M., Mintun, M.A., and Gado, M.H. (1999). Depression duration but not age predicts hippocampal volume loss in medically healthy women with recurrent major depression. *J. Neurosci.* *19*, 5034–5043.

Sheline, Y.I., Wang, P.W., Gado, M.H., Csernansky, J.G., and Vannier, M.W. (1996). Hippocampal atrophy in recurrent major depression. *Proc. Natl. Acad. Sci. U.S.A.* *93*, 3908–3913.

Shimizu, E., Hashimoto, K., Okamura, N., Koike, K., Komatsu, N., Kumakiri, C., Nakazato, M., Watanabe, H., Shinoda, N., Okada, S.-I., et al. (2003). Alterations of serum levels of brain-derived neurotrophic factor (BDNF) in depressed patients with or without antidepressants. *Biol. Psychiatry* *54*, 70–75.

Shirayama, Y., and Chaki, S. (2006). Neurochemistry of the nucleus accumbens and its relevance to depression and antidepressant action in rodents. *Curr Neuropharmacol* *4*, 277–291.

Shirayama, Y., Chen, A.C.H., Nakagawa, S., Russell, D.S., and Duman, R.S. (2002). Brain-derived neurotrophic factor produces antidepressant effects in behavioral models of depression. *J. Neurosci.* *22*, 3251–3261.

Skolnick, P. (1999). Antidepressants for the new millennium. *Eur. J. Pharmacol.* *375*, 31–40.

Sluzewska, A., Sobieska, M., and Rybakowski, J.K. (1997). Changes in acute-phase proteins during lithium potentiation of antidepressants in refractory depression. *Neuropsychobiology* *35*, 123–127.

Slyepchenko, A., Carvalho, A.F., Cha, D.S., Kasper, S., and McIntyre, R.S. (2014). Gut emotions - mechanisms of action of probiotics as novel therapeutic targets for depression and anxiety disorders. *CNS Neurol Disord Drug Targets* *13*, 1770–1786.

Stein, G., and Bernadt, M. (1993). Lithium augmentation therapy in tricyclic-resistant depression. A controlled trial using lithium in low and normal doses. *The British Journal of Psychiatry*.

Suárez, L.M., and Solís, J.M. (2006). Taurine potentiates presynaptic NMDA receptors in hippocampal Schaffer collateral axons. *Eur. J. Neurosci.* *24*, 405–418.

- Svenningsson, P., Berg, L., Matthews, D., Ionescu, D.F., Richards, E.M., Niciu, M.J., Malinger, A., Toups, M., Manji, H., Trivedi, M.H., et al. (2014). Preliminary evidence that early reduction in p11 levels in natural killer cells and monocytes predicts the likelihood of antidepressant response to chronic citalopram. *Mol. Psychiatry* *19*, 962–964.
- Svenningsson, P., Chergui, K., Rachleff, I., Flajolet, M., Zhang, X., Yacoubi, El, M., Vaugeois, J.-M., Nomikos, G.G., and Greengard, P. (2006). Alterations in 5-HT<sub>1B</sub> receptor function by p11 in depression-like states. *Science* *311*, 77–80.
- Szczepankiewicz, A., Leszczynska-Rodziewicz, A., Pawlak, J., Narozna, B., Rajewska-Rager, A., Wilkosc, M., Zaremba, D., Maciukiewicz, M., and Twarowska-Hauser, J. (2014). FKBP5 polymorphism is associated with major depression but not with bipolar disorder. *J Affect Disord* *164*, 33–37.
- Taguchi, R., Shikata, K., Furuya, Y., Ino, M., Shin, K., and Shibata, H. (2016). Selective corticotropin-releasing factor 1 receptor antagonist E2508 has potent antidepressant-like and anxiolytic-like properties in rodent models. *Behav. Brain Res.*
- Tai, H.-C., Besche, H., Goldberg, A.L., and Schuman, E.M. (2010). Characterization of the Brain 26S Proteasome and its Interacting Proteins. *Front Mol Neurosci* *3*.
- Targum, S.D., Rosen, L., and Capodanno, A.E. (1983). The dexamethasone suppression test in suicidal patients with unipolar depression. *Am J Psychiatry* *140*, 877–879.
- Thompson, D., Pepys, M.B., and Wood, S.P. (1999). The physiological structure of human C-reactive protein and its complex with phosphocholine. *Structure* *7*, 169–177.
- Tomaz, V.S., Cordeiro, R.C., Costa, A.M.N., de Lucena, D.F., Nobre Júnior, H.V., de Sousa, F.C.F., Vasconcelos, S.M.M., Vale, M.L., Quevedo, J., and Macêdo, D. (2014). Antidepressant-like effect of nitric oxide synthase inhibitors and sildenafil against lipopolysaccharide-induced depressive-like behavior in mice. *Neuroscience* *268*, 236–246.
- Tonack, S., Jenkinson, C., Cox, T., Elliott, V., Jenkins, R.E., Kitteringham, N.R., Greenhalf, W., Shaw, V., Michalski, C.W., Friess, H., et al. (2013). iTRAQ reveals candidate pancreatic cancer serum biomarkers: influence of obstructive jaundice on their performance. *Br J Cancer* *108*, 1846–1853.
- Toyoda, A., and Iio, W. (2013). Antidepressant-like effect of chronic taurine administration and its hippocampal signal transduction in rats. *Adv. Exp. Med. Biol.* *775*, 29–43.
- Trivedi, M.H., Rush, A.J., Wisniewski, S.R., Nierenberg, A.A., Warden, D., Ritz, L., Norquist, G., Howland, R.H., Lebowitz, B., McGrath, P.J., et al. (2006). Evaluation of outcomes with citalopram for depression using measurement-based care in STAR\*D: implications for clinical practice. *Am J Psychiatry* *163*, 28–40.
- Tsai, N.-P. (2014). Ubiquitin proteasome system-mediated degradation of synaptic proteins: An update from the postsynaptic side. *Biochim. Biophys. Acta* *1843*, 2838–2842.

- Tsai, S.-J., Liou, Y.-J., Hong, C.-J., Yu, Y.W.-Y., and Chen, T.-J. (2008). Glycogen synthase kinase-3beta gene is associated with antidepressant treatment response in Chinese major depressive disorder. *Pharmacogenomics J.* 8, 384–390.
- Valkanova, V., Ebmeier, K.P., and Allan, C.L. (2013). CRP, IL-6 and depression: a systematic review and meta-analysis of longitudinal studies. *J Affect Disord* 150, 736–744.
- Vallebuona, F., and Raiteri, M. (1994). Extracellular cGMP in the hippocampus of freely moving rats as an index of nitric oxide (NO) synthase activity. *J. Neurosci.* 14, 134–139.
- Ventura-Juncá, R., Symon, A., López, P., Fiedler, J.L., Rojas, G., Heskia, C., Lara, P., Marín, F., Guajardo, V., Araya, A.V., et al. (2014). Relationship of cortisol levels and genetic polymorphisms to antidepressant response to placebo and fluoxetine in patients with major depressive disorder: a prospective study. *BMC Psychiatry* 14, 220.
- Vogelzangs, N., Duivis, H.E., Beekman, A.T.F., Kluft, C., Neuteboom, J., Hoogendijk, W., Smit, J.H., de Jonge, P., and Penninx, B.W.J.H. (2012). Association of depressive disorders, depression characteristics and antidepressant medication with inflammation. *Transl Psychiatry* 2, e79.
- Wagner, K.V., Marinescu, D., Hartmann, J., Wang, X.-D., Labermaier, C., Scharf, S.H., Liebl, C., Uhr, M., Holsboer, F., Müller, M.B., et al. (2012). Differences in FKBP51 Regulation Following Chronic Social Defeat Stress Correlate with Individual Stress Sensitivity: Influence of Paroxetine Treatment. *Neuropsychopharmacology* 37, 2797–2808.
- Wang, J.-W., David, D.J., Monckton, J.E., Battaglia, F., and Hen, R. (2008). Chronic fluoxetine stimulates maturation and synaptic plasticity of adult-born hippocampal granule cells. *J. Neurosci.* 28, 1374–1384.
- Webhofer, C., Gormanns, P., Reckow, S., Lebar, M., Maccarrone, G., Ludwig, T., Pütz, B., Asara, J.M., Holsboer, F., Sillaber, I., et al. (2013). Proteomic and metabolomic profiling reveals time-dependent changes in hippocampal metabolism upon paroxetine treatment and biomarker candidates. *J Psychiatr Res* 47, 289–298.
- Webhofer, C., Gormanns, P., Tolstikov, V., Zieglgänsberger, W., Sillaber, I., Holsboer, F., and Turck, C.W. (2011). Metabolite profiling of antidepressant drug action reveals novel drug targets beyond monoamine elevation. *Transl Psychiatry* 1, e58.
- Weckmann, K., Labermaier, C., Asara, J.M., Müller, M.B., and Turck, C.W. (2014). Time-dependent metabolomic profiling of Ketamine drug action reveals hippocampal pathway alterations and biomarker candidates. *Transl Psychiatry* 4, e481.
- Wegener, G., Volke, V., Harvey, B., and Rosenberg, R. (2003). Local, but not systemic, administration of serotonergic antidepressants decreases hippocampal nitric oxide synthase activity. *Brain Res.*
- Westergaard, N., Banke, T., Wahl, P., Sonnewald, U., and Schousboe, A. (1995). Citrate modulates the regulation by Zn<sup>2+</sup> of N-methyl-D-aspartate receptor-mediated

channel current and neurotransmitter release. *Proc. Natl. Acad. Sci. U.S.A.* 92, 3367–3370.

Wieronska, J.M., Klak, K., Palucha, A., Branski, P., and Pilc, A. (2007). Citalopram influences mGlu7, but not mGlu4 receptors' expression in the rat brain hippocampus and cortex. *Brain Res.* 1184, 88–95.

Wildburger, N.C., and Laezza, F. (2012). Control of neuronal ion channel function by glycogen synthase kinase-3: new prospective for an old kinase. *Front Mol Neurosci* 5, 80.

Wong, M.-L., Dong, C., Maestre-Mesa, J., and Licinio, J. (2008). Polymorphisms in inflammation-related genes are associated with susceptibility to major depression and antidepressant response. *Mol. Psychiatry* 13, 800–812.

Wong, M.-L., O'Kirwan, F., Hannestad, J.P., Irizarry, K.J.L., Elashoff, D., and Licinio, J. (2004). St John's wort and imipramine-induced gene expression profiles identify cellular functions relevant to antidepressant action and novel pharmacogenetic candidates for the phenotype of antidepressant treatment response. *Mol. Psychiatry* 9, 237–251.

Wurglics, M., and Schubert-Zsilavecz, M. (2006). *Hypericum perforatum*: a “modern” herbal antidepressant: pharmacokinetics of active ingredients. *Clin Pharmacokinet* 45, 449–468.

Xu, B., Wratten, N., Charych, E.I., Buyske, S., Firestein, B.L., and Brzustowicz, L.M. (2005). Increased expression in dorsolateral prefrontal cortex of CAPON in schizophrenia and bipolar disorder. *PLoS Med.* 2, e263.

Yamamura, T., Okamoto, Y., Okada, G., Takaishi, Y., Takamura, M., Mantani, A., Kurata, A., Otagaki, Y., Yamashita, H., and Yamawaki, S. (2016). Association of thalamic hyperactivity with treatment-resistant depression and poor response in early treatment for major depression: a resting-state fMRI study using fractional amplitude of low-frequency fluctuations. *Transl Psychiatry* 6, e754.

Yang, T.T., Simmons, A.N., Matthews, S.C., Tapert, S.F., Frank, G.K., Max, J.E., Bischoff-Grethe, A., Lansing, A.E., Brown, G., Strigo, I.A., et al. (2010). Adolescents with major depression demonstrate increased amygdala activation. *J Am Acad Child Adolesc Psychiatry* 49, 42–51.

Yao, C., Behring, J.B., Shao, D., Sverdlov, A.L., Whelan, S.A., Elezaby, A., Yin, X., Siwik, D.A., Seta, F., Costello, C.E., et al. (2015). Overexpression of Catalase Diminishes Oxidative Cysteine Modifications of Cardiac Proteins. *PLoS ONE* 10, e0144025.

Yi, J.J., and Ehlers, M.D. (2007). Emerging roles for ubiquitin and protein degradation in neuronal function. *Pharmacol Rev* 59, 14–39.

Yoon, S.J., Lyoo, I.K., Haws, C., Kim, T.-S., Cohen, B.M., and Renshaw, P.F. (2009). Decreased glutamate/glutamine levels may mediate cytidine's efficacy in treating bipolar depression: a longitudinal proton magnetic resonance spectroscopy study. *Neuropsychopharmacology* 34, 1810–1818.

- Yoshimura, R., and Nakano, W.U. (2009). Rapid response to paroxetine is associated with plasma paroxetine levels at 4 but not 8 weeks of treatment, and is independent of serotonin transporter promoter polymorphism in Japanese depressed patients. *Hum Psychopharmacol* 2009 Aug;24(6):489-94 Doi: 101002/Hup1043.
- Yuan, G., Bin, J.C., McKay, D.J., and Snyder, F.F. (1999). Cloning and characterization of human guanine deaminase. Purification and partial amino acid sequence of the mouse protein. *J. Biol. Chem.* 274, 8175–8180.
- Zanardi, R., Serretti, A., Rossini, D., Franchini, L., Cusin, C., Lattuada, E., Dotoli, D., and Smeraldi, E. (2001). Factors affecting fluvoxamine antidepressant activity: influence of pindolol and 5-HTTLPR in delusional and nondelusional depression. *Biol. Psychiatry* 50, 323–330.
- Zangen, A., Nakash, R., and Yadid, G. (1999). Serotonin-mediated increases in the extracellular levels of beta-endorphin in the arcuate nucleus and nucleus accumbens: a microdialysis study. *J. Neurochem.* 73, 2569–2574.
- Zangen, A., Nakash, R., Overstreet, D.H., and Yadid, G. (2001). Association between depressive behavior and absence of serotonin-dopamine interaction in the nucleus accumbens. *Psychopharmacology (Berl.)* 155, 434–439.
- Zhang, H., Hyrc, K., and Thio, L. (2009). The glycine transport inhibitor sarcosine is an NMDA receptor co-agonist that differs from glycine. *The Journal of Physiology*.
- Zhang, Y., Filiou, M.D., Reckow, S., Gormanns, P., Maccarrone, G., Kessler, M.S., Frank, E., Hamsch, B., Holsboer, F., Landgraf, R., et al. (2011a). Proteomic and metabolomic profiling of a trait anxiety mouse model implicate affected pathways. *Mol. Cell Proteomics* 10, M111.008110.
- Zhang, Y., Reckow, S., Webhofer, C., Boehme, M., Gormanns, P., Egge-Jacobsen, W.M., and Turck, C.W. (2011b). Proteome scale turnover analysis in live animals using stable isotope metabolic labeling. *Anal. Chem.* 83, 1665–1672.
- Zhao, J., Jung, Y.-H., Jang, C.-G., Chun, K.-H., Kwon, S.W., and Lee, J. (2015). Metabolomic identification of biochemical changes induced by fluoxetine and imipramine in a chronic mild stress mouse model of depression. *Sci Rep* 5, 8890.
- Zhou, Q.-G., Hu, Y., Hua, Y., Hu, M., Luo, C.-X., Han, X., Zhu, X.-J., Wang, B., Xu, J.-S., and Zhu, D.-Y. (2007). Neuronal nitric oxide synthase contributes to chronic stress-induced depression by suppressing hippocampal neurogenesis. *J. Neurochem.* 103, 1843–1854.
- Zhou, Q.-G., Zhu, L.-J., Chen, C., Wu, H.-Y., Luo, C.-X., Chang, L., and Zhu, D.-Y. (2011). Hippocampal neuronal nitric oxide synthase mediates the stress-related depressive behaviors of glucocorticoids by downregulating glucocorticoid receptor. *J. Neurosci.* 31, 7579–7590.
- Zhu, W., Smith, J.W., and Huang, C.-M. (2010). Mass spectrometry-based label-free quantitative proteomics. *J. Biomed. Biotechnol.* 2010, 840518.
- Zou, Y.-F., Wang, Y., Liu, P., Feng, X.-L., Wang, B.-Y., Zang, T.-H., Yu, X., Wei, J.,

Liu, Z.-C., Liu, Y., et al. (2010a). Association of brain-derived neurotrophic factor genetic Val66Met polymorphism with severity of depression, efficacy of fluoxetine and its side effects in Chinese major depressive patients. *Neuropsychobiology* *61*, 71–78.

Zou, Y.-F., Ye, D.-Q., Feng, X.-L., Su, H., Pan, F.-M., and Liao, F.-F. (2010b). Meta-analysis of BDNF Val66Met polymorphism association with treatment response in patients with major depressive disorder. *Eur Neuropsychopharmacol* *20*, 535–544.

## List of abbreviations

- ACTH: Adrenocorticotrophic hormone
- AdoHcyase: S-adenosyl-L-homocysteine hydrolase
- AdoHcyase 2: S-adenosyl-L-homocysteine hydrolase 2
- ALS: Amyotrophic lateral sclerosis
- AMPA:  $\alpha$ -amino-3-hydroxy-5-methyl-4-isoxazolepropionic acid
- AVP: Arginine vasopressin
- ATIC: Aminoimidazole-4-carboxamide ribonucleotide transformylase/IMP  
cyclohydrolase
- BDNF: Brain-derived neurotrophic factor
- CaMK:  $\text{Ca}^{2+}$ /calmodulin-dependent protein kinase
- cAMP: cyclic adenosine monophosphate
- CAPON: Carboxy-terminal PDZ ligand of *nNOS*
- CPS2: Carbamoyl phosphate synthase 2
- CREB: cAMP response element binding protein
- CRH: Corticotrophin releasing hormone
- CRP: C-reactive protein
- DSM: Diagnostic and statistical manual of mental disorders
- DST: Dexamethasone suppression test
- ERK: Extracellular signal-regulated kinase
- FKBP51: FK506-binding protein 51
- FST: Forced swim test
- FUST: Female urine sniffing test
- GAPDH: Glyceraldehyde-3-phosphate dehydrogenase
- GDA: Guanine deaminase
- GDH1: Glutamate dehydrogenase 1
- GS: Glutamine synthetase
- GSK-3 $\beta$ : Glycogen synthase kinase-3 $\beta$
- HCA: Hierarchical clustering analysis
- HDRS: Hamilton Depression Rating Scale
- HPA: Human Protein Atlas / Hypothalamus-pituitary-adrenal

HPRT: Hypoxanthine-guanine phosphoribosyltransferase  
HRP: Horseradish peroxidase  
ICAT: Isotope-coded affinity tag  
ICD: International statistical classification of diseases and related health problems  
ICPL: Isotope-coded protein label  
IMP: Inosine monophosphate  
iPS: Induced pluripotent stem cell  
ITPase: Inosine triphosphate pyrophosphatase  
iTRAQ: Isobaric tags for relative and absolute quantification  
KEGG: Kyoto Encyclopedia of Genes and Genomes  
LTP: Long-term potentiation  
MAO: Monoamine oxidase  
MARS: Munich Antidepressant Response Signature  
mAST: Mitochondrial aspartate transaminase  
MDD: Major depressive disorder  
MEK: Mitogen-activated protein kinase kinase  
NAc: Nucleus accumbens  
NGF: Nerve growth factor  
NMDA: N-Methyl-D-aspartate  
nNOS: Neuronal nitric oxide synthase  
NO: Nitric oxide  
NR: N-Methyl-D-aspartate (NMDA) receptor subunit  
NT-3: Neurotrophin-3  
NT-4: Neurotrophin-4  
P-CaMKII : Phospho-CaMKII  
P-ERK: Phospho-ERK  
P-GSK-3 $\beta$ : Phospho-GSK-3 $\beta$   
P-MEK: Phospho-MEK  
P-NR1: Phospho-NR1  
P-NR2A: Phospho-NR2A  
P-NR2B: Phospho-NR2B  
PBMCs: Peripheral blood mononuclear cells  
PLF: Paroxetine-treated long-time floating  
PMSA2: Proteasome subunit  $\alpha$  type-2

PNP: Purine nucleoside phosphorylase  
PSD-95: Postsynaptic density protein 95  
PSMA7: Proteasome subunit  $\alpha$ 7  
PSF: Paroxetine-treated short-time floating  
PSMD9: Proteasome 26S non-ATPase subunit 9  
PSMD13: Proteasome 26S non-ATPase subunit 13  
qRT-PCR: Quantitative Reverse Transcription Polymerase Chain Reaction  
RDoC: Research domain of criteria  
SAM: Significant analysis of microarrays (and metabolites)  
sGC- $\beta$ 1: Soluble guanylate cyclase- $\beta$ 1  
SILAC: Stable isotope labeling of amino acids in cell culture  
SILAM: Stable isotope labeling in mammals  
SNPs: Single nucleotide polymorphisms  
SNRIs: Selective norepinephrine reuptake inhibitors  
SSRIs: Selective Serotonin Reuptake Inhibitors  
STXBP1: Syntaxin binding protein 1  
SV2A: Synaptic vesicle glycoprotein 2A  
SYNJ1: Synaptojanin 1  
TCA: Tricyclic antidepressant  
TMT: Tandem mass tag  
TRD: Treatment resistant depression  
Ub: Ubiquitin  
UMP/CMPK: UMP-CMP kinase  
UPS: Ubiquitin-proteasome system

## List of figures

Figure 1. Brain regions that are affected in MDD. ....	1
Figure 2. Diagram of HPA axis.....	4
Figure 3. Monoamine neurotransmission in the synapse.....	5
Figure 4. SILAC and SILAM metabolic labeling methods.....	10
Figure 5. A schematic overview of the workflow.....	24
Figure 6. The effect of chronic paroxetine treatment on FST floating time.....	25
Figure 7. Sub-grouping of paroxetine-treated mice .....	26
Figure 8. The effect of chronic paroxetine treatment on female urine sniffing test (FUST) .....	26
Figure 9. Paroxetine levels in whole brain and plasma .....	27
Figure 10. The effect of age on FST floating time.....	27
Figure 11. The effect of body weight gain on FST floating time.....	28
Figure 12. A volcano plot of hippocampal metabolome and proteome.....	28
Figure 13. A heat map with combined profiles of SAM signatures and their significant correlates .....	29
Figure 14. Hippocampal SAM metabolites and their significant correlates .....	30
Figure 15. Identification of purine and pyrimidine metabolism pathway proteins in proteomics analysis.....	31
Figure 16. Metabolic pathway analysis in the hippocampus.....	31
Figure 17. Purine and pyrimidine metabolite average levels and correlation with FST floating time.....	32
Figure 18. Levels of hippocampal metabolites that are part of pyrimidine metabolism pathway and correlation with FST floating time .....	32
Figure 19. Levels of hippocampal metabolites that are part of purine metabolism pathway and correlation with FST floating time .....	33
Figure 20. The effect of chronic paroxetine treatment on ATIC, CPS2 and HPRT protein expressions in the mouse hippocampus and prefrontal cortex .....	34
Figure 21. Significant plasma metabolite level changes after chronic paroxetine treatment. ....	36
Figure 22. Chronic paroxetine treatment induced differential metabolome alterations in PSF mouse plasma .....	37
Figure 23. Heat maps and identified pathways of PLF groups comparing metabolome at baseline (T0) and following 28 days of treatment (T4).....	38
Figure 24. Plasma metabolite average level changes in the identified pathways. ....	39
Figure 25. Plasma pyrimidine pathway metabolite levels. ....	40
Figure 26. Plasma purine pathway metabolite levels.....	40
Figure 27. Plasma glycine, serine and threonine metabolism pathway metabolite levels.....	41
Figure 28. Common plasma SAM signatures between the PLF and PSF groups.....	41

Figure 29. The effect of chronic paroxetine treatment on ATIC, CPS2 and HPRT protein expressions in the mouse erythrocytes.....	42
Figure 30. Correlation of ATIC, CPS2 and HPRT protein levels with clinical antidepressant treatment response.....	43
Figure 31. Sub-grouping of mice treated with paroxetine.....	44
Figure 32. Proteomics profiles and enriched pathways between the PLF and PSF groups.....	45
Figure 33. A volcano plot comparing PLF and PSF metabolomes.....	46
Figure 34. Glutamate-related metabolite differences between PLF and PSF mice.....	46
Figure 35. Arginine and citrulline levels in PLF and PSF mice.....	47
Figure 36. Affected protein-metabolite network following chronic paroxetine treatment.....	47
Figure 37. NR protein level differences between the sub-groups.....	48
Figure 38. Correlation of NR protein levels with FST floating time.....	48
Figure 39. NMDA receptor signaling protein level differences between the sub-groups.....	49
Figure 40. Correlation of NMDA receptor signaling protein levels with FST floating time.....	49
Figure 41. Differential effect of chronic paroxetine treatment on PSD-95/nNOS complex. PSD-95, nNOS, CAPON and sGC- $\beta$ 1 protein level differences between PLF and PSF mice.....	50
Figure 42. Correlation of PSD-95/nNOS complex with FST floating time.....	50
Figure 43. Glutamate metabolism protein level differences between PLF and PSF mice.....	51
Figure 44. Correlation of glutamate metabolism protein levels of FST floating time.....	51
Figure 45. Synapse and vesicle trafficking-associated protein level differences between PLF and PSF mice.....	51
Figure 46. Correlation of Synapse and vesicle trafficking-associated protein levels with FST floating time.....	52
Figure 47. qRT-PCR data of NRs, PSD95 and nNOS.....	52
Figure 48. Ubiquitinated NR1, NR2A and PSD-95 protein level differences between PLF and PSF groups.....	53
Figure 49. PM2A and ubiquitination level differences between PLF and PSF mice.....	53
Figure 50. Correlation of PM2A and ubiquitination levels with FST floating time.....	53
Figure 51. Western blot analysis in MDD patient's PBMCs.....	54
Figure 52. sGC- $\beta$ 1, PM2A and ubiquitination levels in human PBMCs from antidepressant responder and non-responder patients.....	55
Figure 53. Correlation between the hippocampus and plasma metabolite levels.....	60
Figure 54. Energy-related metabolite ratios in the hippocampus.....	61
Figure 55. Correlation between baseline ubiquitination levels and clinical antidepressant response.....	67
Figure 56. A heatmap of hippocampal UPS pathway proteins comparing PLF and PSF groups.....	68

## List of tables

Table 1. List of primers used for qRT-PCR analysis.....	18
Table 2. Demographic features of antidepressant treatment responder and non-responder patients.....	21
Table 3. Demographic and clinical characteristics of antidepressant responders and non-responders included in ex vivo PBMCs cultivation and paroxetine treatment.....	21

## Publications

**Park, DI.**, Dournes, C., Sillaber, I., Asara J.M., Ising, M., Webhofer, C., Filiou, M.D., Müller M.B., Turck, C.W. Delineation of molecular pathway activities of the chronic antidepressant treatment response suggests important roles for glutamatergic and ubiquitin-proteasome systems. *Submitted*.

**Park, DI.**, Dournes, C., Sillaber, I., Uhr, M., Asara J.M., Gassen N.C, Rein, T., Ising, M., Webhofer, C., Filiou, M.D., Müller M.B., Turck, C.W. Purine and pyrimidine metabolism: Convergent evidence on chronic antidepressant treatment response in mice and humans. *Submitted*.

Shin, M.K., Kim, H.G., Baek, S.H., Jung, W.R., **Park, DI.**, Park, J.S., Jo, D.G., Kim, K.L. Neuropep-1 ameliorates learning and memory deficits in an Alzheimer's disease mouse model, increases brain-derived neurotrophic factor expression in the brain, and causes reduction of amyloid beta plaques. (2014). *Neurobiol Aging*. 35(5):990-1001.

**Park, DI.**, Kim, H.G., Jung, W.R., Shin, M.K., Kim, K.L. Mecamylamine attenuates dexamethasone-induced anxiety-like behavior in association with brain derived neurotrophic factor upregulation in rat brains. (2011). *Neuropharmacology*. 61(1-2):276-82.

Jung, W.R., Kim, H.G., Shin, M.K., **Park, DI.**, Kim, K.L. The effect of ganglioside GQ1b on the NMDA receptor signaling pathway in H19-7 cells and rat hippocampus. (2010). *Neuroscience*. 13165(1):159-67.

## Acknowledgements

First, I should thank my supervisor, Prof. Dr. Christoph W. Turck, for his great support. He provided me with precious chances to develop my thesis and perspective as an independent scientist. I could learn from him how the great scientist should be for the past 4 years.

I greatly appreciate my thesis advisory committee (TAC) members, PD Dr. Mathias Schmidt, Dr. Inge Sillaber and Prof. George Boyan, for the annual supervision and advice.

I would like to acknowledge Prof. Marianne B. Müller and Carine Dournes as well for their contributions, support and establishment of the mouse model and excellent behavioral studies.

My colleagues deserve to get my huge gratitude for the passionate and inspiring discussions. We all shared every single moment in the Max Planck Institute of Psychiatry as group members of AG Turck. All the sweats and toasts we experienced together will remain in my mind for good. They include Luis Rodrigues, Evangelia Tzika, Dr. Chi-Ya Kao, Katja Weckmann, Dr. Christian Webhofer, Dr. Michaela Filiou, Dr. Giuseppina Maccarone, Christiane Rewerts, Dr. Frederik Dethloff, Dr. Ying He, Dr. Shu-Yi Su and Prof. Dr. Daniel Martins-de-Souza.

Dr. Nils C. Gassen, Kathrin Hafner and Dr. Theo Rein also deserve my acknowledgement regarding their generous and passionate collaboration, which improved my thesis and publications a lot.

I am also grateful to Božidar Novak and Christine Huber for their technical and emotional support. I cannot deny that I could not have done some of the experiments easily without their help.

I send my immense thanks to the members of IMPRS-LS coordination office, Dr. Hans-Joerg Schaeffer, Dr. Ingrid Wolf and Maxi, for their assistance here in Munich. Kwanjeong Educational Foundation was the first page of this fairy tale story. Thanks to Jong-hwan Lee, a benefactor who has donated his entire wealths to found this charity. I was able to grab an unimaginable chance studying abroad in a prestigious German research institution.

My greatest appreciation and love are dedicated to my wife, Minyoung Chae. Without her countless sacrifices and support, I would not have been able to go on with

doctoral study abroad in Germany. She has been my best mentor, friend, company and woman. She has stayed next to me all the time going through all imaginable hardships in life. Now I grew up a bit more thanks to her.

Last but not the least, I owe my parents, parents-in-law and a sister-in-law, Sun-Young Chae, a debt of gratitude. I sincerely appreciate their care and patience.

In the end, now I realize that all my achievements have been made with the generous help from society and people around me. I conclude this section by sending my sincere acknowledgement to people who do the best in their places.

## Curriculum Vitae

### *Personal information*

Name: Park, Dongik  
Date of birth: February 19<sup>th</sup>, 1984  
Nationality: South-Korean

### *Education*

**2012-2016 Ph.D.** International Max Planck Research School for Life Science (IMPRS-LS), Max Planck Institute of Psychiatry (MPI-P) (Supervisor: Prof. Dr. Christoph W. Turck)

**2009-2011 M.Sc.** Department of Biological Science, Sungkyunkwan University, Suwon, Korea of Republic (Supervisor: Prof. Dr. Kim, Kil-Lyong)

**2002-2009 B.Sc.** Department of Biological Science, Sungkyunkwan University, Suwon, Korea of Republic

### *Awards and Scholarships*

#### **2012-2016**

Kwanjeong Educational Foundation, Seoul, South-Korea

#### **2014**

Young investigator invitation, National center for Neurology and Psychiatry (NCNP) and MPI-P Joint symposium, Hakone, Japan

#### **2002, 2007-2009**

Excellence scholarship, Sungkyunkwan University, Suwon, South-Korea